Investigation of mono- and polymicrobial antibiofilm activities of Defensin-like antimicrobial peptide-2 against *Candida auris* and *Pseudomonas aeruginosa*

Aimee Piketh (2075118)

5 June 2024

Master's Dissertation

Master of Science in Medicine by research only

Supervisors: Assoc. Prof. Aijaz Ahmad and Dr Vartika Srivastava

Department of Clinical Microbiology and Infectious Diseases

School of Pathology

Faculty of Health Sciences

The University of the Witwatersrand, Johannesburg, South Africa

DECLARATION

I, Aimee Piketh (2075118), declare that this dissertation is my own work. This dissertation is being submitted for the Degree of Master of Science in Medicine (by research) in Clinical Microbiology and Infectious Diseases at the University of the Witwatersrand, Johannesburg, South Africa. It has not been submitted before for any degree or examination at any other University.

Signature:

_____

Date:

____**05 June 2024**____

DEDICATION

This dissertation is dedicated to my loving and unbelievably supportive parents, Sarah Jane Piketh and Stuart John Piketh.

ABSTRACT

Multispecies infections and polymicrobial biofilms continue to increase in prevalence and clinical significance around the globe. These complex infections are challenging to treat, due to their increased expression of resistance and virulence factors, that meaningfully contribute to morbidity and mortality rates. *Candida auris* MRL 6057 and *Pseudomonas aeruginosa* ATCC 27853, have three distinct and clinically significant characteristics in common, they, i) cause nosocomial infections and outbreaks; ii) are multi-drug resistant and iii) can form biofilms. Additionally, defensin molecules have been identified as potent and broad-spectrum potential antimicrobials, in serious need of further evaluation. Therefore, the aim of this study was to determine the therapeutic efficacy of Defensin-like antimicrobial peptide-2 (DLAP-2) against the selected pathogens within mono- and polymicrobial biofilms. The broth microdilution method was used to determine the antimicrobial activity of DLAP-2. Furthermore, the effect of the compound on mono- and polymicrobial biofilms was determined at immature and mature stages of development. This was achieved using a metabolic activity assay and a microbial cell viability assay, following standard protocols. Both treated and untreated biofilms were visualised and validated using fluorescence microscopy. Additionally, the impact of DLAP-2 on membrane integrity of planktonic cell suspensions was evaluated using fluorescence microscopy. For the cytotoxicity assessment of DLAP-2, a haemolytic assay was performed. The results of this study suggest that DLAP-2 shows promising antimicrobial (with MIC and MBC/MFC values ranging from 62,5-250 µg/ml) and antibiofilm activity against polymicrobial biofilms (inhibition levels ranged from 20%-98%). The mode of antimicrobial activity for DLAP-2 was confirmed as cell membrane permeabilization. The haemolytic assay also showed that, at lower concentrations (125 µg/ml and 250 µg/ml), DLAP-2 shows low levels of toxicity (< 10%). However, at higher concentrations, a substantial increase in haemolytic activity was observed. From these results it can be concluded that DLAP-2 shows great promise as a broad-spectrum and multispecies infection, antimicrobial agent. Further development of this anti-infective for commercial use would make DLAP-2 one of the first drugs of its kind.

ACKNOWLEDGEMENTS

I would like to acknowledge the following individuals for their assistance in completing this dissertation:

Associate Professor Aijaz Ahmad and Doctor Vartika Srivastava, thank you for your support and guidance as my supervisors this year.

Mr Jacques Gerber and Dr Derran Reddy at the Unit for Microanalysis and Microscopy (MMU) at the University of the Witwatersrand, for their training and expertise concerning the operation of the fluorescence microscope and visualisation of my microscope slides.

Mr Justice Manyaga for his willingness to share his expertise and help on skills and techniques for performing laboratory related troubleshooting methods.

Professor Jonathan Levin for his patience and guidance in the completion of the biostatistical analysis portion of my project.

To all the staff at the Department of Clinical Microbiology and Infectious Diseases, especially the diagnostic laboratory technicians for your dedication and willingness to go out of your way to help those around you. A special mention to Sanelisiwe Thinasonke Duze, Karren Le Roux, and Professor Mrudula Patel for always answering my long list of questions and for openly and kindly offering guidance.

Finally, to Luyanda Mkhize a fellow master's student, for your moral support and friendship throughout the year.

Funding: This study was funded by the supervisor's National Health Laboratory Service Research Trust Grant (RA21-013).

TABLE OF CONTENT

LIST OF FIGURES

LIST OF TABLES

LIST OF EQUATIONS

LIST OF SCHEMES

LIST OF ACRONYMS, SYMBOLS AND ABBREVIATIONS

%	Percentage
> / <	More/ Less than
˚C	Degrees Celsius
±	Plus-minus
≤	Less than or equal to
α	Alpha
β	Beta
AIDS	Acquired immunodeficiency syndrome
AMB	Amphotericin B deoxycholate
AMR	Antimicrobial resistance
ANOVA	Analysis of variance
AST	Antimicrobial Susceptibility Testing
ATCC	American Type Culture Collection
C. albicans	*Candida albicans*
C. auris	*Candida auris*
CA	California
CDC	The Centers for Disease Control and Prevention
CFUs	Colony forming units
CFUs/ml	Colony forming units per milliliter
CLSI	Clinical and Laboratory Standards Institute
CLSM	Confocal laser scanning microscopy
Con A	Concanavalin A
COVID-19	Coronavirus Diseases of 2019
DCM	Dichloromethane
DIPEA	N, N-diisopropylethylamine
DLAP	Defensin like antimicrobial peptide
DMF	Dimethylformamide
DMSO	Dimethyl sulfoxide
DNA	Deoxyribonucleic acid
eDNA	Environmental DNA
ECM	Extracellular matrix
EPS	Extracellular polymeric substances
EP tubes	Eppendorf tubes®
EUCAST	European Committee on Antimicrobial Susceptibility Testing
FDA	Food and Drug Administration
FUN-1	FUN™ 1 Cell Stain
Gent	Gentamicin
HIV	Human immunodeficiency virus
H_2O	Water molecule
H_2O_2	Hydrogen peroxide
HPLC	High performance liquid chromatography
HβD-3	Human beta-defensin-3
ICU	Intensive Care Unit
IPC	Infection prevention and control
L	Litre
LC-MS	Liquid chromatography- mass spectrometry
MBC	Minimum bactericidal concentration

MFC	Minimum fungicidal concentration
mg	Microgram
MHB	Mueller Hinton Broth
MIC	Minimum inhibitory concentration
ml	Millilitre
MLR	Multiple linear regression
mm	Millimetre
MTT	3- [4,5 dimethylthiazol-2-yl]-2,5-diphenyl-tetrazolium-bromide
NA	Nutrient Agar
NaCl	Sodium chloride- (salt)
NC	Negative control
NHLS	National Health Laboratory Service
nm	Nanometers
OD	Optical density
OFM	Optical fluorescence microscopy
P. aeruginosa	*Pseudomonas aeruginosa*
PBS	Phosphate Buffer Saline
PC	Positive control
PI	Propidium Iodide
PPE	Personal protective equipment
RBC	Red blood cells
RNA	Ribonucleic acid
rpm	Revolutions per minute
SDA	Sabouraud Dextrose Agar
SDB	Sabouraud Dextrose Broth
SEM	Scanning electron microscopy
TFA	Trifluoroacetic acid
TSB	Tryptic Soy Broth
USA or U.S.	United States of America
UV	Ultraviolet
µg	Microgram
µg/ml	Micrograms per milliliter
µl	Microlitre

CHAPTER 1: INTRODUCTION AND LITERATURE REVIEW

Introduction

Humans are a standout species, for our remarkable intellect, the “weapon” with which we have been equipped to survive. This has led to the development and construction of extraordinary civilisations and innovative technology. An impressive aspect to this modernisation, is the establishment of healthcare systems. Additionally, extensive amounts of resources have been allocated to the development of invaluable medical equipment and treatments. Despite this remarkable progress, throughout history, both communicable and non-communicable diseases remain a burden to our population (Baylor College of Medicine, 2023). However, healthcare experts continue to investigate and expand on the current knowledge base, to improve the quality of care that can be offered to communities all around the world.

Two clinically significant, communicable pathogens are the focus of this investigation, namely, *Candida auris* (*C. auris*) and *Pseudomonas. aeruginosa* (*P. aeruginosa*). These microorganisms are known for their predilection for the development of biofilms and increased resistance to the most efficacious mainstream anti-infective agents. Furthermore, biofilms have become a research priority, as this virulence factor causes major challenges to the successful treatment of patients suffering from detrimental cases of infectious diseases (Shaffer, 2023). The ability of microorganisms to exist within biofilms that are made up of multiple species, otherwise known as polymicrobial biofilms, also plays a key role in the persistence of infections and the level of difficultly that is associated with their eradication from human hosts (Wolcott *et al.,* 2013). However, while a profuse database on these complex structures exists, little is known about the cohabitation of *C. auris* and *P. aeruginosa* within these polymicrobial biofilms.

Additionally, defensins are antimicrobial peptides that have been flagged as important potential therapeutic options because of their broad-spectrum activity against various microorganisms (Dhople *et al.,* 2006; Klüver, Adermann, and Schulz, 2006). For this reason, this study aims to contribute to the development of novel treatments for communicable and biofilm related diseases that cause high death rates. The hope is that the defensin peptide under investigation will illustrate potent killing activity against

the two microbial species of interest, a potential antimicrobial and antibiofilm treatment which would be one of the first of its kind.

1.1 Communicable diseases

Of the 1 trillion species of microorganisms on earth, infectious diseases are only caused by pathogenic strains of bacteria, fungi, parasites, and viruses (United States National Science Foundation, 2021). One-hundred million of these have been identified and characterised by humans, and a mere 1400 are thought to be capable of causing infections in humans (Microbiology by numbers, 2011). Globally, less than 1% of all microbial species are responsible for approximately 13.7 million human deaths annually (Gray and Sharara, 2022).

Communicable diseases also contribute more significantly to the burden of disease in low-income countries, with five of the top ten causes of death in these regions being attributed to infectious microorganisms. Such infections include lower respiratory tract infections, diarrheal diseases, malaria, tuberculosis, and human immunodeficiency virus (HIV) with acquired immunodeficiency syndrome (AIDS). The inverse is true in high-income/developed countries, with most deaths related to non-communicable disease such as heart disease, diabetes, and various types of cancer, to name a few (Baylor College of Medicine, 2023).

Treating infectious diseases presents innumerable challenges to healthcare workers as they are caused by pathogens which are highly diverse in their origins, modes of transmission, mechanisms for bringing about disease, clinical presentation as well as approaches for treatment (Baylor College of Medicine, 2023). The main source of infectious diseases is thought to be other animals (zoonotic diseases); however, insects, food, soil, and water have also been established as important reservoirs for contagions. Communicable diseases are spread through modes of transmission which include physical contact with contaminated objects, people or animals and their faeces or bodily fluids, inhalation of infectious aerosols in the atmosphere or droplets generated by infected respiratory tracts of other humans, sexual intercourse or ingestion of contaminated food and water sources (Baylor College of Medicine, 2023).

Throughout history, these diseases have overwhelmed the human population with outbreaks, epidemics, and pandemics. Examples of such occurrences include the bubonic plague pandemic (Black Death) of 1346, or the pandemic of 1918 (Spanish flu), both of which contributed significantly to global death rates. However, the Coronavirus Disease (COVID-19) and pandemic of 2019 demonstrated how even in the wealthiest parts of the modern world, these minute living creatures can wreak havoc, not only on our health, but also on international socio-economic events and stability (Baylor College of Medicine, 2023).

It is for this reason that understanding the pathogenicity of these diseases is of the utmost scientific and medical importance. For medical professionals to properly protect their communities, research and resources need to be dedicated to discovering not only efficacious cures, but also successful means of disease prevention.

1.2 Antimicrobial agents and preventative options

Long before antimicrobials were developed and made commercially available, healthcare practitioners would use a myriad of methods, elixirs, or natural remedies to treat infectious diseases. Two of the most well-known methods used in modern-day clinical settings for the prevention and cure of contagious pathogens are known to be vaccines and antimicrobial agents.

Arguably, vaccines are one of the greatest medical innovations for preventing disease. Vaccines are implemented before the onset of illness, to decrease the risk of disease-associated morbidity or mortality. They are a powerful tool which healthcare professionals use to protect the population from potentially deadly cases of infectious diseases (Centers for Disease Control and Prevention, 2021). For centuries, civilisations around the world have implemented experimental practices which involve intentionally exposing healthy individuals to infectious material in the hopes of preventing fatal cases of such diseases (World Health Organisation, 2024). In 1796 an English physician named Edward Jenner was the first to test this method of prevention using a scientific approach. It was this approach that allowed humans to completely eradicate the existence of a devastating virus known as smallpox (World Health Organization, 2024). Additionally, even in the most recent COVID-19

pandemic, vaccinations played a vital role in our ability to control and manage the spread of this once novel pathogen (World Health Organization, 2024). Unfortunately, development of safe and effective vaccines requires large amounts of time, money, and expertise. Furthermore, there are many drawbacks associated with these intervention methods and, currently, they are only available for the prevention of some bacterial and viral diseases. No vaccines for fungal and parasitic infections exist yet. This means that their usefulness is subject to major limitations in the global fight against the public health threat that is infectious disease.

A second major discovery in the field of medicine was that of antimicrobial agents which could treat infections caused by bacteria and fungi. In 1928, Alexander Fleming discovered penicillin, and thus began the age of antibiotics (Gaynes, 2017). For almost a century, humans have been using various classes of antimicrobial agents to treat bacterial infections. Subsequently, the development of nystatin in 1950 introduced another major drug class of antifungals for the treatment of superficial infections. A mere five years later, amphotericin B deoxycholate was found to be an effective antifungal capable of treating complex and invasive fungal infections (Nett and Andes, 2015).

These are just a few of the many methods, both past and present, which medical advancements have introduced for preventing and treating infectious diseases. The objective of the discussion is just to offer insight into a few of the more widely used options and highlight some of their shortcomings, not least of which is the limited availability, especially to developing or under-developed countries.

1.3 Antimicrobial resistance and the need for novel drug discovery

One of the greatest challenges facing the healthcare industry in the twenty-first century, regarding effective treatment of infections, is the development of antimicrobial resistance (AMR) (Fletcher, 2015). Pathogenic microorganisms are considered immaculate examples of rapid, modern-day evolution. When a microbial population is exposed to antimicrobial agents, the drug acts as an environmental pressure, replicating that of natural selection (Fletcher, 2015). This means that cells capable of

resisting or persisting through the inhibitory or killing effects of a drug are the ones that survive (Fletcher, 2015). From here, it is the resistant cells that go on to replicate and replace the previously susceptible population of cells with a new and resistant one. Additionally, over time, a lack of access to clean water and sanitation, inadequate infection prevention and control (IPC) strategies, poor clinical practices, along with a lack of adherence to antimicrobial stewardship strategies, has led to an increase in the spread of resistant strains of infection. Resistance has been identified in bacterial, fungal, and even viral microorganisms (Fletcher, 2015), and have been observed in microbes against -static (inhibits growth of cells) and -cidal (kills cells) antimicrobial agents (Fletcher, 2015).

AMR comes about through genetically coded attributes in the nucleic acid of microorganisms and resistance can be intrinsic or acquired (Fletcher, 2015). Intrinsic resistance is due to natural or inborn (innate) genes whereas acquired resistance develops throughout the lifespan of a microbial cell. Acquired resistance can be achieved through mutations that alter antimicrobial drug target sites on the cell itself. A second mechanism for bringing about acquired resistance is through the horizontal transfer of novel genes from a microbial cell that already possess or exhibits resistance to specific classes of antimicrobial agents. This transfer of resistance factors can even occur on an interspecies basis (Fletcher, 2015).

These resistance mechanisms develop and result in previously effective antimicrobial agents causing treatment failure in patients who have become infected with resistant strains (Fletcher, 2015). As a result of this, it is imperative for the medical community to research and discover alternative means of treatment whilst also performing routine monitoring of the development of resistance patterns in existing microorganism-antimicrobial relationships (Fletcher, 2015). There are several well-established methods for achieving both objectives, and these are collectively known as antimicrobial susceptibility testing (AST). The Clinical and Laboratory Standards Institute (CLSI) as well as the European Committee on Antimicrobial Susceptibility Testing (EUCAST) are examples of recognised organisations that provide annually updated guidelines on treatment options and breakpoints for detecting resistance in laboratory settings. The importance of these organisations and their outputs cannot be understated, as they work to keep healthcare professionals up to date with the most

effective treatments. Because *C. auris* and *P. aeruginosa* are the organisms that were selected for this study, further details will be centred around fungal and bacterial forms of infectious diseases.

1.4 Candida auris

1.4.1 Epidemiology

C. auris was initially detected in a Japanese healthcare facility in the year 2009. The novel microorganism was isolated from a female patient's ear canal sample (Horton and Nett, 2020; Jeffery-Smith *et al*., 2018). This emerging pathogen is hypothesized to have evolved due to global warming and, through genetic analysis, research shows that *C. auris* has emerged concurrently in multiple global regions (Du *et al.,* 2020) More than a decade later, it has been isolated in clinical settings in over forty countries, across six different continents. *C. auris* isolates were originally grouped by whole genome sequencing analyses, into four distinct clades which each demonstrate unique characteristics. These clades have been categorized based on the geographical locations from which the strains were isolated. Namely, Clade I- South Asian, Clade II- East Asian, Clade III- South African, and Clade IV- South American (Narayanan *et al.,* 2022). Recently, a novel clade has been isolated in Iran and is called Clade V (Du *et al.,* 2020).

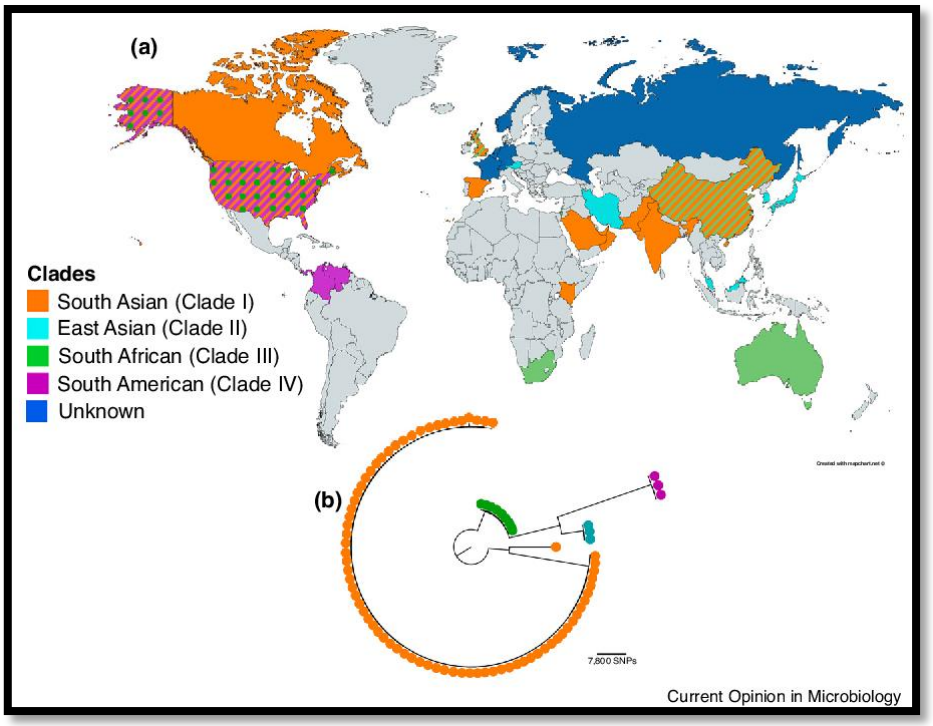

Figure 1.1. **(a)** Globally distributed clades of *C. auris.* **(b)** Phylogenetic tree (circle tree) showing the relationships amongst the geographically unique *C. auris* clades. The phylogeny was determined using the Randomized Accelerated Maximum Likelihood program (Rhodes and Fisher, 2019).

1.4.2 Microbiological characteristics

This eukaryotic organism has a defined nucleus with supplementary intracellular components that are bound by an outer membrane (Gleichmann, 2021). *C. auris* belongs to the Kingdom Fungi, and by extension, to the largest fungal phylum known as *Ascomycota*. *C. auris* is a haploid species of fungal yeast that, unlike its close relative *Candida albicans* (*C. albicans*), was thought to be incapable of undergoing a morphological transition from yeast to filamentous forms of growth. However, this theory has since been proven wrong and whilst this occurrence is still extremely rare in *C. auris*, it has been observed under very selective growth conditions (Du *et al.,* 2020).

This microorganism can be grown on Sabouraud Dextrose Agar (SDA), at its optimal growth temperature of 37 ºC. Colonies have a pink/beige, smooth, and shiny appearance when grown on solid media (Jeffery-Smith *et al*., 2018). Under favourable

growth conditions, the microorganism has an oval morphology with cells that are approximately 2.5-5 µm in size with no hyphae structures (Jeffery-Smith *et al*., 2018). However, when exposed to less favourable culture conditions, its morphology becomes less consistent, with an elongated circular/ovoid cell shape and the development of pseudo-hyphae. When the Gram-stain technique is used, these cells show Gram-positive staining with a blue/purple colour (Jeffery-Smith *et al*., 2018) as can be seen in Figure 1.2.

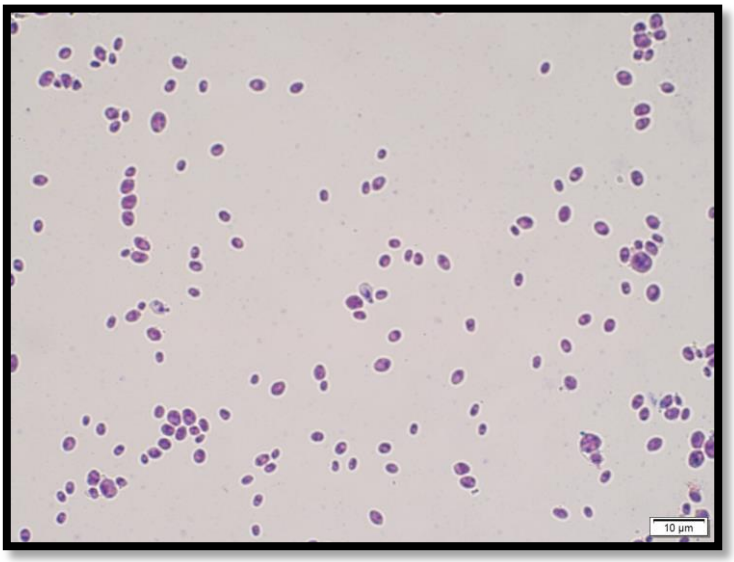

Figure 1.2. *C. auris* MRL 6057 planktonic cells were Gram-stained and visualised using an Olympus BX 63 OFM microscope. A 100X oil immersion objective lens was used (Scale bar: 10 µm).

This species of *Candida* shares a close relation with *Candida haemulonii* and *Candida lusitaniae,* with a more removed genetic relation to the most clinically prevalent, diploid *C. albicans*. A common challenge associated with this pathogen is that it is often misidentified when using routine laboratory techniques (Du *et al.,* 2020). However, two key characteristics set *C. auris* apart and contribute to its ability to persist in harsh environments even outside of its host. Firstly, its thermotolerance, which means it can grow at temperatures of up to 42 ºC and, secondly, its osmotolerance (Du *et al.,* 2020). Osmotolerance allows this yeast to alter its morphology in response to stressful environmental conditions. Furthermore, when grown in undesirable levels of salt (NaCl), *C. auris* presents with pseudo-hyphal like formations (Du *et al.,* 2020).

1.4.3 Clinical characteristics

C. auris is capable of high levels of host colonization and has superior survival skills. This well-established ability to persist on living tissue and even on abiotic surfaces outside of its host—for weeks—means that *C. auris* is a notable causative agent of nosocomial infection[1]. Notably, *Candida* species are the number one fungal cause and the number four overall cause of nosocomial infections (Du *et al.,* 2020).

Transmission occurs through direct contact with contaminated surfaces and medical equipment or internal medical devices, or through physical contact with an infected individual, even if they are asymptomatic (Horton and Nett, 2020). This means that when IPC strategies are not adhered to, *C. auris*, along with other opportunistic infections, are able to run rampant in medical facilities, causing burdensome outbreaks. Such IPC intervention practices include regular disinfection of equipment, washing of hands by healthcare workers in-between each patient visit or donning of personal protective equipment (PPE), just to name a few. Worse still is the resistance patterns to commonly used disinfectants that have been observed in certain strains of this pathogen, which act as driving factors for the development of outbreaks (Du *et al.,* 2020).

Whilst there is a very low risk of infection with *C. auris* in healthy individuals, hospitals are a primary site for transmission and infection as they are filled with an immunocompromised population (Du *et al.,* 2020). Those who are critically ill and who occupy ICUs face the most significant threat of infection (Du *et al.,* 2020). A few of the risk factors and comorbidities associated with these infections include old age, diabetes mellitus, open surgery, invasive medical devices such as catheters, patients undergoing haemodialysis, and use of broad-spectrum antimicrobials for extended periods of time (Du *et al.,* 2020). Consequently, patients afflicted with risk factors for infection need to be more carefully managed. For example, invasive medical devices are a dangerous source of severe infection and, therefore, these sites need to be meticulously cared for. When patients begin to recover, regular assessments for their removal, need to be prioritised. Moreover, in cases of open surgical procedures, if a

[1] Infections acquired by a patient during their stay in a healthcare facility, also known as healthcare-associated infections. (Sikora and Zahra, 2023).

patient has been found to be colonized with this microorganism, additional precautions for disinfection of surgical sites needs to take precedence.

Fortunately, despite the myriad of risk factors, *C. auris* mainly colonizes hosts and causes mild/superficial infections of the skin which are easily managed and can be treated with topical antifungal agents (Du *et al.,* 2020). In more serious instances, however, this pathogen has been isolated from the bladder, the liver or gallbladder, parts of the upper respiratory system such as the ears and nostrils, the axilla or even the rectum (Du *et al.,* 2020). The most severe and alarming cases of infection are septicaemia (infection of the blood) which in some cases can lead to life-threatening sepsis. Around the world, *Candida* species are reportedly identified as the aetiology of roughly 400,000 incidents of septicaemia, every year (Du *et al.,* 2020). Unfortunately, the mortality rate associated with invasive infections in the immunocompromised population has been reported as a staggering 30-60% (Horton and Nett, 2020). It is important to note that this pathogen is incapable of surviving in the oxygen deficient human digestive system, as opposed to its more virulent counterpart, *C. albicans* (Du *et al.,* 2020).

Infection with this pathogen can lead to the onset of symptoms such as fever and chills or hypothermia, pain, severe fatigue, hypotension, and tachycardia (Cleveland Clinic, 2023). Successful treatment of *C. auris* infections can be considerably more challenging when accounting for its multi-drug resistant profile (Du *et al.,* 2020). Furthermore, this AMR may be exacerbated by the ability of *C. auris* to form complex and protective biofilm structures (Horton and Nett, 2020).

1.4.4 Mechanisms of antimicrobial resistance and approaches to treatment

Due to *C. auris* having "superbug" status[2], there are a limited number of antifungals that can treat more critical cases of these infections. Many strains of *C. auris* that cause clinical infections demonstrate resistance patterns to two mainstream antifungals, namely amphotericin B and fluconazole (Centers for Disease Control and Prevention, 2022). Moreover, there are currently no available formalised clinical breakpoints against any antifungal agents that have been recorded for *C. auris*, or any other *Candida* species for that matter (Jeffery-Smith *et al*., 2018). This serves as an additional challenge for healthcare practitioners who have been tasked with treating candidiasis. However, despite this, the Centers for Disease Control and Prevention (CDC) has recommended the first-line class of drugs for treatment—in adults, children, and neonates—to be echinocandins. This is because most clinical isolates remain susceptible to their antimicrobial activity. Although this class is made up of anidulafungin, caspofungin and micafungin, anidulafungin has not been approved for treatment in children and neonates (Centers for Disease Control and Prevention, 2022). Even though a lower proportion of clinical isolates are resistant to echinocandins, the development of resistance in this species of *Candida* is rapid.

Table 1.1 summarises the antifungal agents commonly used to treat these infections, as well as describes mechanisms by which this microorganism (*C. auris*) become resistant to their antimicrobial effects. Understanding resistance mechanisms to our most valuable clinical treatments is imperative for the development of novel and efficacious drugs.

[2] Microorganisms that are resistant to most of the antimicrobials that are usually prescribed to treat the diseases which they cause (Du *et al.,* 2020)

Table 1.1. Classes and antifungal drugs most used to treat clinical infections of *C. auris* and their mechanisms of action, their drawbacks, as well as mechanisms that bring about resistance to their antimicrobial activity (Ghannoum and Rice, 1999; Houšť, Spížek, and Havlíček, 2020).

Antifungal drug classes and drugs	Drug mechanism of action	Resistance mechanisms	Drawbacks
Polyenes • Nystatin (topical treatment for superficial infections) • Amphotericin B This class of antifungals shows broad-spectrum activity and is often used to treat invasive fungal infections (Ghannoum and Rice, 1999).	Removes ergosterol from fungal cell membranes. Ergosterol plays an influential role in maintaining plasma membrane integrity (Ghannoum and Rice, 1999).	Mutations occur in the genes of pathogens. Alterations target genetic components involved in the modulation of ergosterol biosynthesis. This leads to changes in the cell membrane ergosterol composition. These changes make polyenes, less effective (Houšť, Spížek, and Havlíček, 2020).	High levels of toxicity for mammalian cells (specifically causes nephrotoxicity) (Ghannoum and Rice, 1999).
Azoles 1. ***Imidazole*** 2. ***Triazole*** • Fluconazole • Itraconazole • Posaconazole • Voriconazole • Isavuconazole	Works by preventing ergosterol biosynthesis. Ergosterol forms a fundamental part of fungal plasma membranes and controls permeability and fluidity (Ghannoum and Rice, 1999).	Azole resistance mechanisms differ widely from one species of fungi to another and a few non-albicans species demonstrate intrinsic resistance to azoles. Resistant strains modify the amount and constituents of target enzymes and can also decrease access to the antimicrobial target (Ghannoum and Rice, 1999). They can also overexpress target biosynthesis which contributes to insufficient concentrations of antifungal drugs.	Due to azoles being fungistatic in nature, they actively select for and promote survival of resistant strains. Resistance mechanisms also cause cross-resistance to multiple drugs within this class (e.g. fluconazole and itraconazole). This makes effectively treating infections even more challenging. (Ghannoum and Rice, 1999).

Antifungal drug classes and drugs	Drug mechanism of action	Resistance mechanisms	Drawbacks
<u>Echinocandins</u> • Caspofungin • Micafungin • Anidulafungin Most widely used in invasive candidiasis, especially in seriously ill and neutropenic patients. This class of drug provides an important treatment alternative in resistant strains of *Candida* (Ghannoum and Rice, 1999).	These drugs work as non-competitive inhibitors of an integral enzyme known as 1,3-β-glucan synthase. This enzyme is involved in cell wall synthesis. Drug activity, therefore, causes strain and compromises cell wall integrity (Ghannoum and Rice, 1999).	The most significant means of resistance development encompasses amino acid changes. These changes are due to mutations in 1,3-β-glucan synthase associated genes, which decreases fungal cell enzyme sensitivity to the antifungal drugs (Ghannoum and Rice, 1999; Houšť, Spížek, and Havlíček, 2020).	These drugs are completely ineffective at treating *Cryptococcus* infections, as this pathogen remains inherently resistant to this class of drug (Ghannoum and Rice, 1999).

Consequently, to prevent the development of pan-resistance (resistance to all drug classes), healthcare professionals are required to closely monitor patients, order multiple and regular follow-up AST panels as well as treat pan-resistant or recurring infections with liposomal forms of amphotericin B or combination therapies (Centers for Disease Control and Prevention, 2022).

Figure 1.3 below shows the distribution of endemic and multidrug resistant strains of *C. auris*. Reports indicate that North America, parts of Canada, South America, the Middle East, and India are more detrimentally afflicted with cases of resistant *C. auris*. Interestingly, even South Africa has been flagged as an area of major concern in this regard.

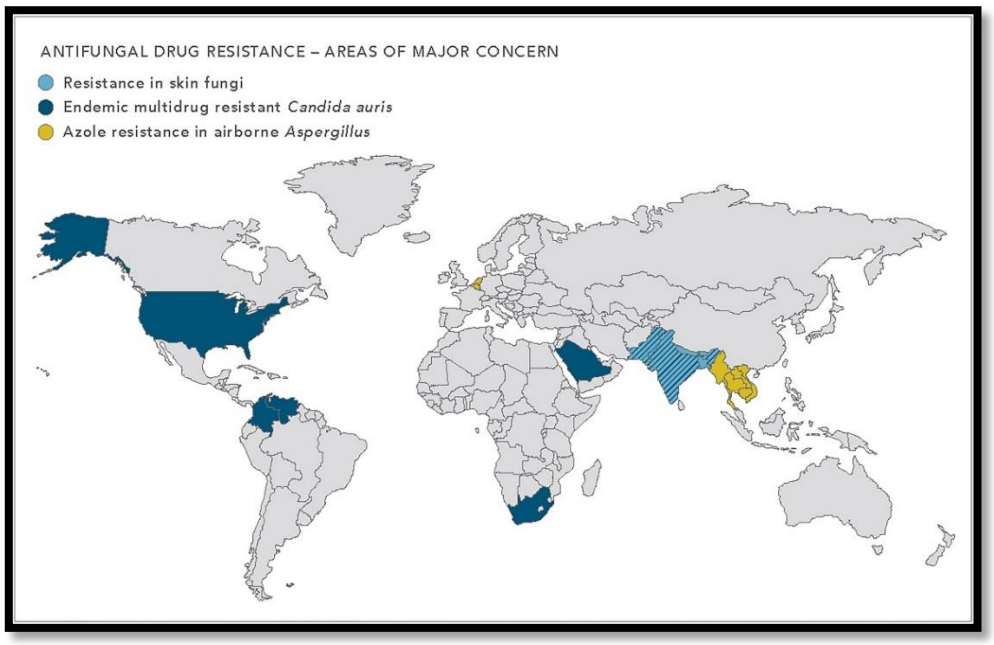

Figure 1.3. A world map summarising the distribution of antifungal drug resistance and areas of major concern (McDermott, 2022).

If *C. auris* causes non-invasive infection at anatomical sites like the skin, the bladder or even the upper respiratory tract, it is recommended that no antimicrobials be prescribed if patients present as asymptomatic (Centers for Disease Control and Prevention, 2022). However, implementing IPC measures is imperative even in cases with no signs of disease, because as described above, this pathogen can still be spread under these conditions, especially within hospital settings (Centers for Disease Control and Prevention, 2022).

1.5 Pseudomonas aeruginosa

1.5.1 Epidemiology

P. aeruginosa is a ubiquitous bacterium (Fourie and Pohl, 2019) that makes up one of the six ESKAPE pathogens[3], highly virulent microorganisms which have been flagged for their clinically significant contributions to morbidity and mortality rates, as well as their predilection for developing resistance to antibiotics. Detailed data on the global distribution of varying *P. aeruginosa* strains is scarce, however, records of clinical isolates have been reported on major continents such as North and South America, Australia, Africa, Asia, and Europe, in a myriad of countries (Reynolds and Kollef, 2021). Moreover, the distribution of resistant strains of this pathogen will be discussed later.

A substantial point-prevalence study based on international observations showed that *P. aeruginosa* accounted for 16,2% of all ICU infections and 23% of ICU-associated nosocomial infections (Reynolds and Kollef, 2021). These statistics put into perspective the reality of the public health threat and burden that this contagion poses to healthcare systems around the world. Additionally, significant diversity exists across the different strains of this pathogen, especially in those that are found in varying geographical locations. These genomic variations lead to an array of expressed phenotypic characteristics, meaning that approaches to the treatment for each individual case of infection can be quite unique. This poses a challenge for healthcare workers when attempting to diagnose and effectively treat the diseases which *P. aeruginosa* can cause.

1.5.2 Microbiological characteristics

P. aeruginosa is considered a more primitive prokaryotic organism, which lacks a nucleus and other organelles that are well defined by associated membranes (Gleichmann, 2021). This microorganism belongs to the Monera Kingdom, and more specifically, the phylum Proteobacteria. It is rod-shaped, with dimensions of 1–5 µm long and 0.5–1.0 µm in wide (Bassetti *et al.,* 2018; Diggle and Whiteley, 2020). In

[3] *Enterococcus faecium*, *Staphylococcus aureus*, *Klebsiella pneumoniae*, *Acinetobacter baumannii*, *Pseudomonas aeruginosa* and *Enterobacter* spp. (Wang, 2021).

addition, it is a Gram-negative (Gram-stain red/pink as seen in Figure 1.4 below), aerobic-facultatively-anaerobic, and non-spore forming bacterium. Attachment, surface adhesion and motility of this microbe are achieved by means of a membrane-bound, polar flagellum and bacterial surface pili which contribute to its virulence and facilitate the cells' ability to swim and twitch. Cellular motility remains advantageous for several reasons: cells are better suited for acquiring nutrients, evading lethal substances, and for effective navigation to more favourable sites within a host (Diggle and Whiteley, 2020).

When cultured, this microorganism can optimally multiply at temperatures of 37 °C, although it is also known for its thermotolerance at temperatures as high as 42 °C. When grown on solid media such as agar, it appears in colonies with a glassy blue-green colour, a hue known to be caused by the production of the pigment pyocyanin—synthesized with powerful antimicrobial properties—which plays a central role in facilitating intra- and inter-species communication for *Pseudomonas* (Diggle and Whiteley, 2020).

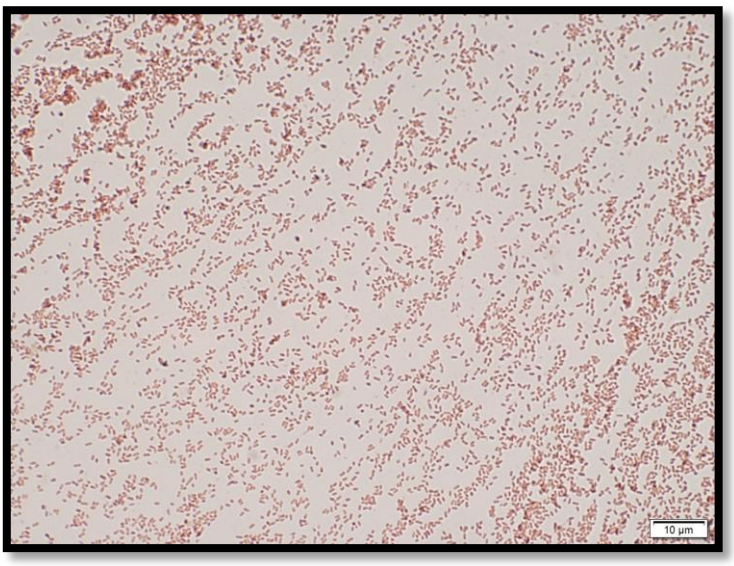

Figure 1.4. *P. aeruginosa* ATCC 27853 planktonic cells were Gram-stained and visualised using an Olympus BX 63 OFM microscope. A 100X oil immersion objective lens was used (Scale bar: 10 µm).

1.5.3 Clinical characteristics

P. aeruginosa exists sparsely in natural sources such as soil and water but is predominantly known to colonize human and animal associated environments (Diggle

and Whiteley, 2020). This pathogen is considered an opportunistic and nosocomial infection, which in close quarters and poorly ventilated spaces is also known to be spread from person to person (Cleveland Clinic, 2023), which leads to difficult to manage outbreaks. Like *C. auris*, *P. aeruginosa* rarely causes disease in healthy members of the population, with most infections occurring in individuals with weakened immune systems (Cheong et al.,2008). *P. aeruginosa* has also established itself as the most burdensome bacteria (Bassetti *et al.,* 2018), as invasive cases involving the immunocompromised have a reported mortality rate of 18-61% (Zhang *et al.,* 2022). Additionally, there are several characteristics which make this pathogen clinically significant, viz., its infectiousness, its high levels of existing and its rapid development of new resistance to antimicrobials, as well as its ability to persist in environments for extended periods, which may stem from its increased thermotolerance (it can grow at temperatures of up to 42 ºC) (Diggle and Whiteley, 2020). The mode of transmission of this microbe is contact with contaminated objects, medical equipment and invasive devices which have not been properly sterilized, as well as direct contact with skin (Cleveland Clinic, 2023). Additionally, exposure to infected water, food, and soil can also lead to the onset of associated diseases (Cleveland Clinic, 2023).

Infections occur at diverse sites within the human body and can cause diseases such as bacteraemia, ventilator or community associated pneumonia, infection of the tissues, ears, gastrointestinal and urinary tract, just to name a few (Bassetti *et al.,* 2018). Examples of clinical symptoms can include pain in the infected area, inflammation, pyrexia, nausea, vomiting, headaches, and diarrhoea (Cleveland Clinic, 2023). Risk factors for the onset of such infections include invasive medical devices, compromised immunity (e.g. HIV), recent (within the last 90 days) use of broad-spectrum antibiotics, as well as extended periods of hospitalization—especially if this has included time in the ICU (Bassetti *et al.,* 2018). There are multiple comorbidities associated with more severe and even fatal cases of *Pseudomonas,* including, being elderly, suffering from hypertension, diabetes mellitus, renal or liver disease which requires haemodialysis, tumours, those who have undergone an organ transplant, structural lung issues like cystic fibrosis or chronic obstructive pulmonary disease, and finally, trauma to any bodily tissues (Bassetti *et al.,* 2018). Moreover, moisture and warmth are significant preferences of this pathogen and as a result, infections of the

skin and soft tissue pose a substantial challenge to treatment when contaminated with *Pseudomonas*. Two clinical syndromes remain at the forefront of such infections, (1) ecthyma gangrenosum, and (2) trauma from deep tissue burns (Bassetti *et al.,* 2018), where burn victims are faced with staggering risks of morbidity and mortality when afflicted with multi-drug resistant strains of *P. aeruginosa*. Additionally, as a model bacterium used for the investigation of virulence factors such as the secretion of toxins, quorum sensing and most notably, biofilm formation (Reynolds and Kollef, 2021), these characteristics make treating such infections difficult and thus significantly increases the risk of mortality (Cheong *et al.,*2008).

1.5.4 Mechanisms of antimicrobial resistance and approaches to treatment

P. aeruginosa is notorious for its often-extensive resistance profile as there are strains of this pathogen known to be resistant to all major classes of antibiotics (Bassetti *et al.,* 2018). Consequently, routine AST panels can classify clinical isolates into one of three categories: (1) multi-drug resistant organisms which are resistant to one or more antimicrobials in three or more antibiotic classes, (2) extensively drug-resistant strains which are resistant to one agent or more in all categories except for two or less; and (3), pan-drug resistance which occurs when the strain is not susceptible to any antimicrobial agents (Bassetti *et al.,* 2018).

The primary mechanisms of resistance include, altering drug target sites, producing enzymes that can dismantle antimicrobial compounds or decreasing antibiotic access to target sites (Bassetti *et al.,* 2018). The main challenge with *P. aeruginosa* is that it possesses both intrinsic resistance (natural or inborn traits encoded within its genetic material) and acquired resistance traits (obtained through genetic mutation or the intra-/interspecies horizontal transfer of portable resistance genes) (Bassetti *et al.,* 2018). Table 1.2 summarises important characteristics associated with the antibiotic classes and drugs that are routinely used to treat *Pseudomonas* infections.

Table 1.2. The most effective and widely used antipseudomonal drugs, their mechanisms of antimicrobial action, drawbacks as well as the mechanisms by which *P. aeruginosa* develops resistance to them (Bassetti *et al.,* 2018; Healthline Medical Network, 2023).

Antibiotic class and drugs	Drug mechanism of action	Bacterial resistance mechanisms to drugs	Drawbacks of drugs
β-lactams	Bactericidal agents that work to prevent cell wall synthesis.	**<u>Intrinsic resistance traits</u>** (Bassetti *et al.,* 2018) • Naturally has low levels of outer cell membrane permeability meaning drugs cannot penetrate the cell and take effect. • Hyperexpression of genes associated with transport proteins such as efflux pumps, means that drugs are pumped out of the cell and cannot take effect. • Producing enzymes capable of antibiotic-inactivation (cephalosporinases), specifically of the cephalosporin drug class. **<u>Acquired resistance traits</u>** (Bassetti *et al.,* 2018) • Chromosomal mutations that bring about resistance are selected for and expressed. • Horizontal transfer of broad-spectrum resistance associated genes on an intra- or interspecies basis.	• Fever • Stevens-Johnson syndrome • Blood conditions such as leukopenia and thrombocytopenia (Healthline Medical Network, 2023).
<u>Penicillin</u> • Piperacillin • Ticarcillin • Tazobactam • Clavulanate	Inhibition of cross-linking activity and direct prevention of bacterial cell walls from forming (Bassetti *et al.,* 2018).		Negative gastrointestinal side effects like diarrhoea, nausea, and vomiting (Healthline Medical Network, 2023).
<u>Cephalosporin</u> • Ceftazidime • Cefepime • Cefoperazone • Ceftolozane	Interfering with cell wall enzymes (Bassetti *et al.,* 2018).		• Negative gastrointestinal side effects like diarrhoea, nausea, and vomiting • Seizures (Healthline Medical Network, 2023).
<u>Carbapenems</u> • Imipenem • Meropenem • Doripenem Last-line drug for highly resistant strains of infection.	Inhibition of bacterial cell wall synthesis (Bassetti *et al.,* 2018).		• Available treatment alternatives for carbapenem-resistant strains of P. aeruginosa are challenging and limited. This is due to the diverse mechanisms of resistance that these strains usually pose.

Antibiotic class and drugs	Drug mechanism of action	Bacterial resistance mechanisms to drugs	Drawbacks of drugs
		• Production of diverse and unique enzymes that are capable of breaking open β-lactam rings (β-lactamases), which render drugs ineffective. • Production of enzymes which make aminoglycosides ineffective. • Transport proteins known as efflux pumps are used to pump antibiotics out of the cell. • Porins are outer membrane proteins which when decreased in number, allow cells to decrease membrane permeability, meaning drugs cannot enter the cell and take effect. • Modification of drug target sites.	• Seizures (Healthline Medical Network, 2023).
<u>Monobactams</u> • Aztreonam	Running interference with the biosynthesis of peptidoglycan, along with cell division (Bassetti *et al.,* 2018).		
<u>non-β-lactam, β-lactamase inhibitor</u> • Avibactam			
<u>β-lactamase inhibitor</u> • Tazobactam			
<u>Aminoglycosides</u> • Gentamicin • Tobramycin • Amikacin (less afflicted by antibiotic inactivation enzymes)	Inhibition of protein synthesis (Bassetti *et al.,* 2018).		• Ototoxicity • Nephrotoxicity (at higher concentrations). • Neuromuscular blockade (Healthline Medical Network, 2023). Additionally, these drugs do not penetrate lung tissue well, and are therefore not suitable for treatment of pneumonia (Bassetti *et al.,* 2018).
<u>Fluoroquinolones</u> • Ciprofloxacin • Levofloxacin	Prevents DNA from replicating and inhibits the synthesis		• Causes severe side effects in patients at risk of heart valve issues.

Antibiotic class and drugs	Drug mechanism of action	Bacterial resistance mechanisms to drugs	Drawbacks of drugs
	and division of cells (Bassetti *et al.,* 2018).		• Seizures • Tendonitis • Negative gastrointestinal side effects • Dizziness, insomnia, and headaches (Healthline Medical Network, 2023). Additionally, these drugs exhibit high levels of resistance in certain parts of the world (e.g. Europe) (Bassetti *et al.,* 2018).
<u>Polymyxin E</u> • Colistin (last resort drug)	Acts by disrupting the outer cell membrane and causes intracellular components to leak out of the cell (Bassetti *et al.,* 2018).		• Nephrotoxicity Neurotoxicity. • Dizziness • Numbness, tingling, prickling, burning sensation, especially in the extremities and tongue (Healthline Medical Network, 2023).
<u>Phosphonic</u> • Fosfomycin	Inhibits bacterial cell wall synthesis (Bassetti *et al.,* 2018).		

A study published in 2023 investigated how host colonization with multiple strains of *P. aeruginosa* impacted the development of AMR (Diaz Caballero *et al.,* 2023). In it, *P. aeruginosa* was used as a model microorganism because of its known ability to co-exist with a myriad of strains within a single host (Diaz Caballero *et al.,* 2023). The most significant findings were that resistance patterns emerged more expeditiously in patients who were colonized with various strains of *P. aeruginosa*. The cause of this phenomenon was thought to be the increased diversity of novel resistance alleles within the microorganism population. The selection and expression of these genetic traits was therefore associated with resistance to an increased number of antibiotics, and ultimately resulted in treatment failure and poor patient outcomes (Diaz Caballero *et al.,* 2023). Superinfection with multiple strains of this pathogen has therefore been identified as a main factor in the exponential development of AMR in *P. aeruginosa* infections (Diaz Caballero *et al.,* 2023).

The survival and recovery of patients with *P. aeruginosa* infections is directly linked to several factors, including but not limited to, early diagnosis and detection of the causative agent and source of infection. The second factor is the swift start of appropriate antimicrobial therapy, this involves performing continuous AST assays to ensure that the chosen treatment regimen adequately eradicates the infectious pathogen. Additionally, drug resistant strains are usually treated with a combination or “cocktail” of antibiotics, which is unique to the type of infection. Lastly, the effective management and control of underlying risk factors and comorbidities is essential for reducing the threat of worsened patient outcomes.

When dealing with pan-drug resistant *P. aeruginosa*, two last-line antibiotic drug classes exist, namely, carbapenems and polymyxins. Strains that can only be treated with these anti-infectives are considered to have significantly dangerous resistant profiles. Figure 1.5 below, shows reported levels of resistance to one of these last-line drugs (carbapenems) across the globe. We can see that resistance levels are most worrying in places such as Russia, numerous parts of South America, Mexico, Korea, parts of Southeast Asia, the Ukraine and South Africa. These regions have reported resistance levels that exceed 25% from their collected isolates.

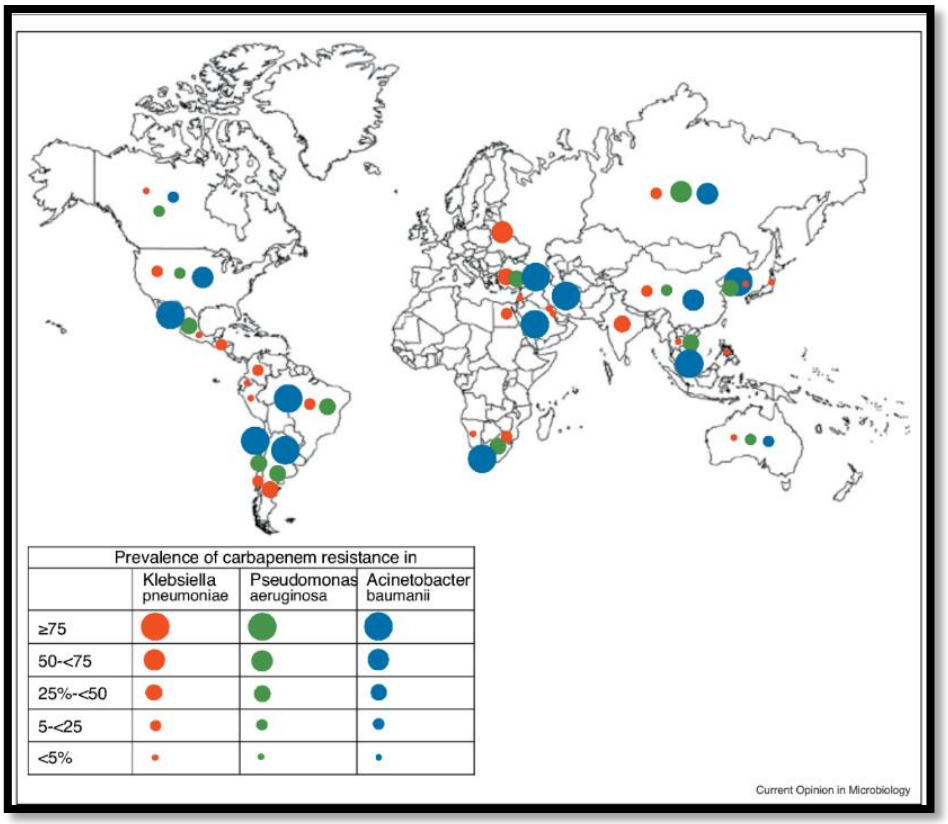

Figure 1.5. A world map that indicates the distribution of carbapenem resistance in three major ESKAPE pathogens (including *P. aeruginosa*) (Theuretzbacher, 2017).

To put these resistance patterns into a local perspective, a graph summarising the reported levels of resistance to numerous drug classes in South Africa, from 2011-2016, has also been included in this review of the literature (Figure 1.6).

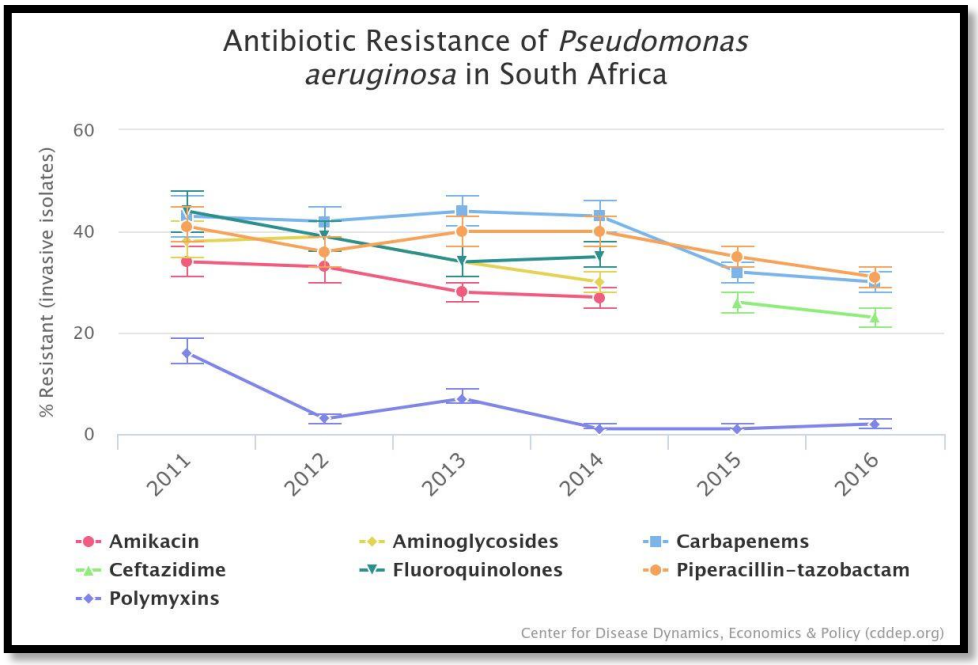

Figure 1.6. Antibiotic resistance levels (percentage resistance to antibiotics in isolated cultures of invasive infection) in *P. aeruginosa,* in South Africa (OneHealthTrust, 2024).

Overall, the graph shows a decreasing trend in the development of resistance over the six-year period. This may be due to efforts to adhere to antimicrobial stewardship practices more strictly. Furthermore, in 2016, the reported levels of resistance to each antibiotic class were as follows: for carbapenems, ±30%; for ceftazidime (cephalosporin), ±23%, for the widely used antibiotic "cocktail" piperacillin-tazobactam, ±31%, and finally, resistance to polymyxins (such as the last-resort antibiotic, colistin), ±2%. However, considering the approximate eight years between 2016 and 2024, these patterns may have significantly changed. This graph also corresponds with the levels of carbapenem resistance that was reported in South Africa for *P. aeruginosa* (25% - < 50%) as shown in Figure 1.5. Whilst these statistics may not seem significantly high, they are of great concern to healthcare workers and the medical community as increasing levels of resistance directly translate to limited treatment options and, by extension, a higher number of AMR associated deaths.

1.6 Biofilms

Biofilms are complex, surface dependent structures composed of sessile microorganism cells and an extracellular matrix (O'Toole *et al.,* 2000). These structures form on biotic and abiotic surfaces and are abundant in natural, industrial and hospital environments. Within clinical settings, these surfaces include various types of human tissue, implanted medical devices like urinary or central venous catheters, prosthetic heart valves or pacemakers and medical equipment, such as ventilators (O'Toole et al., 2000). Rigorous and effective sterilisation of such equipment is complicated. Therefore, when persistent structures are not successfully removed, complicated infections continue to spread to other patients who come into contact with these pieces of equipment.

Biofilms offer microorganisms protective factors like increased resistance to antimicrobial agents, protection from mechanical damage, inhibition of host defence mechanisms and increased survival capabilities in unfavourable environmental conditions (Wolcott *et al.,* 2013)**.** Such protective factors can lead to treatment failure in infected patients and significantly increases the risk of morbidity and mortality rates (Shaffer, 2023).

When biofilms are isolated from natural or healthcare associated environments, they are most likely to consist of multiple types of microorganisms, these are called polymicrobial biofilms (Wolcott *et al.,* 2013). It has been established that these polymicrobial cell suspensions and biofilms exhibit superior tendencies for antimicrobial resistance (Orazi and O'Toole, 2019). Furthermore, mature biofilms that have reached the stationary phase in cell growth are also more prone to showing higher levels of antimicrobial tolerance (Sharma, Misba and Khan, 2019). Antimicrobial agents that have antibiofilm properties and antimicrobial activity against fungi and bacteria are extremely rare. Discrepancies in antimicrobial cell targets and mechanisms that cause resistance in fungi and bacteria are further causes of treatment associated challenges (Ghannoum and Rice, 1999). For this reason, this study aims to assess the antimicrobial and antibiofilm capabilities of an untested compound in the hopes that it will display fungicidal, bactericidal, and antibiofilm properties for potential therapeutic use against polymicrobial biofilms.

Fungal and Bacterial Cohabitation

There are a multitude of examples of interactions between prokaryotic and eukaryotic organisms in nature (Fourie and Pohl, 2019). Some of the most notable and non-pathogenic interactions occur within the gastrointestinal tract and on the skin of the human body. The plethora of microorganisms that can be isolated from these sites make up the human microbiome and are essential for survival (Fourie and Pohl, 2019). However, the interactions described in this study are more focused on those that are harmful to human health. More specifically, the interactions between two pathogens of great clinical significance, each of which belong to unique biological kingdoms. *C. auris* belongs to the Kingdom Fungi (eukaryotic) *and P. aeruginosa* to the Kingdom Monera (prokaryotic) (Gleichmann, 2021). Figure 1.7 is a micrograph of a mixed cell suspension which includes the two pathogens of interest.

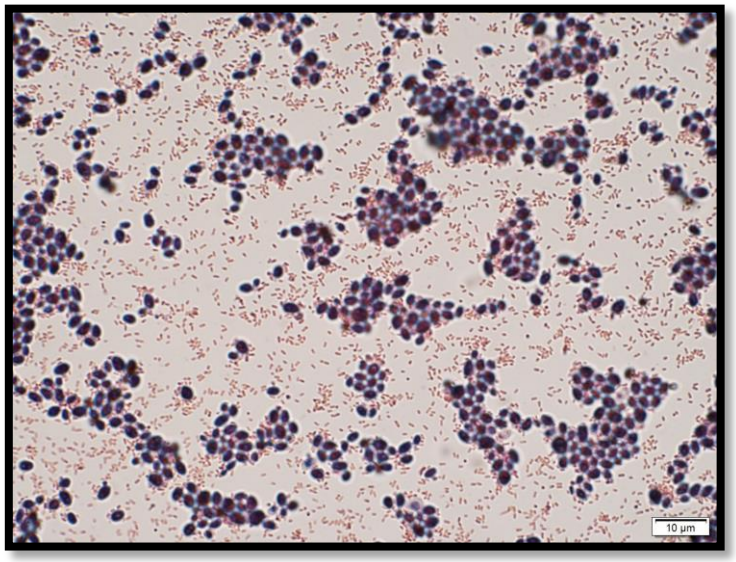

Figure 1.7. A mixed planktonic cell-suspension of *P. aeruginosa* ATCC 27853 (pink rod-shaped cells) and *C. auris* MRL 6057 (purple ovoid cells) were Gram-stained and visualised using an Olympus BX 63 OFM microscope. A 100X oil immersion objective lens was used (Scale bar: 10 µm).

Microorganisms that make up the constituents of polymicrobial cell suspensions and biofilms can interact in several ways. The types of interactions between genetically distinct species of microbes are extremely diverse and unique, adding another layer of complexity to the treatment of such infections. Polymicrobial interactions can be categorized as either synergistic or antagonistic. Synergism involves the collective

effect of two or more microbes which facilitates superior pathogen persistence at the site of infection (Wolcott *et al.,* 2013). This relationship benefits both pathogens and leads to an increased disease severity when compared with similar monomicrobial biofilms (Wolcott *et al.,* 2013). However, antagonism describes a dynamic between two or more microorganisms which are continuously in competition for essential but limited nutrients. This causes more challenging living conditions for the cohabiting pathogens and is associated with alterations in metabolic activity and expression of virulence factors within all species. For an infected patient, these tumultuous associations can still lead to an increased risk of morbidity and mortality.

As stipulated above, this study hopes to focus on the relationship between *C. auris* and *P. aeruginosa* under polymicrobial conditions. However, it is a severely under-researched relationship dynamic between two highly burdensome pathogens. The review of available literature only yielded results for an interaction between *P. aeruginosa* and *C. albicans*, a close relative of *C. auris* (Fourie and Pohl, 2019). Collected clinical samples containing *P. aeruginosa* and *C. albicans* demonstrated growth inhibition of *Candida* cells. The variables that contribute to the inhibition of *Candida* cells are intricate and convoluted. They include cell wall components, interactions between quorum sensing molecules (phenazine molecules like pyocyanin play a very important role) and fatty acid metabolites, as well as a rivalry for the intake of essential minerals like iron. These multispecies infections are more prevalent and problematic in the urinary tract, the lungs, open wounds, and the gastrointestinal tract (Fourie and Pohl, 2019).

Due to the lack of information regarding polymicrobial biofilms that are made up of *C. auris* and *P. aeruginosa,* this study hopes to serve as a stepping stone for the further investigation of the factors that influence these multispecies infections. Additionally, this can be described as the gap in the existing knowledge base, which, at least to some extent, might be addressed with this study's findings.

1.6.1 Biofilm formation

Biofilm forming ability of Candida auris

There is an array of fungal species known for their biofilm forming capabilities, of which, the most predominant species is *Candida*. *C. auris* is amongst those belonging to this genus which exhibits remarkable biofilm forming capabilities (Watkins et al., 2022). Unlike the more virulent *C. albicans*, *C. auris* is not usually capable of undergoing the same morphological switching from yeast to hyphae which can create more dense biofilms (Watkins et al., 2022). However, biofilms still contribute in a significant way to the increased virulence, AMR, and survival capabilities of *C. auris* in external environments and within an infected host. Certain strains of *C. auris* show greater tendencies to generate biofilms. Clade III (South African) illustrates the greatest biofilm forming capabilities (Watkins et al., 2022). This is a significant finding when analysing such infections within a local context.

The initial stages of biofilm development in *C. auris* can be visualised as a monolayer of yeast cells on a surface (Horton *et al.,* 2020). The overall procedure for biofilm formation consists of distinguishable major steps (Horton *et al.,* 2020). An overview of the most important phases of biofilm development is visually represented in Figure 1.8. The process begins with planktonic yeast cells attaching themselves to a surface by means of adhesin proteins to initiate a biofilm state (this usually takes about 90-minutes under *in vitro* conditions). From here, a protective extracellular matrix (ECM) is secreted, which in these yeast cells has been found to consist primarily of mannan-glucan polysaccharides (Watkins *et al.,* 2022). If these initial stages of adherence remain undisrupted, the biofilm layers can then begin to thicken through the continued proliferation of sessile yeast cells and the continued secretion of ECM (Watkins *et al.,* 2022). Once the biofilm has matured (this usually takes up to 24-hours under *in vitro* conditions), an impenetrable barrier is formed, offering sessile cells protection from host immune responses and antifungal drugs. This biofilm acquired ability to resist the effects of antifungal drugs is thought to be due to the upregulation of efflux pump associated genes when cells are within a biofilm (Watkins *et al.,* 2022). The increased number of efflux pumps available in cellular membranes means that antifungal drugs can be ejected at an increased rate thus leading to decreased efficacy of these agents.

The final stages of biofilm development involve the redistribution (or dispersion) of sessile cells out of the biofilm and back into the host environment where they revert to their planktonic state and seek out new and favourable areas for colonization and infection (Watkins *et al.,* 2022).

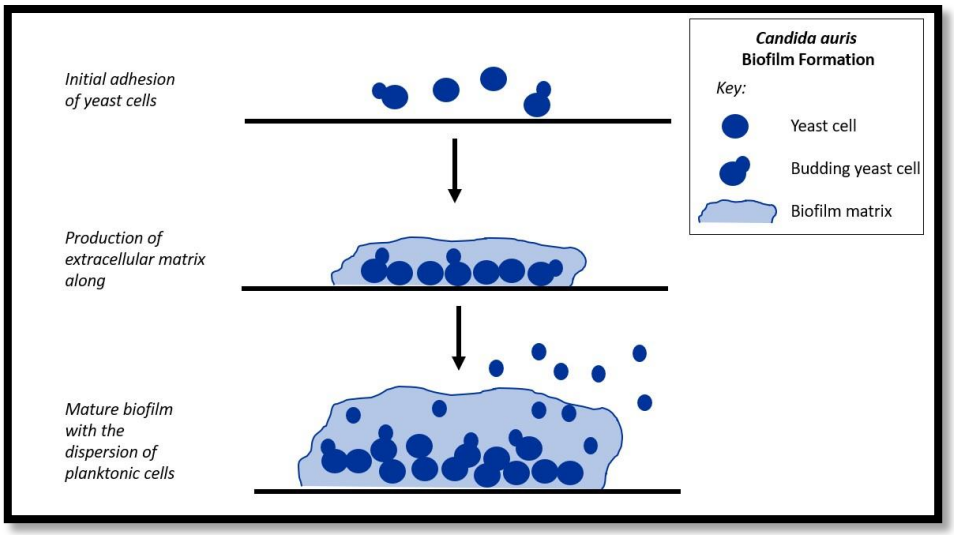

Figure 1.8. Diagrammatical representation of the steps involved in the development of *C. auris* biofilms (Adapted from: Piketh, Alam and Ahmad, 2023).

Biofilm forming ability of Pseudomonas aeruginosa

As previously mentioned in section 1.5, *P. aeruginosa* has advanced abilities for forming biofilms, and is therefore often used as a model bacterial species for the study of these complex structures. Distinct strains and varying nutritional or environmental conditions leads to development of biofilms that have individualistic phenotypic expression (Rasamiravaka *et al.,* 2015). The biofilm development cycle for *P. aeruginosa*, consists of important primary steps. First, planktonic bacterial cells reversibly anchor themselves onto a surface that is suitable for growth. Secondly, the irreversible attachment of these bacterial cells through the continued secretion of adhesin proteins occurs. Thirdly, the microcolonies of these cells also begin to secrete extracellular polymeric substances (EPS)[4]—this is known as biofilm initiation. *P. aeruginosa* manufactures at least three distinct types of polysaccharides. These

[4] EPS has a fundamental function, maintaining the structure and integrity of a biofilm. It also makes up about 85% of the total biofilm biomass. Moreover, its major constituents include biomolecules, exopolysaccharides, extracellular DNA (eDNA), and polypeptides (Rasamiravaka *et al.,* 2015).

polysaccharides are essential for biofilm stability and structure. environmental DNA (eDNA) is also a fundamental component, without which biofilms cannot be formed (Rasamiravaka *et al.,* 2015). Interestingly, when eDNA is targeted and removed from these structures, biofilms become more susceptible to compounds that can eradicate them. *P. aeruginosa* is also known to have extracellular appendages like flagella, pili, and fimbriae. These structures are usually responsible for cell motility but, during biofilm development, they demonstrate an adhesive function in the irreversible cell-to-surface interactions (Rasamiravaka *et al.,* 2015).

As bacterial cell proliferation and EPS secretion continues, the biofilm expands and begins to take on a three-dimensional shape—known as biofilm maturation. With *P. aeruginosa*, bacterial microcolonies will usually continue to grow until the entire surface is colonized with these structures. The fifth and final step involves sessile bacterial cells being dispersed, exiting the biofilm structure, and reverting to their planktonic state. This process facilitates the spread of these cells so that other appropriate surfaces within the host can be colonized (Rasamiravaka *et al.,* 2015).

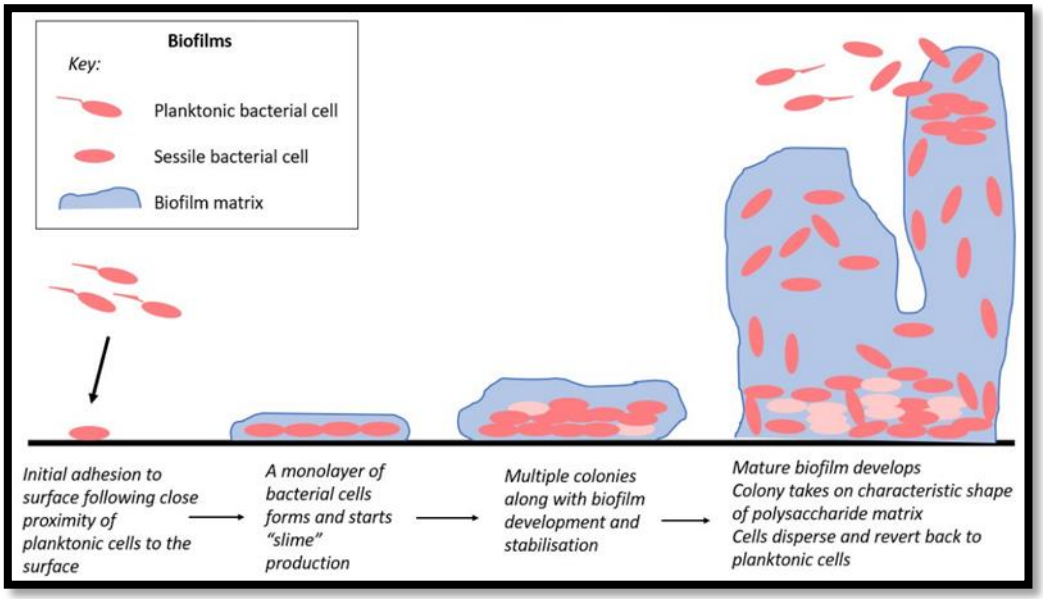

Figure 1.9. Biofilm formation cycle of bacterial cells (Adapted from: Piketh, Alam and Ahmad, 2023).

1.7 Defensins

Defensins are tiny, cationic, amphipathic, and water-soluble molecules that belong to a family of well-known antimicrobial peptides (Liu *et al.,* 2008; Pachón-Ibáñez *et al.,* 2017). These endogenous peptides can be found in a myriad of living creatures and play a crucial role in the immune response of plant and animal hosts when colonized with microbial pathogens (Barroso *et al.,* 2021; Dhople *et al.,* 2006; Henrik *et al.,* 2009; Hughes, 1999; Otvos, 2000).

Those of human origin can be categorised as either alpha (α)- or beta (β)-defensins (Liu *et al.,* 2008). These peptides are expressed in various tissues throughout the body. For example, α-defensins are secreted by neutrophils and gastrointestinal tract associated cells, while β-defensins originate in the skin as well as in epithelial cells that line protective mucous membranes (Klüver, Adermann, and Schulz, 2006; Liu *et al.,* 2008). Defensins have an abundant supply of cysteine molecules which have unique intramolecular bonds. Made up of a blend of a single α-helical domain, they are joined to a double-stranded and antiparallel β-sheet domain by means of several disulfide bonds. These stabilizing disulfide bridges are thought to significantly contribute to their antimicrobial abilities (Pachón-Ibáñez *et al.,* 2017).

Defensins can identify and rapidly negate any harmful infectious microorganisms or toxic substances, as they form an integral part of the innate immune response within humans (Liu *et al.,* 2008). The cells that make up the human body are covered in surface associated proteins called antigens. In healthy individuals, the immune system is programmed to identify these antigens but not stimulate an immune response in their presence (Marshall *et al.,* 2018). However, potentially harmful microorganisms and even toxic or foreign substances and structures are also known to be covered in antigenic proteins. When these alien antigens are detected, the immune response is activated and attempts to neutralize and destroy these invasive and unwelcome particles (Marshall *et al.,* 2018). This non-specific immune reaction is the body's first line of defence and is known as the innate immune system. An additional function of this system is to stimulate the onset of the highly selective adaptive immune response, also known as the second line of defence (Marshall *et al.,* 2018).

The existing literature reports that human defensins have demonstrated broad-spectrum antimicrobial activity against enveloped viruses, Gram-positive and Gram-negative bacteria, fungi, and even some species of parasites. Studies have also shown (Dhople *et al.,* 2006; Klüver, Adermann, and Schulz, 2006) that defensins illustrate antimicrobial activity even against bacteria with high levels of resistance to mainstream antibiotics (Liu *et al.,* 2008). Antimicrobial activity from any compound is brought about by a mechanism of action that targets essential structures or functions within a microorganism cell. By destroying such structures or intervening with crucial functions, these compounds can inhibit growth or cause a cell to die. The primary mechanism of antimicrobial action for defensin peptides has been identified as cellular membrane permeabilization (Liu *et al.,* 2008). These molecules work to disrupt and compromise pathogenic cell membranes which leads to cell lysis and eventual death (Liu *et al.,* 2008). Furthermore, the lack of cellular target specificity—as most microorganisms have cell membranes—means the development of resistance to these peptides is extremely rare. These peptides are of great importance, especially for the treatment of pathogens that are known for their ability to develop resistance to a vast array of mainstream drugs. As described above, *C. auris* and *P. aeruginosa* are notoriously difficult to treat when patients become infected with multi-drug resistant strains. This study therefore also aims to contribute further research into the discovery of a synthetically engineered defensin—a defensin-like antimicrobial peptide—and its potential contribution to effectively treat complex infection.

Defensin-like Antimicrobial Peptide-2

Defensin-like antimicrobial peptides are structurally and functionally similar to naturally occurring defensins. The defensin-like antimicrobial peptide (DLAP) which was investigated for its antimicrobial activity in this study, was synthetically generated in a chemical laboratory—please see Chapter 2 for further information. These peptides were designed and synthesized by tweaking the amino acid sequences of naturally occurring and known human defensins. The target amino acid sequence for this artificially derived peptide (DLAP-2) was stipulated as; **AVLSCLPKEEQIGKCSTRGERKCCRKK** as shown in Figure 1.10.

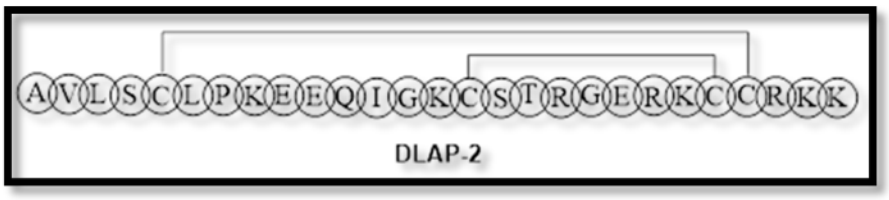

Figure 1.10. Structure and amino acid sequence of synthetically produced DLAP-2.

When this amino acid sequence was compared to those of human defensins, its sequence was most like that of a β-defensin known as, human β-defensin-3 (HβD-3), as seen in Figure 1.11 below. β-defensins are found exclusively in mammals and birds (Klüver, Adermann, and Schulz, 2006). There are several β-defensins all with a unique set of features. The antimicrobial potency of these molecules is thought to be associated with parametric characteristics like primary structure (also known as linear amino acid sequences), peptide surface-associated charge, hydrophobicity, and tertiary structure (the three-dimensional shape of the peptide) which facilitates species-specific microbial cell wall interfaces (Klüver, Adermann, and Schulz, 2006).

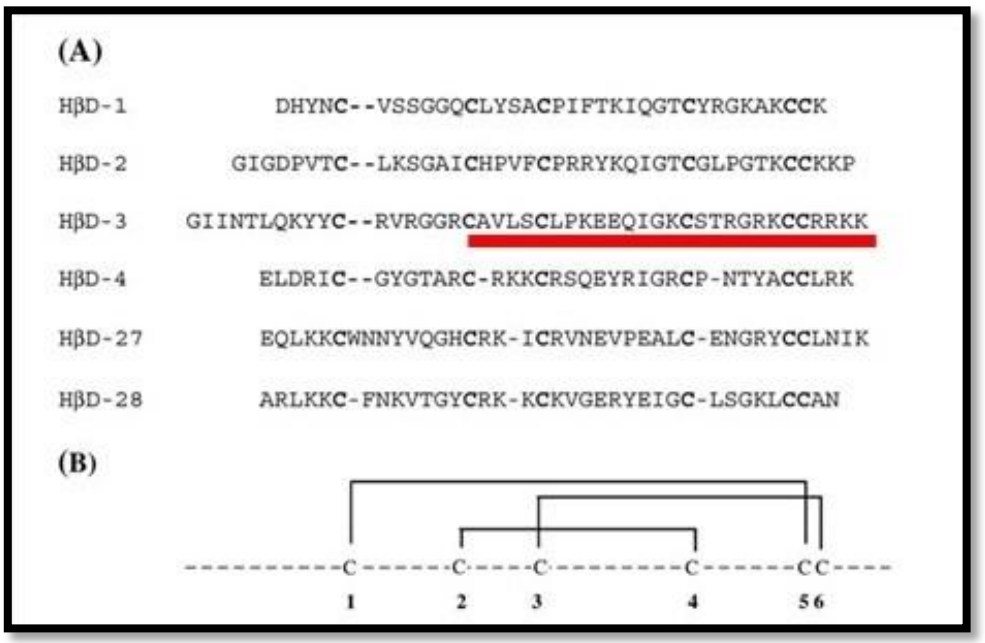

Figure 1.11. **(A)** represents the primary amino acid sequences and **(B)** represents the disulfide connections as seen in β-defensins. A portion of the HβD-3 peptide has been underlined in red, as it is this section of the sequence which most closely resembles that of DLAP-2. (Dhople *et al.,* 2006).

Cyclic and linear analogues of HβD-3 were investigated and a structure-function relationship that contributes to their antimicrobial capabilities was discovered. Additionally, it was found that most HβD-3 analogues can also selectively interact with natural and synthetic liposomes—biological drug delivery systems, which is thought to contribute to their ability to inhibit the growth of Gram-positive and Gram-negative bacteria (Liu *et al.,* 2008).

Moreover, whilst membrane permeabilization has been described as the main mechanism of antimicrobial activity for all peptides that belong to this family, it has also been stipulated that various types of defensins exhibit multiple and unique modes of activity. For example, HβD-3 has a reported mode of action against bacteria that works by inhibiting the biosynthesis of cell walls which leads to cell lysis (Pachón-Ibáñez *et al.,* 2017). Further laboratory analysis also elucidated the potential for these peptides to neutralize the harmful effects of bacterial endotoxins that bring about problematic side effects within the human body, for example, inflammation. Additionally, bactericidal activity has been reported against some species such as: *Escherichia coli, Klebsiella pneumoniae, Pseudomonas aeruginosa, Stenotrophomonas maltophilia, Acinetobacter baumannii, Enterococcus faecium, Staphylococcus aureus, Streptococcus pneumoniae, and Streptococcus pyogenes* (Pachón-Ibáñez *et al.,* 2017). Membrane permeabilization and depletion of cellular energy sources have also been found to be mechanisms of activity against specific strains of fungi, for example, *C. albicans*. Finally, antiviral activity has also been observed against *Vaccinia virus,* Influenza A, as well as certain strains of herpes simplex virus and HIV, by blocking viral cell binding to receptors and fusion and induction of cellular aggregation (Pachón-Ibáñez *et al.,* 2017).

Their reported antimicrobial power has led to an increase in the need for scientific investigations. These experimental procedures should involve the synthesis of various and individualistic β-defensin analogues. Synthetically engineered linear analogues can be used to elucidate the structure–function relationships that make defensins potentially invaluable sources of novel drugs for use in the treatment of clinical infections (Klüver, Adermann, and Schulz, 2006). For this reason, this study hopes to contribute to the much-needed demand for further research into synthetically engineered defensins.

1.8 Problem statement and research justification

C. auris and *P. aeruginosa* are infectious pathogens that share distinct characteristics which make them clinically significant. These attributes include: i) their elevated ability to persevere in clinical environments, ii) their tendency to be multidrug resistant, iii) their ability to be easily transmitted, iv) their potential to cause nosocomial outbreaks, and lastly vi) their biofilm forming capabilities. Biofilms are a principal virulence factor which have been identified as an etiological structure leading to the development of resistance and reoccurring clinical infections. For this reason, the discovery of new and highly effective antimicrobial agents that are capable of not only eradicating planktonic cells, but that can also dismantle and attenuate complex biofilm architecture, has never been so important. The limited knowledge available in the existing literature calls for further investigation of the relationship between the two pathogens of interest in polymicrobial biofilms. Furthermore, *in vitro* testing and analyses for the discovery of antimicrobial and antibiofilm drugs should be considered important research and therefore a major public health priority.

1.9 Aims

The aim of this study is to investigate the mono- and polymicrobial antibiofilm activities of DLAP-2 against *C. auris* and *P. aeruginosa*.

1.10 Objectives

- To assess the antimicrobial activity of DLAP-2 against *C. auris* and *P. aeruginosa* in single and mixed planktonic cell conditions by determining the minimum inhibitory concentrations (MIC) and minimum bactericidal/fungicidal concentrations (MFC/MBC).
- To determine the antibiofilm activity of DLAP-2 on mono- and polymicrobial biofilms.
- To study the impact of DLAP-2 on membrane integrity in single and mixed planktonic cell conditions.
- To determine the *in vitro* cytotoxicity of DLAP-2 by performing a haemolytic assay.

CHAPTER 2: MATERIALS AND METHODS

2.1 Chemistry of defensin-like antimicrobial peptide-2

DLAP-2 was synthesized by Dr. Mohmmad Y Wani, in the Department of Chemistry at the University of Jeddah in Saudi Arabia. Standard Solid Phase Peptide Synthesis protocols were used as shown in Scheme 2.1. The procedure started with chlorotrityl chloride resin (1.52 mmol) and Fmoc-amino acids (2.5mmol) which were subjected to a solid-phase reactor containing N, N-diisopropylethylamine (DIPEA) (3.5mmol), and dimethylformamide (DMF) which were agitated for 2 hours. Methanol (1mL) was then added to the resin and agitated for another 20 minutes. The resin was subsequently washed with DMF and dichloromethane (DCM). To assemble the desired peptide sequence, the Fmoc-protecting group was removed using piperidine, following repetition of the coupling cycle. The peptide was then cleaved from the resin using trifluoroacetic acid (TFA) and purified with high performance liquid chromatography (HPLC). To ensure that each coupling step was completed, the Kaiser test was used. As DLAP-2 has a longer amino acid sequence, it was synthesized using the Microwave Peptide Synthesizer instrument (Liberty, CEM). To confirm > 95% purity for all resulting compounds Liquid chromatography–mass spectrometry (LC-MS) was used. The resulting yellow powder was dissolved in dimethyl sulfoxide (DMSO), to acquire a stock solution with a concentration of 1000 µg/ml. Additionally, this solution was stored in the laboratory fridge at 4°C and thawed as needed.

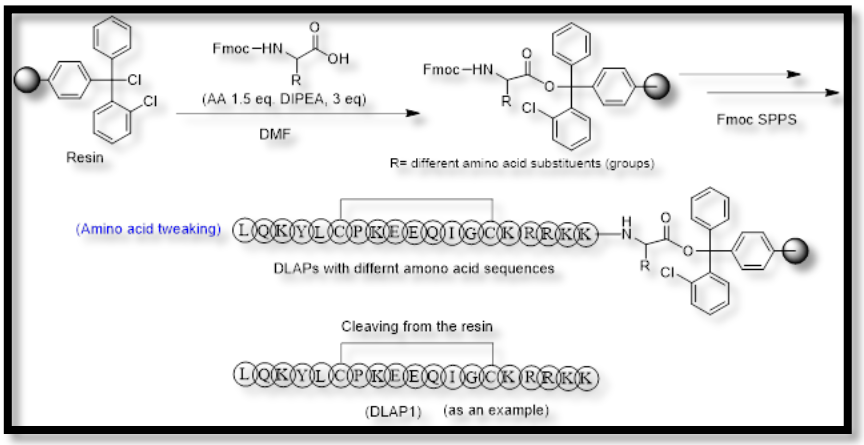

Scheme 2.1. Synthesis procedure for the target DLAPs

2.2 Ethics

This study involved using cultures of previously characterized and preserved microorganism specimens that were stored in the Department of Clinical Microbiology and Infectious Diseases at the University of the Witwatersrand. Additionally, equine red blood cells (RBCs) were used for the cytotoxicity assay and were obtained from the National Health Laboratory Service (NHLS). Therefore, interaction with patients and the collection of samples or confidential patient data is not applicable. It is for this reason that an ethics waiver was the most appropriate level of ethical clearance needed. This ethical clearance was obtained from the Human Research Ethics committee of the University of the Witwatersrand, Johannesburg, South Africa (Protocol No.: W-CBP-230509-01/Ref: R14/49). Please see Appendix I- Ethical clearance, for the official document.

2.3 Microorganism strains and growth

In this study, *C. auris* MRL 6057 and *P. aeruginosa* ATCC 27853 were used for all the assays. *C. auris* MRL 6057 was selected based on its known ability to form biofilms and reported resistance to amphotericin B deoxycholate (Srivastava and Ahmad, 2020). *P. aeruginosa* ATCC 27853 on the other hand was the only readily available strain for use in this study and was deemed suitable due to its known predilection for the formation of biofilms. Both pathogens were revived from glycerol stocks that were stored at −80 ºC in the Department of Clinical Microbiology and Infectious Diseases at the University of the Witwatersrand. Revival and maintenance of microbes from glycerol stocks was achieved using their respective agar media plates. Sabouraud Dextrose Agar (SDA) was used to grow *C. auris* and Nutrient Agar (NA) was used for *P. aeruginosa*. Glycerol stocks were thawed and a metal loop that had been sterilised with alcohol and by flame was then submerged in the clearly labelled glycerol stock sample and streaked onto the appropriate agar plates. The resulting agar plates were incubated for 24-48 hours at 35 ºC ± 2 ºC. These were known as the master plate, and from here, single colonies of either yeast or bacteria were used to inoculate a liquid growth media (broth).

2.3.1 Preparation of inocula

Appendix IV includes all the recipes that were used to prepare the broth, agar and additional reagents that were used for this study. Additionally, Sabouraud Dextrose Broth (SDB) was used for *C. auris* and Mueller Hinton Broth (MHB) for *P. aeruginosa.* Twenty millilitre aliquots of broth were prepared and inoculated with microorganism colonies from solid media. These inoculums were then incubated at 35 °C ± 2 °C at 200 rpm for 24 hours. The cell suspensions were then transferred into sterile, 50 ml falcon tubes and were centrifuged for 10 minutes at 4000 rpm. The resulting supernatant was discarded and the pellet that was formed at the bottom of the falcon tube was then washed twice by adding 20 ml of Phosphate-Buffered Saline (PBS) and centrifuging for 5 minutes at 4000 rpm. Once washed, 20 ml of the appropriate growth media was added. These cell suspensions were then used to make the appropriate 0.5 McFarland Standard solutions, the correct readings for which were determined by a turbidity meter. A 0.5 McFarland Standard Solution corresponds with a turbidity meter reading of between 0,06- 0,1 and Table 2.1 shows the corresponding CFU's/ml for suspensions made of bacteria or yeast.

Table 2.1. CFU's/ml for cell suspensions of yeast or bacteria in a 0.5 McFarland Standard.

Microorganism	CFU's/ml in a 0.5 McFarland Standard
Fungi (Yeast)	1-5 x 10^6
Bacteria	1,5 x 10^8

2.4 Antimicrobial activity

As discussed in the above literature review, AST is a useful tool for monitoring the development of resistance to mainstream antimicrobial agents, but also for the discovery of new and effective drugs which can be used to eradicate severe cases of clinical infections. The broth microdilution method was chosen as it is affordable, highly accurate and considered to be one of the gold-standard reference methods for evaluating MICs of antimicrobials (Salam *et al.,* 2023). Additionally, it allows the researcher to manipulate the concentrations of compound as needed.

In this study the antimicrobial potential of DLAP-2 was evaluated against planktonic cells under single and mixed conditions. This was determined using a broth microdilution assay following CLSI guidelines (Clinical and Laboratory Standards Institute, 2022), for which quantitative values were recorded. Minimum concentrations required to inhibit growth (MIC's) were determined visually, as the microtiter plate well that demonstrated no observable turbidity at the lowest possible concentration of antimicrobial. The minimum concentrations needed to kill almost all the bacterial and fungal cells were recorded as MBC/MFC values and were taken as the first plated out well for which no growth could be seen on the appropriate agar plates. For all the broth microdilution assays run in this experiment, a DLAP-2 stock solution (1000 µg/ml) was serially diluted. The calculated concentrations for each well can be seen in Table 2.2 below. The concentration gradient starts with the highest concentrations on the left-hand side of the microtiter plate (column 1) and gradually decreased towards the right with the lowest concentration in column 12.

Table 2.2. DLAP-2 serial dilution concentrations (µg/ml) in each well of the first two rows of a 96-well microtiter plate.

	1	**2**	**3**	**4**	**5**	**6**	**7**	**8**	**9**	**10**	**11**	**12**
A	250	125	62,5	31,25	15,62	7,81	3,91	1,96	0,98	0,49	0,24	0,12
B	250	125	62,5	31,25	15,62	7,81	3,91	1,96	0,98	0,49	0,24	0,12

2.4.1 Single planktonic microbial populations

This experiment was set out as follows; 100 µl of growth media was added to all the appropriate wells in a 96-well, U-bottomed microtiter plate. A 100 µl aliquot of a 1000 µg/ml stock solution of the DLAP-2 was then serially diluted in the 12 wells of 1 row of the microtiter plate. The final 100 µl mixture left in the pipette after the dilution was complete was discarded. Once this step was completed, 100 µl of a 0.5 McFarland standard cell suspension was added to each of the same wells. Sterility controls, negative controls (or growth controls) as well as positive controls were also set up and run simultaneously. Sterility controls consisted exclusively of 100 µl of growth media, growth controls consisted of 100 µl of growth media as well as 100 µl of a cell suspension. Lastly, positive controls were set up using 100 µl of growth media, and serially diluted stock solutions (1000 µg/ml) of amphotericin B (for *C. auris*) and

gentamicin (for *P. aeruginosa*). The resulting concentration gradient for positive control wells in a single microtiter plate row was therefore identical to those as seen in Table 2.2 for DLAP-2. These plates were then incubated at 35 °C± 2 °C for 24 hours. From here, the MIC values were recorded. Furthermore, using the same plates prepared for the MIC portion of the investigation, 10 µl of the contents of each microtiter plate well were then sub-cultured onto SDA and NA plates. These agar plates were subsequently incubated at 35 °C± 2 °C for 24 hours. From these agar plates, the MBC/MFCs were recorded. It is also important to note that the MIC and MBC/MFC values were determined relative to the growth as seen on the negative or growth controls, in both single and mixed cell conditions.

2.4.2 Mixed planktonic microbial populations

The MIC and MBC/MFC values of DLAP-2 against mixed planktonic cell populations of *C. auris* and *P. aeruginosa* were evaluated using pre-established procedures (Li *et al.,* 2015). The procedure used to set up the MIC plates in section 2.4.1 was conserved for section 2.4.2, with a few minor adjustments to accommodate both pathogens. Along with 50 µl of *C. auris* in TSB growth media, 50 µl of *P. aeruginosa* was added to each relevant well in the 96-well microtiter plate. Negative or growth controls and sterility control wells were also set up. Negative or growth control wells contained 100 µl of TSB media and 50 µl of *P. aeruginosa* cell suspension along with 50 µl of *C. auris* cell suspension. The sterility control contained 100 µl of TSB growth media only. The plates were then incubated at 35 °C ± 2 °C for 24 hours. Following incubation, plates were visually observed to determine MIC values. Thereafter, from the same plates, the MBC/MFC's were recorded by following the procedure as described in section 2.4.1 above. However, for the mixed culture conditions, contents were plated out onto two sets of agar plates; the first being SDA that had been supplemented with bactericidal concentrations of gentamicin (15,62 µg/ml) and NA that had been supplemented with fungicidal concentrations of amphotericin B (31,25 µg/ml). These plates were supplemented with MBC/MFC concentrations of antibiotic and antifungal agents so that the growth patterns of each individual pathogen could be determined. The gentamicin (mainstream antibiotic) works to inhibit the growth of *P. aeruginosa* so that *C. auris* growth could be visualised separately, and amphotericin B (mainstream

antifungal) works to inhibit the growth of *C. auris* so that *P. aeruginosa* growth could be visualised separately.

2.5 Antibiofilm activity of DLAP-2

The antibiofilm potential of DLAP-2 on mono- and polymicrobial biofilms was determined, using the most effective concentrations as recorded in section 2.4 of this study. Two stages of the biofilm growth process were investigated, namely for, (a) the initial or cell adhesion stages of biofilm development (immature biofilms), and for (b) biofilms that had a significant period to grow (mature biofilms) (Scheunemann *et al.,* 2021).

Monomicrobial biofilms were grown in the designated wells of flat-bottomed 24-well microtiter plates. A 200 µl aliquot of the respective growth media (SDB for *C. auris* and MHB for *P. aeruginosa*) was added to the appropriate wells, followed by 200 µl of a 0.5 McFarland Standard microbial cell-suspension. On the other hand, polymicrobial biofilms were grown by adding 100 µl each of *P. aeruginosa* and *C. auris* and 0.5 McFarland Standard cell-suspensions to 200 µl of TSB medium (Sigma-Aldrich, USA). Subsequently, these separate microtiter plates were then incubated at 35 °C ± 2 °C for 90 minutes (immature biofilms) and 24 hours (mature biofilms). Post-incubation, the contents of each well was gently removed using a pipette without disrupting the biofilms that had formed on the bottom of the plate wells. In three separate Eppendorf tubes® (EP tubes), 200 µl of a 1000 µg/ml stock solution of DLAP was serially diluted in 200 µl of the appropriate growth media which had been aliquoted into each tube. The three highest concentrations of DLAP-2 were used (62,5 µg/ml, 125 µg/ml, and 250 µg/ml). The resulting 200 µl of diluted compound was then gently aliquoted into the appropriate wells of the microtiter plate. For the negative or growth control wells, 200 µl of growth media only was used to replace the original growth media- cell suspension solution. The plates were then once again incubated at 35 °C ± 2 °C for 24 hours. Post-incubation, the growth media and compound solutions were removed, and the biofilms were then delicately washed with 100 µl of PBS to remove any remaining planktonic cells. Next a quantitative value for the metabolic activity of the freshly washed sessile cells were determined using an MTT (MTT, Thiazolyl Blue Tetrazolium, M2128, Sigma, Sigma-Aldrich, Chemie GmbH, Taufkirchen, Germany) assay.

Therefore, for this experiment a stock solution of MTT in PBS with a concentration of 5 mg/ml was further diluted to create a working solution with a concentration of 0,075 mg/ml—a concentration found to be appropriate when performing assay optimizations. A 100 µl aliquot of this solution was added to each of the respective wells, after which the plates were incubated again for another 2 hours at 35 °C ± 2 °C (until a light purple, colour change was observed). Next, the liquid solution was removed from the appropriate wells and 100 µl of 100% DMSO was added, followed by 15 minutes of room temperature incubation (after which another colour change is observed-deep/dark purple). These plates were then mounted onto a spectrophotometry instrument and the absorbance readings were recorded at 570 nm (SpectraMax iD3 multi-mode microplate reader, Molecular Devices, CA, USA). From here, the recorded values were plugged into the equation below so that the percentage biofilm inhibition (%) could be calculated (Srivastava and Dubey, 2016).

$$\% \text{ Biofilm inhibition} = [(\text{control OD}_{570\text{nm}} - \text{test OD}_{570\text{ nm}})/\text{control OD}_{570\text{ nm}}] \times 100$$

Equation 2.1. Calculating percentage biofilm inhibition from quantitative readings as determined by the SpectraMax iD3 multi-mode microplate reader.

2.6 Biofilm microbial cell viability

Fernandes and co-workers (2020) established a method for determining fungal and bacterial cell viability, which was adopted for this study. This involves calculating the colony forming units (CFUs) of each microorganism of interest (individually as well as in combination) from the formed immature (incubated for 90-minutes) and mature (incubated for 24-hours) biofilms (Rather *et al*., 2023). A 96-well microtiter plate was used and 100 µl of growth media was added to the 12 wells of a single row. The following step involves incorporating an additional 100 µl of the appropriate cell suspension. For the combination plate, 50 µl of each pathogen was added to every well. Once the initial incubation (35 ºC ± 2 ºC) period was complete, the contents of each well were removed using a pipette and replaced with varying concentrations of a growth media and DLAP-2 solution. From the growth control wells, the growth media and cell suspension mixtures were also removed and replaced with 200 µl of just

growth media. The plates were then incubated for a second period of 24 hours at 35 ºC ± 2 °C. The contents of each well were then gently removed using a pipette. Next, 100 µl of PBS was used to carefully wash the biofilms which had now developed on the walls of each microtiter plate well, after which this PBS was removed. A 100 µl aliquot of PBS was added again and used to scrape the remaining biofilms off the walls of each well. This 100 µl was then aliquoted into a labelled EP tube. Subsequently, a unique number of EP tubes containing 90 µl of PBS each were then set up and 10 µl of the original biofilm sample was aliquoted out and used to perform a serial dilution. Wells that were expected to contain a higher number of viable cells in their biofilms (for example growth controls or treated samples exposed to lower concentrations), had a higher dilution factor. This means that they had to be further diluted to achieve an acceptable number of CFUs when plated out and grown on agar plates. From here, 30 µl of this diluted sample was plated out onto SDA plates which were enhanced with bactericidal concentrations (15,62 µg/ml) of gentamicin, and NA agar plates that had been supplemented with fungicidal concentrations (31,25 µg/ml) of amphotericin B (Rather *et al*., 2023). These plates were supplemented to ensure that the growth of each pathogen could be visualised individually, even under mixed culture conditions. These plates were incubated for 24 hours at 35 °C ± 2 °C and were analysed and counted for the number of visible colonies that had formed, these values were then recorded.

This entire process was repeated 3 times. The formulas below were then used to calculate the CFU's/ml in the original sample, and finally the mean Log10 CFU/ml values were determined and plotted on a graph (Fernandes *et al.,* 2020).

Step 1:

$$\text{CFU's/ml in diluted sample} = \frac{Number\ of\ colonies\ counted\ on\ agar\ plate}{Volume\ of\ diluted\ sample\ added\ to\ agar\ plate\ (ml)}$$

Step 2:

$$\text{CFU's/ml in original sample} = \frac{CFU's\ per\ ml\ in\ diluted\ sample}{Dilution\ factor\ of\ the\ diluted\ sample}$$

Equation 2.2. Calculating the CFU's/ml in the diluted and original samples taken from a biofilm microtiter plate.

2.7 Fluorescence microscopy for the visualisation of biofilms

For the analysis of microbial biofilms, two main fluorescent dyes were exploited, namely Concanavalin A -Alexa Fluor 488 conjugate (ConA). Con A (Invitrogen, Thermo Fisher Scientific, ZA; excitation wavelength = 485 nm and emission wavelength = 610 nm) and FUN ™ 1 Cell Stain (FUN-1) (Invitrogen, Thermo Fisher Scientific, ZA; excitation wavelength = 495 nm and emission wavelength = 519 nm) exclusively binds to the cell membrane and cell wall components of fungi and bacteria. This dye fluoresces green and stains both biofilm matrix and the cell membranes of live and intact cells (Rather *et al*., 2023). FUN-1 on the other hand is uniquely capable of displaying two-colour fluorescence (Thermo Fisher Scientific Inc., 2023). When this dye undergoes passive diffusion into fungi and bacterial cells, it stains the cytoplasm green. Subsequently, if cells are metabolically active and have maintained cell membrane integrity, this dye is processed further within the cell and exhibits red fluorescence (Thermo Fisher Scientific Inc, 2023).

The protocol for performing the antibiofilm property validation was adopted from Rather and co-workers (2023). For monomicrobial biofilms, separate 0.5 McFarland Standard cell-suspensions of *C. auris* and *P. aeruginosa* were set up in SDB and MHB growth media respectively. Sterile square glass coverslips were then placed into flat bottomed, 6-well microtiter plates. 1,5 ml of growth media and cell-suspension were then added to each well. For polymicrobial biofilms, 750 µl of *C. auris* and 750 µl of *P. aeruginosa* cells, suspended in TSB media, were also added. Immature biofilm plates were incubated for 90-minutes and mature biofilms for 24-hours under biofilm forming conditions at (35 ºC ± 2 ºC). After this initial phase of growth and incubation, the growth media and cell-suspension solutions were delicately removed. 1,5 ml of serially diluted DLAP 2 was then added to the appropriate wells (concentrations used were 250 µg/ml and 125 µg/ml). To the negative or growth control wells, a 1,5 ml mixture of the appropriate cell suspension and growth media was added. These plates were then incubated for an additional 24 hours at 35 ºC ± 2 ºC. This was followed by the planktonic cells and growth media being aspirated, after which PBS was used to gently wash the biofilms. To each well, 500 µl of PBS and 10 µl of FUN-1 (stock solution concentration: 10 mM) and Con A (stock solution concentration: 5 mg/ml) were each added. These plates were incubated in darkness at room temperature for 30 minutes

before the solution from each well was then removed. Subsequently, the glass coverslips were carefully removed, flipped over, and mounted onto glass microscope slides for visualisation on an Olympus BX63 OFM Microscope. The resulting images consisting of red (FUN-1), and green (Con A) fluorescence were then recorded individually and simultaneously using multitrack mode. These results were recorded as photomicrographs.

2.8 Cell membrane integrity

The integrity of the microbial cell membrane of selected planktonic pathogens was determined using the Propidium Iodide (PI) staining method (Suchodolski *et al.,* 2017; Rather *et al*., 2023). PI (Sigma-Aldrich, USA; excitation wavelength = 535 nm and emission wavelength = 615 nm) stains DNA or RNA by binding to the nucleic acid through intercalation in nucleotide bases. This means that only dead cells, or cells with compromised membranes will fluoresce (orange/red in colour). This assay was used to confirm the mechanism of antimicrobial activity for DLAP-2.

A 0.5 McFarland Standard cell-suspension of *P. aeruginosa* and *C. auris* cells (under both single and mixed conditions) was suspended in PBS and exposed to various concentrations of DLAP 2 (MIC and MBC/MFC) in 1 ml samples. Additionally, a negative (or growth) control was established using cells suspended in PBS alone, while the positive control was established using a 30% hydrogen peroxide (H_2O_2) solution and suspended cells. After these samples had been incubated at 35 °C ± 2 °C, under agitation conditions at 200 rpm for 4 hours, they were subsequently centrifuged for 5 minutes at 4000 rpm and the pellet was washed with PBS. The cells were then resuspended in 250 µl of PBS and stained with 5 µl of PI (stock solution concentration: 1mg/ml), after which they were stored in a dark fridge for 2 hours. Cells were then once again washed and centrifuged at 4000 rpm for 3 minutes. From here a final 250 µl of PBS was added to the individual EP tubes. A pipette was used to aliquot 50 µl onto glass slides before a glass coverslip was added. These samples were then kept in the dark before being viewed by means of a fluorescence microscope (Olympus BX63 OFM Microscope). The results were recorded as photomicrographs.

2.9 Cytotoxicity

A cell cytotoxicity evaluation was performed to determine if the antimicrobial agent of choice is in anyway toxic to living RBCs under laboratory conditions. A haemolytic assay was performed using equine (horse) RBCs. Haemolysis occurs when living RBCs are exposed to stress. As a result, they are damaged and burst open to release their cell contents. A previously reported method was used for this experiment (Lone and Ahmad, 2020; Rather *et al*., 2023). This procedure involved aliquoting 10 ml of horse blood into a sterile 50 ml falcon tube. This tube was centrifuged for 10 minutes at 2000 rpm, which separated RBCs from platelets and plasma. As the blood is separated, the heavier RBCs sink to the bottom to create a pellet. The supernatant was then discarded, and the pellet was washed three times with 15 ml of ice-cold PBS, after which it was resuspended in 90 ml of chilled PBS. 500 µl samples were created in EP tubes, made up of 200 µl of the blood solution and varying concentrations of the DLAP-2 (MIC, 2×MIC and 3×MIC). For this part of the experiment, a positive control was established using Triton X-100 (1%) and a negative control using PBS. These mixtures were incubated at 35 °C ± 2 °C for 1 hour. Once incubation was complete, cells were centrifuged at 2000 rpm for 10 minutes and the supernatant was pipetted into a 24-well flat-bottomed microtiter plate. From here, the absorbance was determined at a wavelength of 450 nm by means of spectrophotometry (SpectraMax iD3 multi-mode microplate reader, Molecular Devices, CA, USA). The following equation was used to calculate the percentage haemolysis:

$$\%\ \text{haemolysis} = \left[\frac{\text{A450 of test compound treated sample} - \text{A450 of buffer treated sample}}{\text{A450 of 1 \%Triton X}-100\ \text{treated sample} - \text{A450 of buffer treated sample}}\right] \times\ 100\%$$

Equation 2.3. Calculating the percentage haemolysis from quantitative readings as determined by the SpectraMax iD3 multi-mode microplate reader.

2.10 Statistical analysis

All experimental procedures in this study were completed in triplicate. Data analysis was achieved using multiple linear regression (MLR) models as well as one-way ANOVA models on Stata statistical package software (STATA/ SE- Standard Edition 17.0 – StataCorp). Additionally, all p-values $\leq$ 0,05 were taken as statistically significant. For experimental data that is not suitable for the above-mentioned statistical analysis models, descriptive statistics were used.

CHAPTER 3: RESULTS

3.1 Antimicrobial activity

From the results below (Table 3.1), DLAP-2 had higher antimicrobial activity against *C. auris* in single culture samples. The MIC and MFC values were 62,5 µg/ml and 125 µg/ml, respectively. However, when *C. auris* was allowed to grow in mixed cultures with *P. aeruginosa*, the concentration of DLAP-2 needed to inhibit its growth or kill its cells increased to 125 µg/ml and 250 µg/ml, respectively. *C. auris* was also run against a mainstream antifungal known as amphotericin B, to establish positive controls (MIC-15,62 µg/ml). According to reported CDC tentative MIC breakpoints, this strain is therefore resistant to amphotericin B (Centers for Disease Control and Prevention, 2020; Uprety and Lockhart, 2022).

Conversely, *P. aeruginosa* was run against mainstream antibiotic, gentamicin, with an observed MIC of 3,91 µg/ml, when compared to the CLSI breakpoints, the sample was classified as susceptible (Clinical and Laboratory Standards Institute, 2022).
The antimicrobial activity of DLAP-2 against *P. aeruginosa* under single planktonic conditions yielded an MIC of 125 µg/ml and an MBC of 250 µg/ml (as seen in Table 3.1). Furthermore, under combination planktonic cell suspension conditions, the MIC and MBC values for *P. aeruginosa* remained identical. This means that there were no observable changes to its resistance patterns in mixed culture conditions with *C. auris*.

3.1.1 Single planktonic microbial populations

The resulting 96-well microtiter MIC plates for single cell conditions can be seen in Figure 3.1 below.

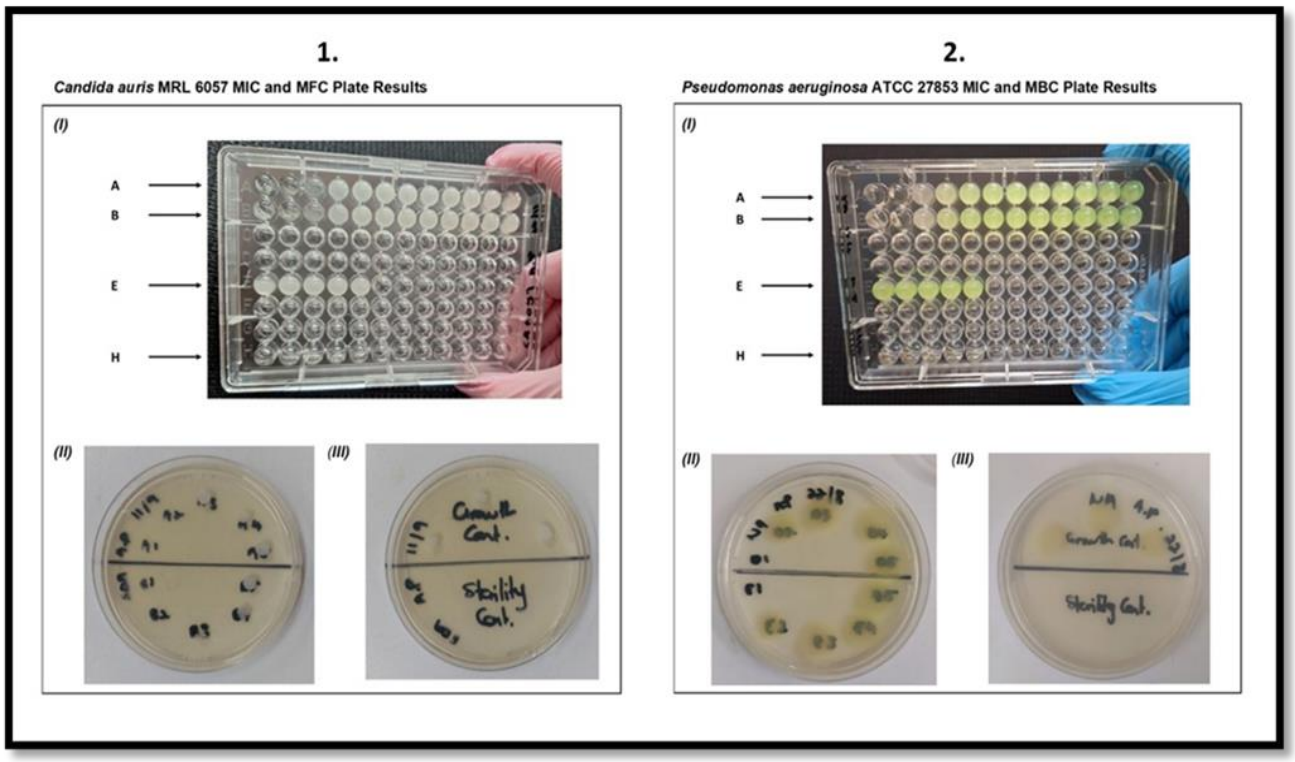

Figure 3.1. MIC and MBC/MFC plate results for single *C. auris* MRL 6057 (**1**) and *P. aeruginosa* ATCC 27853 (**2**). The MIC plates ***(I)*** have been labelled as follows: **A** and **B**- these wells were used to set up a serial dilution of the DLAP-2 compound. **E**- the growth or negative control wells which were unexposed to antimicrobial compounds. **H**- the sterility control was set up to ensure no contamination was present. The images labelled ***(II)*** show the MBC/MFC results which were obtained from agar plates. The final image ***(III)*** is of the agar plates that were used to set up growth control wells as well as the sterility control wells.

3.1.2 Mixed planktonic microbial populations

The resulting AST 96-well microtiter plate for combination cell populations can be seen in Figure 3.2 below.

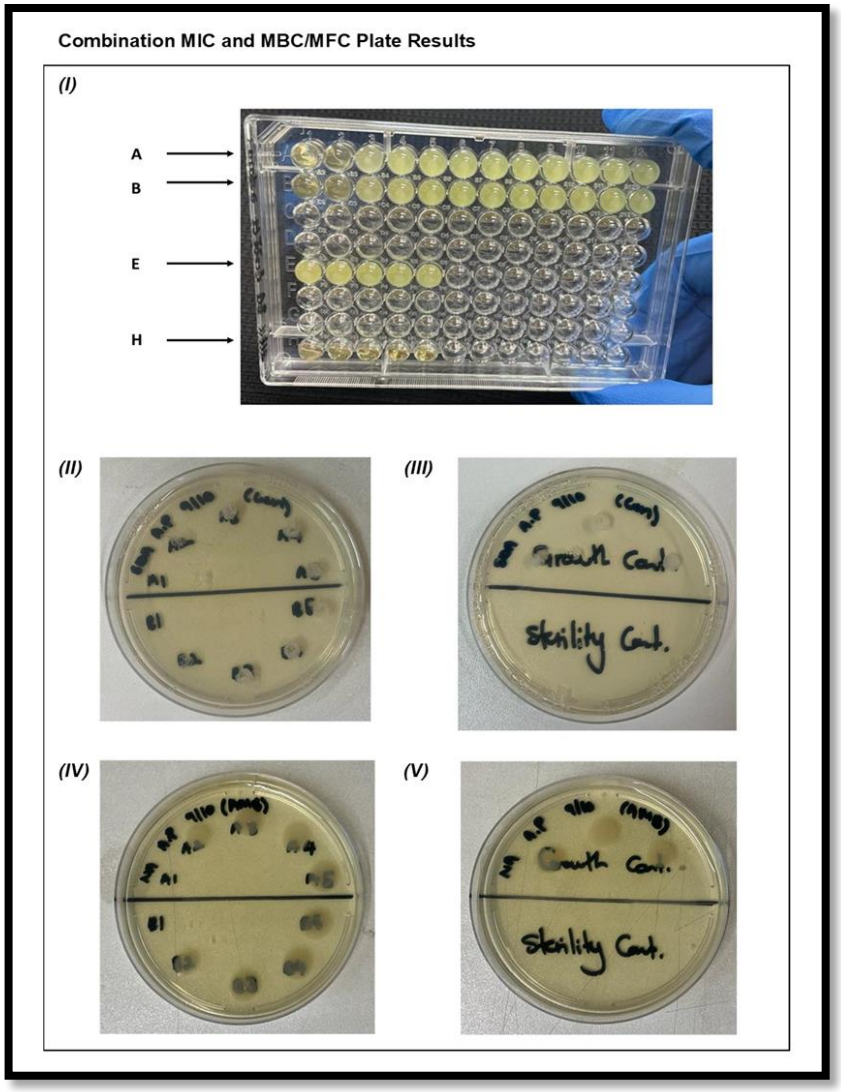

Figure 3.2. MIC and MBC/MFC plate results for the mixed cell suspensions, consisting of *C. auris* MRL 6057 and *P. aeruginosa* ATCC 27853. The MIC plate ***(I)*** has been labelled as follows: **A** and **B**- these wells were used to set a serial dilution of the DLAP-2 compound. **E**- the growth or negative control wells which were unexposed to antimicrobial compounds. **H**- the sterility control was set up to ensure no contamination was present. The image labelled ***(II)*** and ***(IV)*** show the MBC/MFC results which were obtained from supplemented agar plates. These plates were supplemented with complementary mainstream antimicrobials to ensure that each pathogen would grow and could be observed individually (selective media). The final images ***(III)*** and ***(V)*** are of the plated-up growth control wells and the sterility control wells.

Table 3.1 MIC and MBC/MFC values for single and mixed cell cultures of *C. auris* and *P. aeruginosa* against the test compound DLAP-2.

Microorganism	**MIC (µg/ml)** **Mean (*n*=*6*)**	**MBC/ MFC (µg/ml)** **Mean (*n*=*6*)**
C. auris MRL 6057	62,5	125
P. aeruginosa ATCC 27853	125	250
Combination	125	250

*****The results from the experimental repeats were identical, therefore, no standard deviations have been included.

Descriptive statistics were used for the above analysis. The values obtained for the six repeat tests of each pathogen, individually as well as in combination, were identical. In other words, for all six repeats there were no deviations from the values as listed in the table above, and by extension, there were no deviations in the overall mean values that were calculated. Therefore, each value shows a standard deviation of zero.

3.2 Antibiofilm activity of DLAP-2

The MTT assay that was performed gave an indication of the number of viable cells within the biofilms being studied (Gutiérrez *et al.,* 2017). This study yielded mean percentage biofilm inhibition values which have been summarised in Table 3.2, Figure 3.3, Figure 3.4, and Figure 3.5, below. These results show a trend for all three types of biofilms that were evaluated. As the concentration of DLAP-2 increased, so the percentage biofilm inhibition increased. At higher concentrations, fewer sessile cells survive. Therefore, at concentrations of 250 µg/ml, the least number of viable cells were present when compared to the growth controls, according to the MTT assay results. This trend can be seen in both immature and mature biofilms. However, the effect of duration (time for which previously established biofilms were allowed to grow) on the outcome variable was less predictable and consistent as the pathogenic constituents of the study biofilms changed.

C. auris monomicrobial biofilms (Figure 3.3) for example, only exhibited biofilm inhibition percentages that exceeded 50% at DLAP-2 concentrations of 125 µg/ml (53,17%), and 250 µg/ml (55,54%) in immature biofilms and only at concentrations of 250 µg/ml (56,6%) in mature biofilms.

On the other hand, at all 3 concentrations of DLAP-2, monomicrobial biofilms made up of *P. aeruginosa* (Figure 3.4), showed higher percent biofilm inhibition values in immature biofilms that were only given 90 minutes to develop. From a cursory glance of the *P. aeruginosa* data, it seems that as the duration increases, so the percentage biofilm inhibition decreases. Treated biofilm samples that had been exposed to the highest concentration of DLAP-2 (250 µg/ml), showed inhibition readings of 49,86% in immature and 38,79% in mature biofilms. The above data shows that DLAP-2 was least effective at eradicating biofilms made up of *P. aeruginosa* on its own, as percentage biofilm inhibition outcomes did not exceed 50% at any of the tested concentrations of DLAP-2.

For combination biofilm plates (Figure 3.5) that were made up of both *C. auris* and *P. aeruginosa* sessile cells, most of the results showed the highest levels of biofilm percentage inhibition when compared to all three datasets. This data therefore suggests that DLAP-2 demonstrates the best antimicrobial and antibiofilm activity against polymicrobial biofilms. In polymicrobial biofilms, the percentage biofilm inhibition values exceeded 50% in immature and mature biofilms at two concentrations,

namely, 125 µg/ml and 250 µg/ml. When DLAP-2 concentrations were set at 125 µg/ml, the percentage biofilm inhibition values were found to be 53,62% in immature biofilms and this increased to 55,54% in mature biofilms. In comparison, at DLAP-2 concentrations of 250 µg/ml, the inhibition values were recorded as 63,55% in immature biofilms, and 64,59% in mature biofilms.

Table 3.2. Mean percentage biofilm inhibition values with the corresponding concentrations of DLAP-2 against 90-minute (immature) and 24-hour (mature) biofilms of *C. auris* and *P. aeruginosa*.

DLAP-2 Concentration (µg/ml)	**Percentage Biofilm Inhibition (%) Mean (*n*=6)**					
	90-minute biofilms			**24-hour biofilms**		
	C. auris	*P. aeruginosa*	*Combination*	*C. auris*	*P. aeruginosa*	*Combination*
62,5	33,63	21,46	48,25	42,11	19,08	32,55
125	53,17	38,23	53,62	47,61	34,99	55,54
250	55,54	49,86	63,55	56,6	38,79	64,59

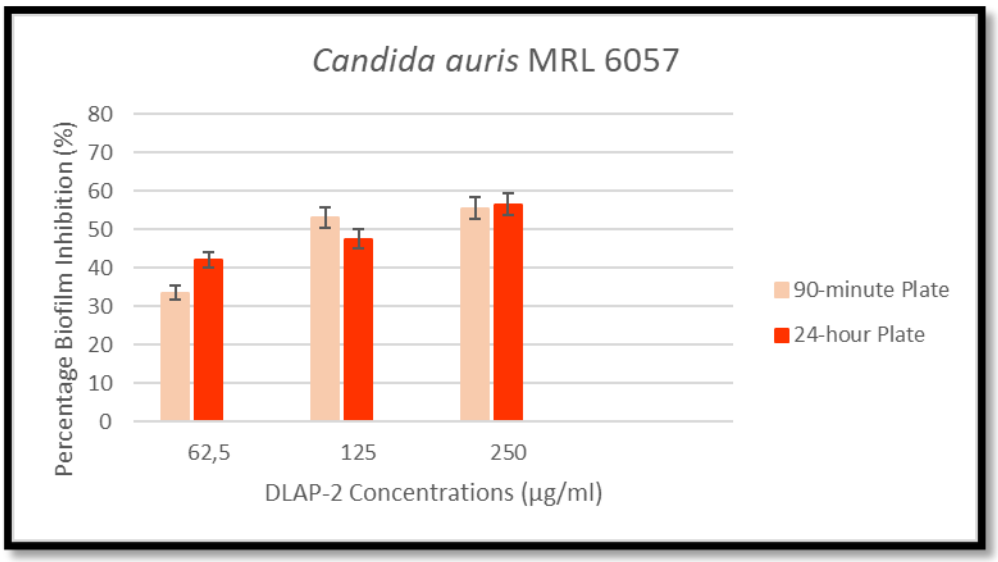

Figure 3.3. The percentage biofilm inhibition of 90-minute (immature) and 24-hour (mature) monomicrobial biofilms of *C. auris.* Biofilms were exposed to 62,5 µg/ml, 125 µg/ml, and 250 µg/ml of DLAP-2 (p-value = 0,0073).

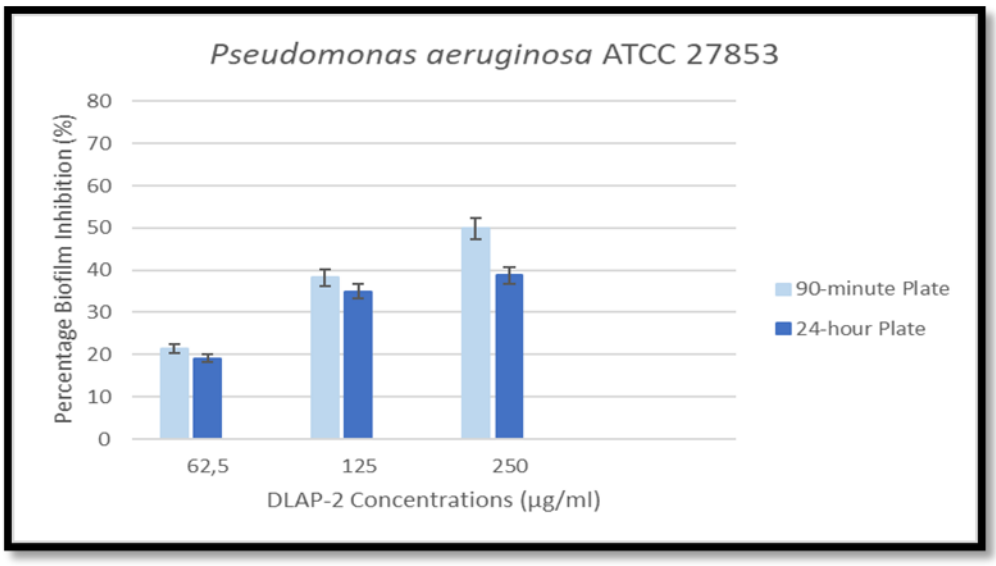

Figure 3.4. The percentage biofilm inhibition of 90-minute (immature) and 24-hour (mature) monomicrobial biofilms of *P. aeruginosa*. Biofilms were exposed to 62,5 µg/ml, 125 µg/ml, and 250 µg/ml of DLAP-2 (p-value = 0,0761).

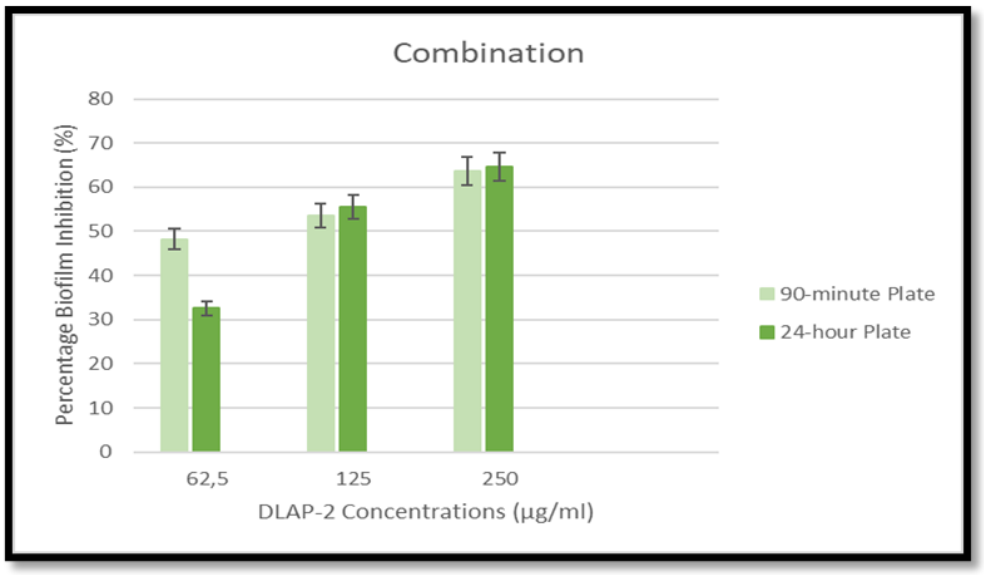

Figure 3.5. The percentage biofilm inhibition of 90-minute (immature) and 24-hour (mature) polymicrobial biofilms of *C. auris* and *P. aeruginosa*. Biofilms were exposed to 62,5 µg/ml, 125 µg/ml, and 250 µg/ml of DLAP-2 (p-value < 0,0001).

The statistical analysis of the biofilm percentage inhibition data was performed using a multiple linear regression (MLR) model. These models use statistical procedures to determine the effect of two or more independent variables on the outcome of a dependent variable. This technique outlines the variation of the model and the comparative influence of each independent variable on the total variance (Hayes, 2023). Additionally, it was important to test for an interaction between the two categorical, independent variables in this experiment. Such an interaction can be found in a dataset when the effect of one variable on the outcome values, depends on the corresponding value of another variable. To this end, a 'Wald Chi-Squared Test' was performed—a parametric, quantitative value for verifying whether the individual as well as the collective effect of two or more independent variables is statistically significant for a model or not (StatisticsHowTo.com, 2023). If the resulting p-value from this test is found to be statistically significant (p-value < 0,05), further analysis is needed to account for the identified interaction. The qualitative data for this and any other statistical analysis in this study is summarized in Appendix III.

From the MLR models of all three datasets, it was determined that at concentrations of 125 µg/ml and 250 µg/ml there was a positive correlation with the dependent variable, biofilm percentage inhibition. For monomicrobial biofilms of *C. auris* and *P. aeruginosa* this correlation was statistically significant, with p-vales < 0,05. However, for polymicrobial biofilms this correlation was statistically significant at a concentration of 250 µg/ml (p-value = 0,026) and not statistically significant for a concentration of 125 µg/ml (p-value = 0,414). In essence, this means that (at statistically significant concentration levels), as the concentration of DLAP-2 increases, so does the biofilm percent inhibition.

The Wald Chi-Squared test that was performed for both sets of monomicrobial data, yielded a p-value of 0,31 for *C. auris* and 0,48 for *P. aeruginosa*. This means that there was no statistically significant interaction between concentration and duration, hence, it was not included in the models. Additionally, the correlation between duration and biofilm percentage inhibition was found to be positive for *C. auris* and negative for *P. aeruginosa*. This correlation, however, was statistically significant for monomicrobial biofilms of neither *C. auris* (p-value = 0,708) nor *P. aeruginosa* (p-value = 0,17). Conversely, the results from the Wald Chi-Squared of polymicrobial biofilms yielded a p-value of 0,007. This means that the interaction between concentration and duration

in this model was statistically significant. An interpretation of this interaction showed that the effect of duration on biofilm inhibition was much stronger for the lower concentration group (62,5 µg/ml). For the higher concentration groups (125 µg/ml and 250 µg/ml), duration did not seem to have any effect, as there was no significant difference in the percentage biofilm inhibition of immature (90-minutes) and mature (24-hours) biofilms. A defining characteristic of the polymicrobial biofilm dataset, however, was the fact that the negative correlation between duration and biofilm percent inhibition was statistically significant (p-value = 0,001). This means that, as the duration for which biofilms were allowed to develop increased, so biofilm percent inhibition caused by DLAP-2 decreased.

3.3 Biofilm microbial cell viability

The results of the biofilm cell viability count assay revealed that concentration of DLAP-2 and duration played a central role in determining the inhibitory effects on the development and maintenance of previously established biofilms. This statement holds true for immature (90-minute) and mature (24-hour) biofilms of varying microbial composition. More simply put, when the concentration of DLAP-2 was increased, the Log10 CFU's/ml values were significantly decreased in mono- and polymicrobial biofilms alike.

The calculated Log10 CFUs/ml values for *C. auris* cells in monomicrobial biofilms (Figure 3.6) decreased from 10,62 to 4,82 (immature biofilms) and from 10,99 to 8,99 (mature biofilms) when comparing negative control quantities to samples that were exposed to 2XMIC (125 µg/ml) concentrations of DLAP-2. Furthermore, in monomicrobial biofilms of *P. aeruginosa* (Figure 3.7) which were exposed to 2XMIC (250 µg/ml) concentrations of DLAP-2, the outcomes also demonstrated reduced Log10 CFU/ml quantities. From 10,83 to 3,5 (in immature biofilms) and from 12,98 to 4 (in mature biofilms). It is also important to note that in monomicrobial biofilms under growth control conditions, *P. aeruginosa* boasted higher Log10 CFU/ml values than *C. auris*. This directly translates to an increased number of Log10 CFU's/ml in *P. aeruginosa* biofilms. In addition to this difference, *P. aeruginosa* has a doubling time of 25 minutes to 1,5 hours (LaBauve and Wargo, 2012) which is significantly shorter than the recorded 1 to 2,5 hours (Gustavo and Lorenz, 2021) doubling time of *C. auris*. The values that were recorded for this experiment also showed that under mature (24-hour) biofilm conditions, DLAP-2 seemed to reduce the Log10 CFU/ml values of *P. aeruginosa* more so than for *C. auris* at a concentration of 62,5 µg/ml. In contrast to the monomicrobial biofilms, polymicrobial biofilms were set up on two sets of agar plates when visually determining the number of CFUs. Agar plates had to be supplemented with mainstream antimicrobial agents so that the growth of each biofilm microbe constituent could be determined individually. It is for this reason that there are double the number of recorded Log10 CFU's/ml values for the polymicrobial biofilms. Keeping this in mind, we can now say that the same trend was observed in polymicrobial biofilms (Figure 3.8). When negative or growth control readings were compared to samples that had been exposed to 2XMIC (250 µg/ml) concentrations of DLAP-2, the Log10 CFU/ml quantities were decreased. Values for counts of *C. auris*

went from 7,19 to1,82 and for *P. aeruginosa* from 9,43 to 2,16 (90-minute). Similarly, in mature biofilms (24-hour), Log10 CFU/ml values for *C. auris* went from 8,9 to 5,35 and for *P. aeruginosa* from 11,31 to 6,01. For all samples, higher Log10 CFU/ml values were obtained for *P. aeruginosa.* Further studies would need to be conducted to confirm whether this observed trend can be attributed to a unique interaction relationship between the two pathogens.

The raw data for CFUs/ml in the original sample (which can be found in Appendix II-A.2.2) was also used to deter3lk1`mine the percentage reduction in viable cells found in biofilms. For these calculations, the growth control or unexposed (0 µg/ml) samples were compared to exposed samples. The results of these calculations showed that the number of viable cells found within mono- and polymicrobial biofilms was reduced by a minimum of 98% in all samples that were exposed to DLAP-2 at concentrations of 125 µg/ml or above.

Table 3.3. Mean microbial cell viability values (Log10 CFU's/ml) for 90-minute and 24-hour biofilms that had been exposed to varying concentrations of DLAP-2. (NC- negative control made up of untreated biofilm cells which were allowed to grow unhindered).

Biofilms	**Concentrations (µg/ml)**	**Log10 CFU/ml values Mean (*n=3*)**		**Log10 CFU/ml values Mean (*n=3*)**	
Monomicrobial		**90-minute biofilms**		**24- hour biofilms**	
C. auris	0 (NC)	10,71		10,96	
	62,5	6,78		10,88	
	125	4,82		8,99	
	250	3,16		7,54	
P. aeruginosa	0 (NC)	10,83		12,99	
	62,5	7,71		10,33	
	125	4,68		7,34	
	250	3,5		4	
Polymicrobial		***C. auris***	***P. aeruginosa***	***C. auris***	***P. aeruginosa***
Combination	0 (NC)	7,2	9,43	8,9	11,31
	62,5	4,92	7,34	6,44	9,58
	125	3,54	4,28	5,75	7,81
	250	1,82	2,16	5,35	6,01

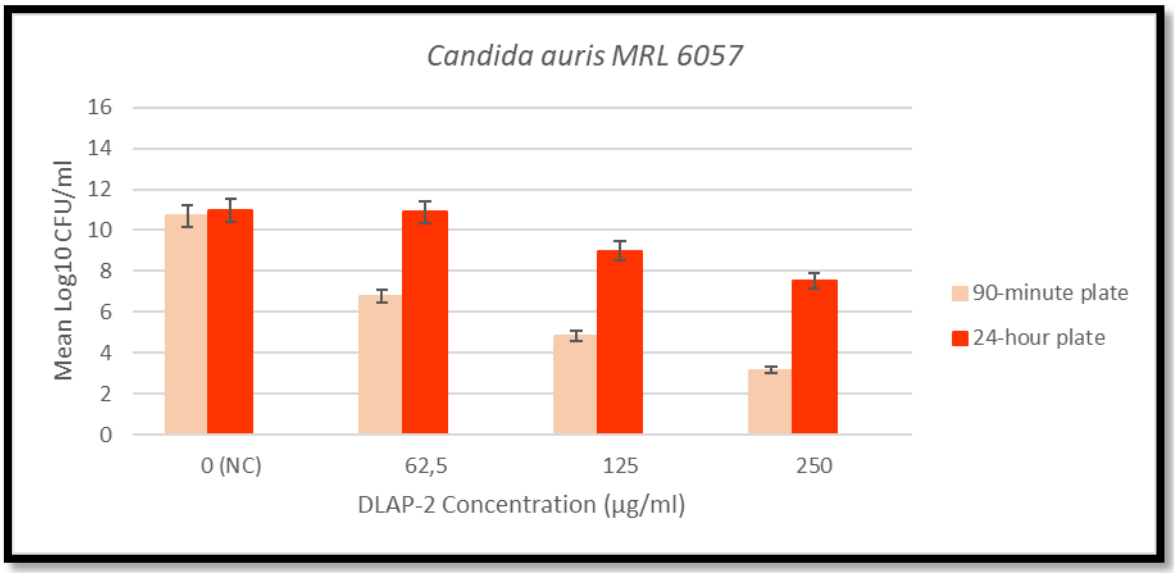

Figure 3.6. Results of a viability assay for monomicrobial biofilms, made up of *C. auris* (sessile cells only). Biofilms were exposed to three different concentrations of DLAP-2, and the corresponding CFU counts were recorded (p-value < 0,0001). The 0 µg/ml (NC) dataset is the negative control, otherwise known as the growth or untreated control.

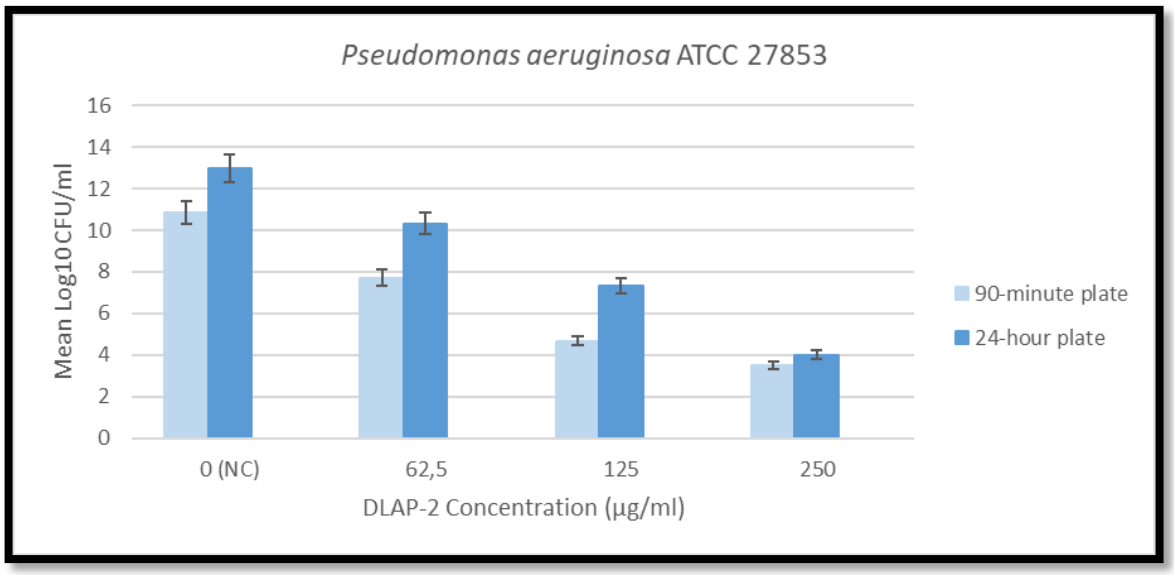

Figure 3.7. Results of a viability assay for monomicrobial biofilms, made up of *P. aeruginosa* (sessile cells only). Biofilms were exposed to three different concentrations of DLAP-2, and the corresponding CFU counts were recorded (p-value < 0,0001). The 0 µg/ml (NC) dataset is the negative control, otherwise known as the growth or untreated control.

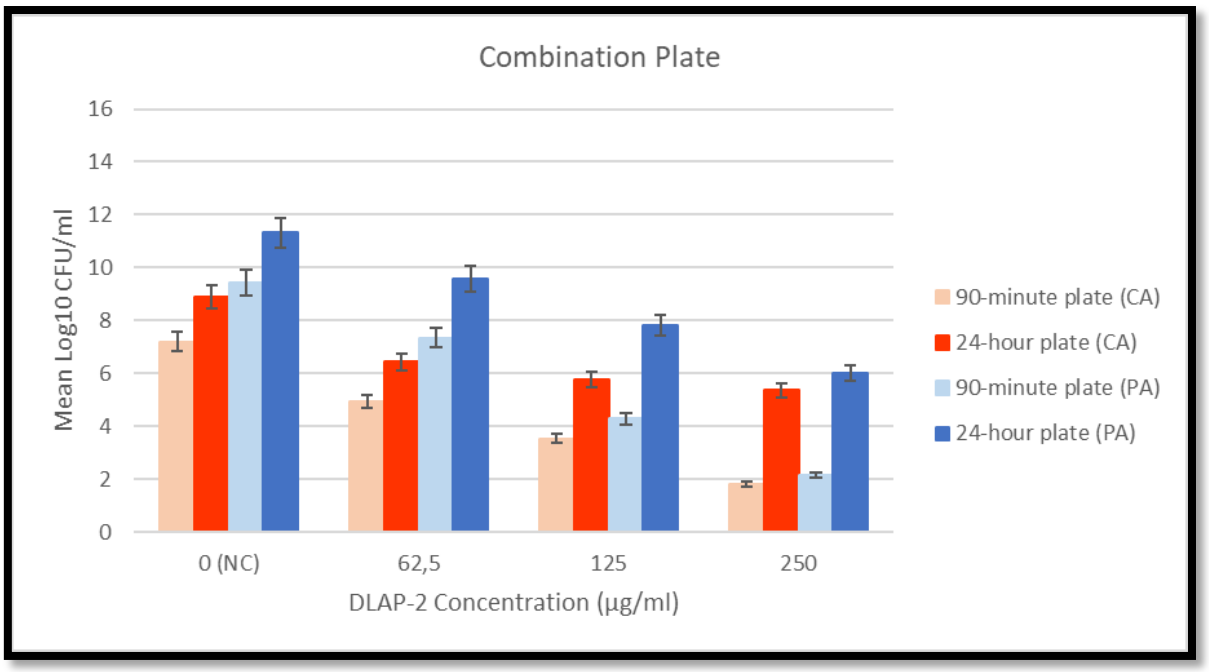

Figure 3.8. Results of a viability assay for polymicrobial biofilms, made up of *C. auris* and *P. aeruginosa* (sessile cells only). Biofilms were exposed to three different concentrations of DLAP-2, and the corresponding CFU counts were recorded (p-value < 0,0001). The 0 µg/ml (NC) dataset is the negative control, otherwise known as the growth or untreated control.

The qualitative data for this statistical analysis is summarized in Appendix III- A.3.2. The MLR models were run for cell viability assays of monomicrobial biofilms of *C. auris* and *P. aeruginosa* as well for polymicrobial biofilms. All three concentration groups and the number of viable cells found in a biofilm sample (Log10 CFU/ml) have a negative correlation in all the datasets, all of which were also statistically significant (p-value < 0,05). In other words, the data shows that, as the concentration of DLAP-2 that each biofilm was exposed to increased, so the number of viable cells found in the corresponding biofilm sample (Log10 CFU/ml) decreased. Duration was also found to be positively correlated with the number of viable cells found in a biofilm sample (Log10 CFU/ml) for all three datasets. Therefore, as the duration (amount of time for which biofilms are allowed to develop), increased, so the number of viable cells found in a biofilm also increased. This relationship was statistically significant with identical p-values < 0,001, for all datasets.

The Wald Chi-Squared test was also performed for each dataset and the interactions between duration and concentration were statistically significant for all datasets. For the respective monomicrobial biofilms, *C. auris* had a p-value < 0,0001 while *P.*

aeruginosa had a p-value = 0,0002. For the polymicrobial biofilm plate, *C. auris* had a p-value < 0,0001 while *P. aeruginosa* had a p-value = 0,003. The nature of the interaction between the two independent variables for monomicrobial biofilms made up of *C. auris* shows that for the negative control (0 µg/ml) duration had no effect on the recorded Log10 CFU/ml values (the number of viable cells within the biofilm). However, as the concentration of DLAP-2 increased (62,5 µg/ml, 125 µg/ml, and 250 µg/ml), so the Log10 CFU/ml values decreased. Additionally, mature biofilms had more viable cells than the immature ones, even after exposure to the chosen antimicrobial peptide.

For monomicrobial biofilms made up of *P. aeruginosa*, duration had no effect on the highest concentration group (250 µg/ml). Yet for the negative control and two lower concentrations, duration showed a positive correlation. Increased time for biofilm development led to an increased Log10 CFU/ml value.

Finally, for the polymicrobial biofilms, similar trends were observed. An increase in duration led to an increase in the number of viable biofilm-associated cells (Log10 CFU/ml values). This means that the longer biofilms were allowed to develop for, the more cells could survive exposure to lethal concentrations of DLAP-2. Furthermore, as the concentration of DLAP-2 increased, so the number of viable cells decreased.

3.4 Fluorescence microscopy for the visualisation of biofilms

In the micrograph summary of each biofilm slide, four images were included. Image A represents the DIC grey microscopy visualisation mode which clearly displays cell morphology and distribution. Image B shows FUN-1 fluorescence which, is red and indicates viable and metabolically active cells. Increased fluorescent intensity in these images corresponds with increased levels of cell viability. Image D shows Con A fluorescence which is green and indicates the presence of intact cells with polysaccharides in their cell walls. Due to the presence of polysaccharides in biofilm matrix, this structure will also exhibit green fluorescence. Increased intensity of green fluorescence in these images is associated with an increased number of intact cells as well as more intricate, three-dimensional biofilm networks. Finally, image C is a multitrack image which shows DIC grey, FUN-1 and Con A attributes simultaneously. The green fluorescence in image C can be considered biofilm matrix exclusively whilst yellow fluorescence is synonymous with cells that are metabolically active and that have intact cell-walls.

These photomicrographs were visually studied, and several conclusions could be drawn from them. The 90-minute (immature) and 24-hour (mature) growth control biofilms, specifically for *P. aeruginosa* and combination plates (Figure 3.12 and Figure 3.15, respectively), presented with densely arranged and metabolically active cells in conjunction with complex biofilm structures (seen by intensive levels of red and green fluorescence). In comparison, although *C. auris* untreated controls (Figure 3.9) were still concentrated with cells, they showed less compact biofilm arrangements. Moreover, when comparing the density of 90-minute and 24-hour growth controls, an evident difference could only be observed with *C. auris* biofilm slides (Figure 3.9). In mixed growth control biofilm samples (Figure 3.15), fewer *C. auris* cells could be identified when compared to the number of *P. aeruginosa* cells in the same sample as well as compared to *C. auris* cells in monomicrobial growth controls. *C. auris* cells also seemed to be enveloped and entangled by the overwhelming cell population size of *P. aeruginosa*. A second observable difference between the mixed 90-minute and 24-hour growth control sample also showed an increased number of *C. auris* cells in the immature biofilm.

Analysis of the treated samples showed that the inhibition of biofilm development was found to be concentration dependent. Samples of monomicrobial and polymicrobial biofilms were exposed to concentrations of DLAP-2 (125 µg/ml and 250 µg/ml) to investigate the peptides antibiofilm properties. Monomicrobial biofilms made up of *C. auris* were exposed to 250 µg/ml of DLAP-2 as seen in Figure 3.11. When this sample was compared to its growth control, decreased numbers and more sparsely distributed cells were seen. This observation was also accompanied by decreased levels of red fluorescent intensity. A decrease in the presence of strong green fluorescence also indicated diminished development of biofilm matrices. These same treated samples were also established for monomicrobial biofilms of *P. aeruginosa* (Figure 3.14) as well as for polymicrobial biofilms made up of both pathogens (Figure 3.17). Similarly, the observations as described for the former (*C. auris* biofilms) were the same as for the latter (*P. aeruginosa* and combination biofilms). This decrease in the quantity and distribution of viable cells in treated samples can be seen in both immature (90-minute) and mature (24-hour) biofilms. Biofilms that were allowed to grow for only 90-minutes showed an increased level of biofilm inhibition when compared to 24-hour biofilms. At lower concentrations, significant variations can be seen between growth controls and

the treated samples. However, in samples that were exposed to 125 µg/ml of DLAP-2 (Figure 3.10- *C. auris*; Figure 3.13- *P. aeruginosa* and Figure 3.16- Combination) the difference between levels of inhibition in immature and mature biofilms becomes less distinguishable. Occasionally, in DIC grey images (A) of treated samples, there were observable reductions in the size of cells as well as increased inconsistencies in cell morphology. To confirm this however, further studies that utilise confocal laser scanning microscopy (CLSM) as well as scanning electron microscopy (SEM) should be completed as these techniques offer more detailed photomicrographs of a cell's structure and surface.

In summation, DLAP-2 concentrations of 125 µg/ml and 250 µg/ml can diminish complex structures associated with previously established mono- and polymicrobial biofilms. This statement holds true for biofilms made up of *C. auris* and *P. aeruginosa* in both immature (90-minute) and mature (24-hour) phases of development.

3.4.1 Monomicrobial Biofilms

***C. auris* MRL 6057**

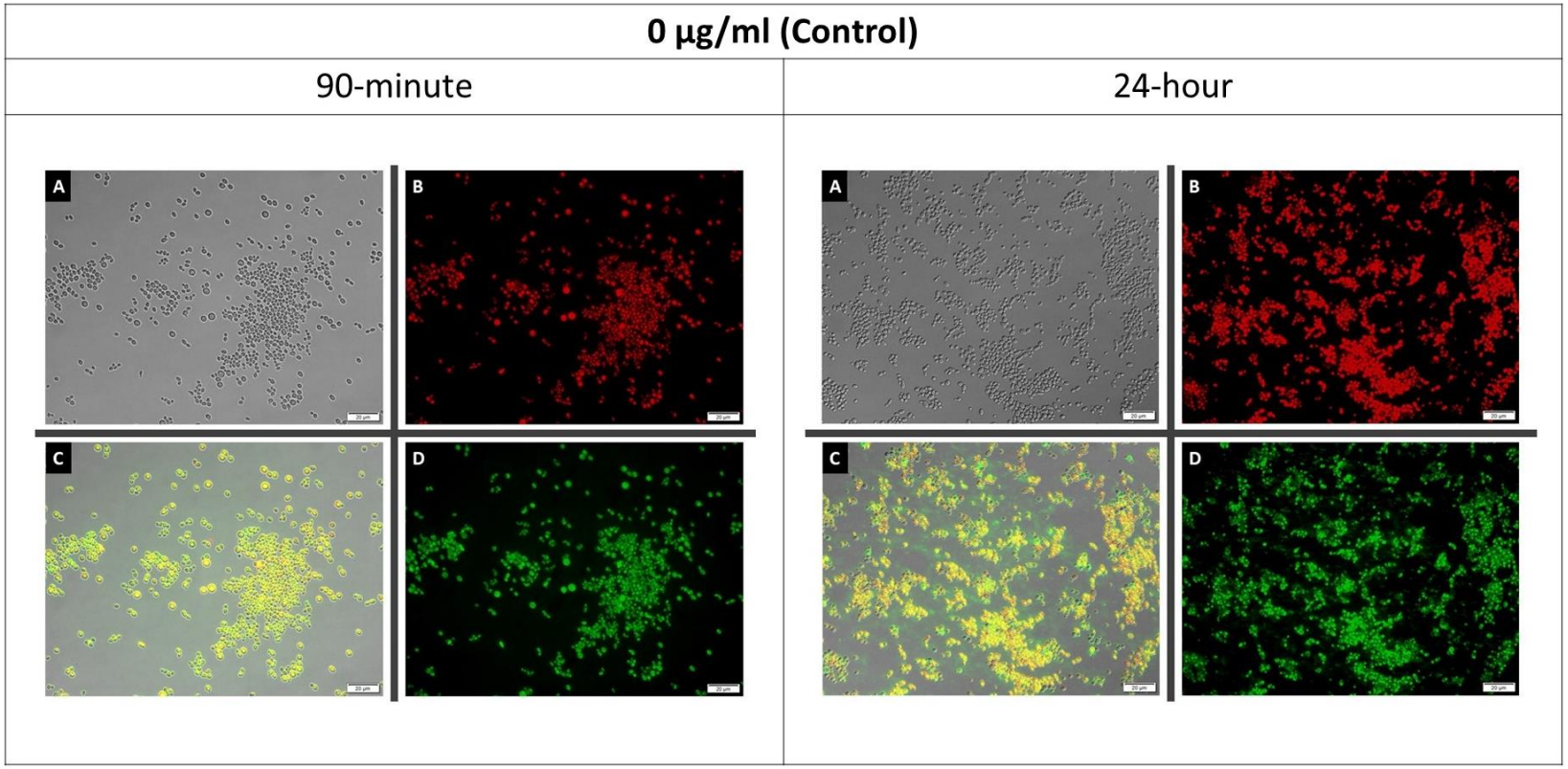

Figure 3.9. Micrographs for the 90-minute and 24-hour control biofilms of *C. auris*. Micrographs were taken on the Olympus BX63 OFM. Observation of cells was achieved using a 60X oil immersion objective lens (Scale Bar: 20 µm). A- DIC Grey; B- FUN-1 fluorescent dye; C- Multitrack mode; D- Con A fluorescent dye. Green fluorescence- all intact cells (dead or alive) and biofilm matrix; red fluorescence- metabolically active cells.

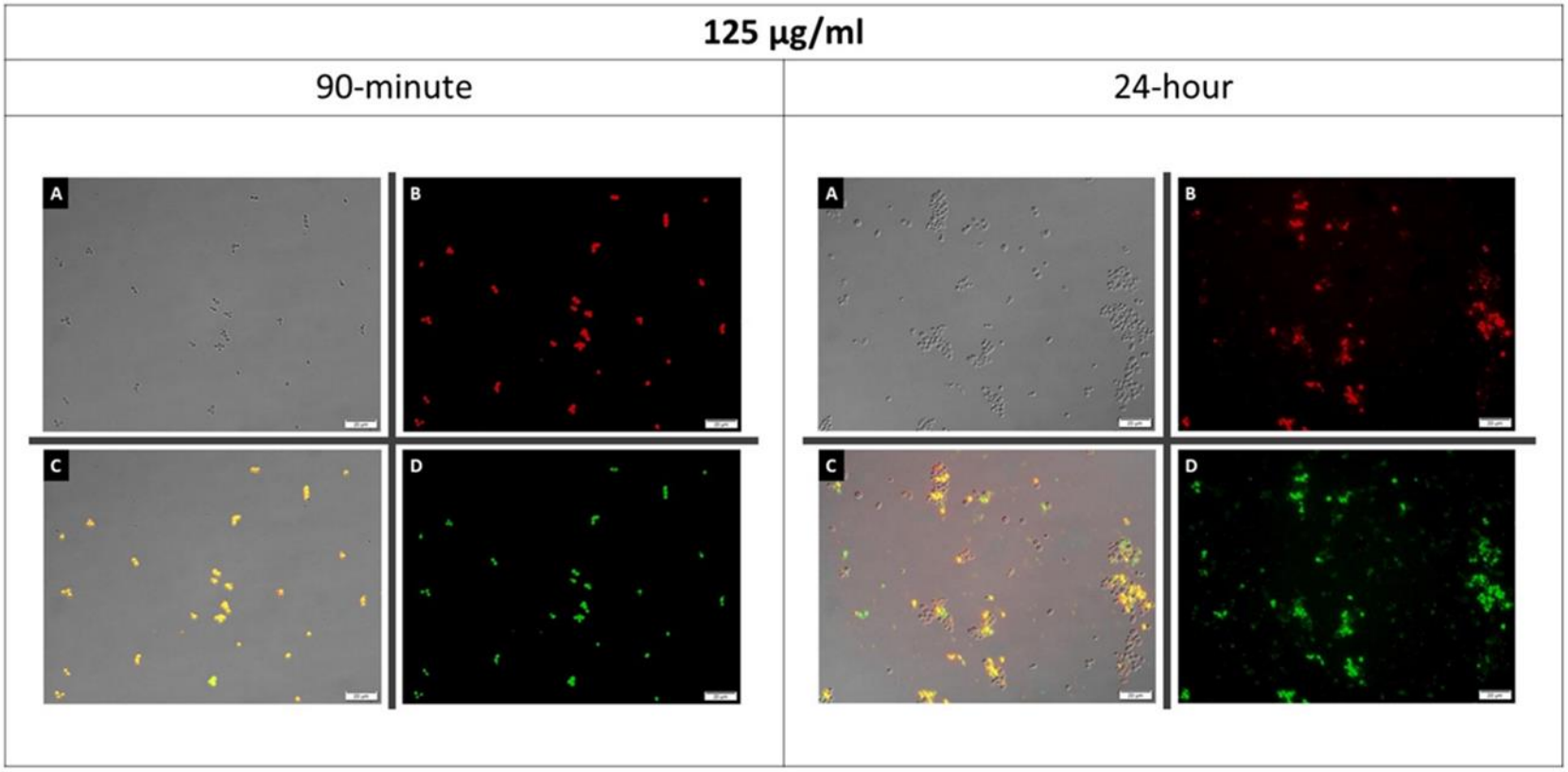

Figure 3.10. Micrographs for the 90-minute and 24-hour biofilms of *C. auris* that had been exposed to 125 µg/ml of DLAP-2. Micrographs were taken on the Olympus BX63 OFM. Observation of cells was achieved using a 60X oil immersion objective lens (Scale Bar: 20 µm). A- DIC Grey; B- FUN-1 fluorescent dye; C- Multitrack mode; D- Con A fluorescent dye. Green fluorescence- all intact cells (dead or alive) and biofilm matrix; red fluorescence- metabolically active cells.

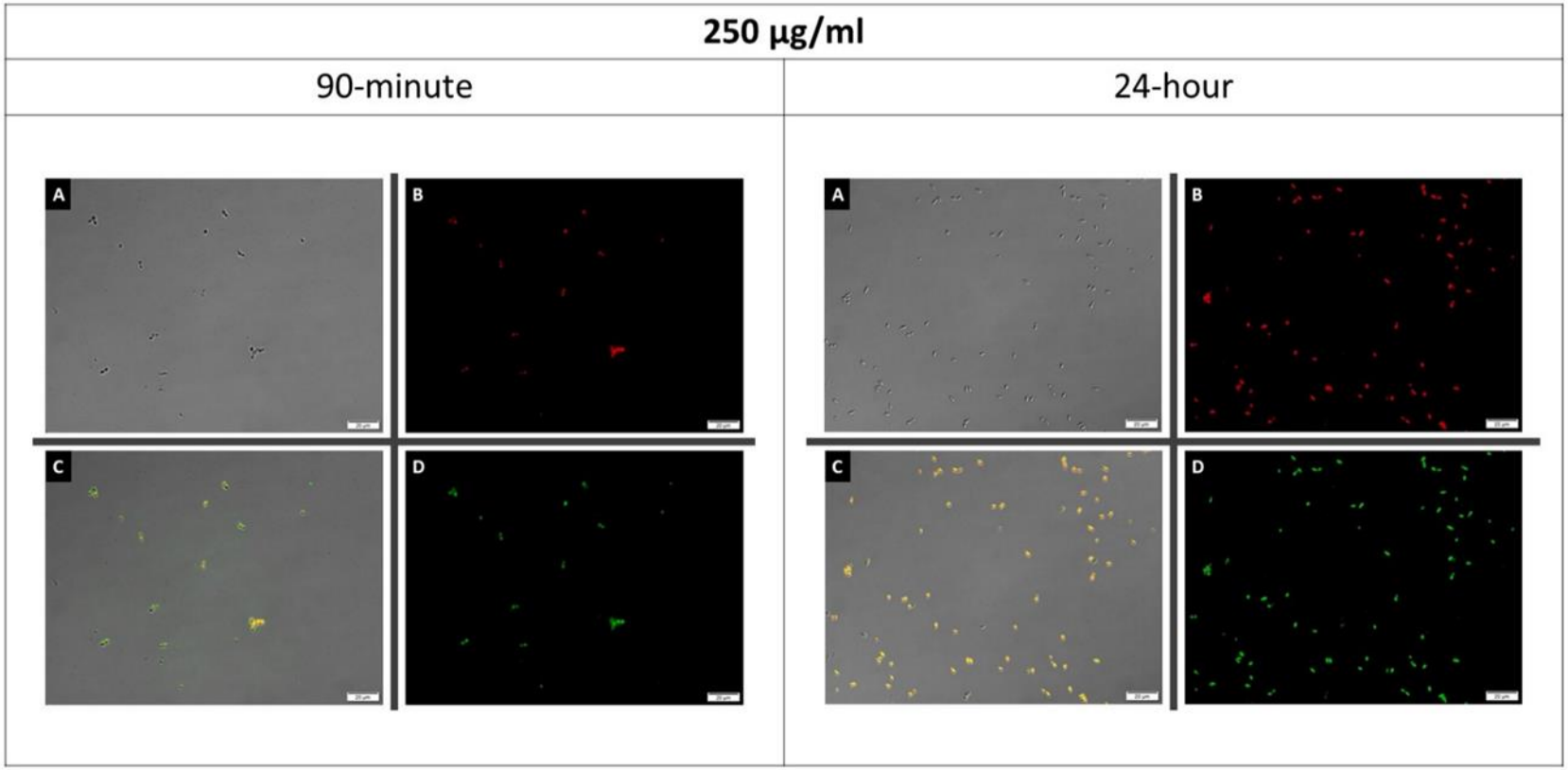

Figure 3.11. Micrographs for the 90-minute and 24-hour biofilms of *C. auris* that had been exposed to 250 µg/ml of DLAP-2. Micrographs were taken on the Olympus BX63 OFM. Observation of cells was achieved using a 60X oil immersion objective lens (Scale Bar: 20 µm). A- DIC Grey; B- FUN-1 fluorescent dye; C- Multitrack mode; D- Con A fluorescent dye. Green fluorescence- all intact cells (dead or alive) and biofilm matrix; red fluorescence- metabolically active cells. Green fluorescence- all intact cells (dead or alive) and biofilm matrix; red fluorescence- metabolically active cells.

***P. aeruginosa* ATCC 27853**

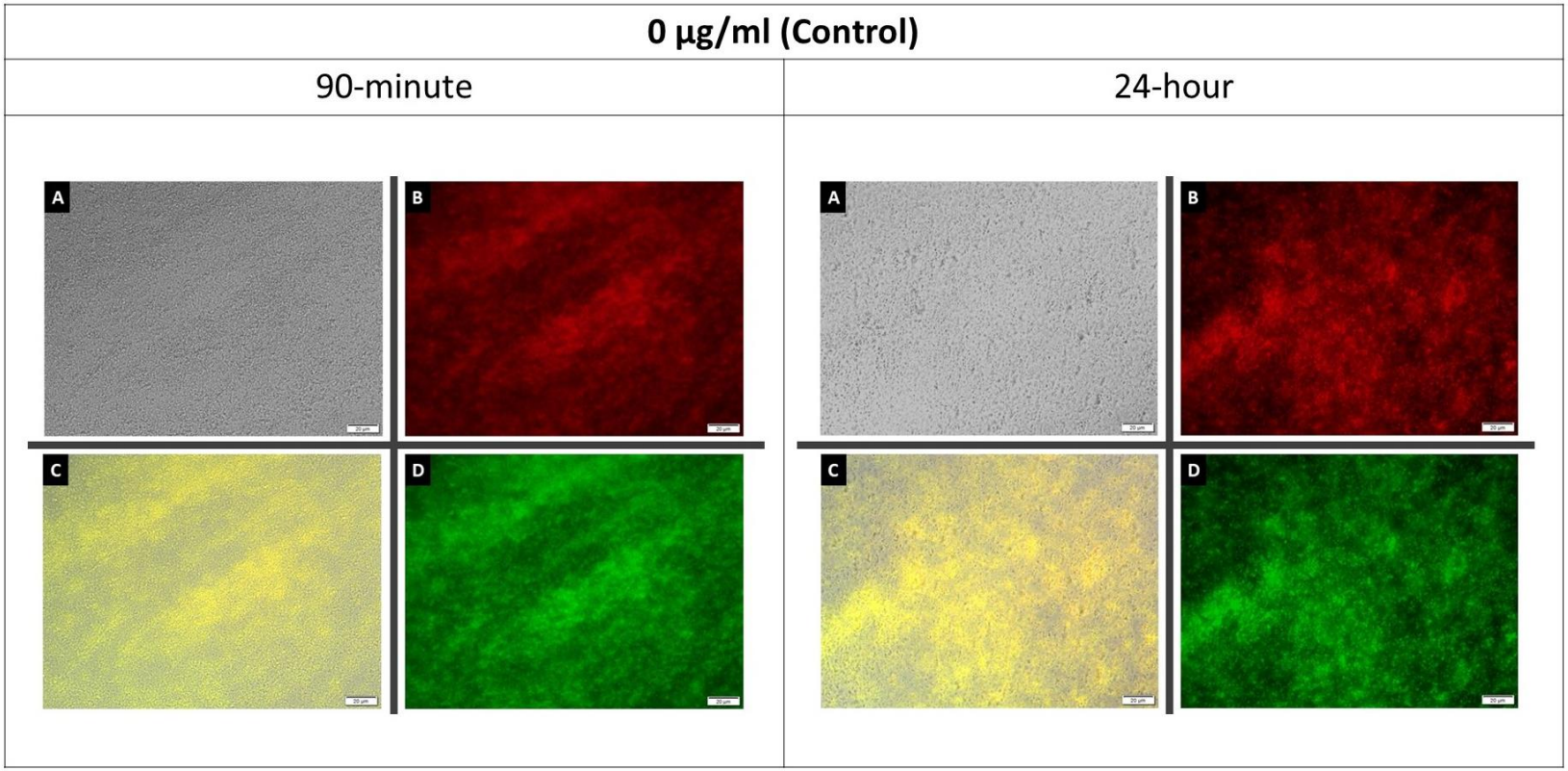

Figure 3.12. Micrographs for the 90-minute and 24-hour control biofilms of *P. aeruginosa*. Micrographs were taken on the Olympus BX63 OFM. Observation of cells was achieved using a 60X oil immersion objective lens (Scale Bar: 20 µm). A- DIC Grey; B- FUN-1 fluorescent dye; C- Multitrack mode; D- Con A fluorescent dye. Green fluorescence- all intact cells (dead or alive) and biofilm matrix; red fluorescence- metabolically active cells.

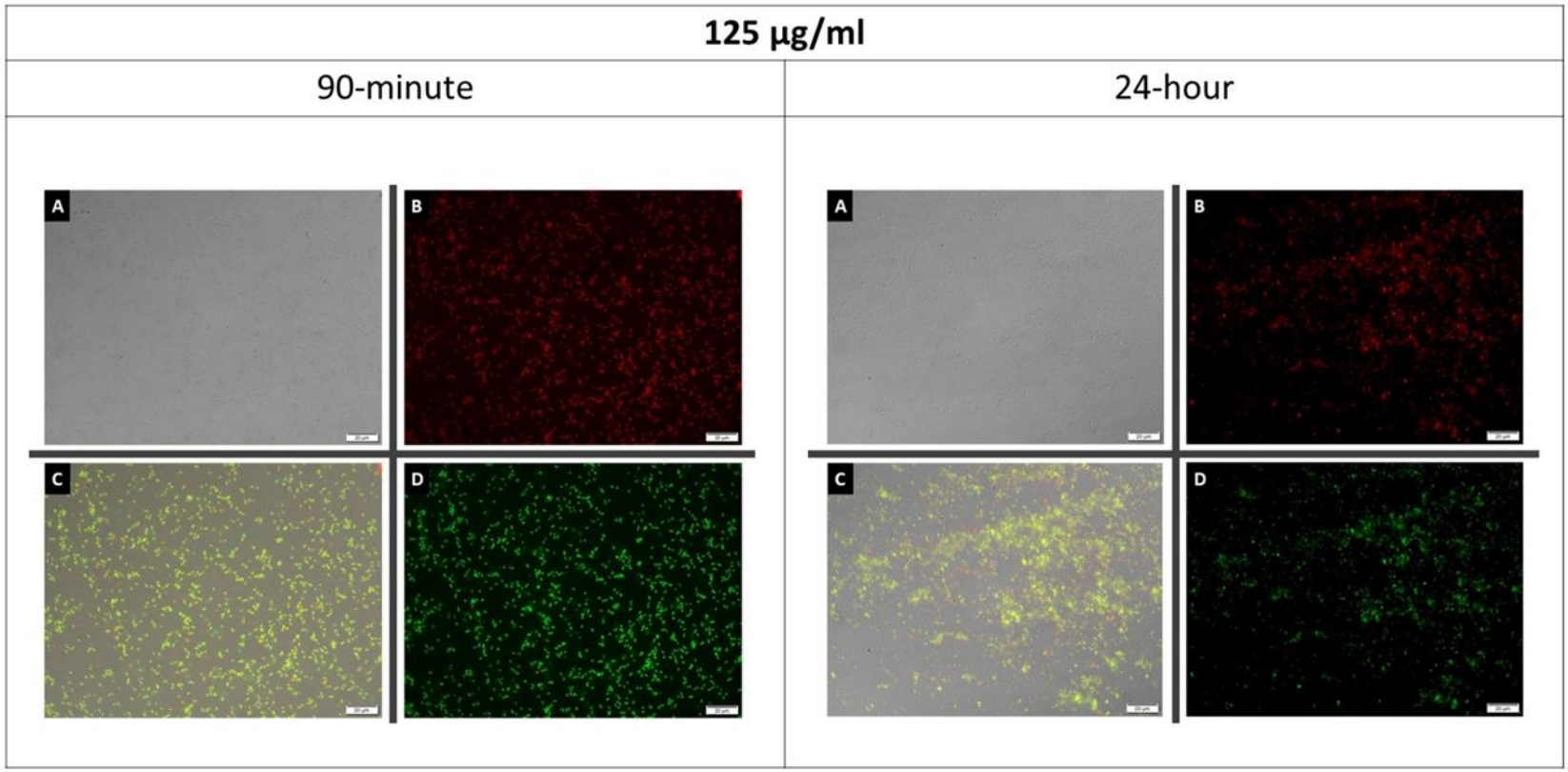

Figure 3.13. Micrographs for the 90-minute and 24-hour biofilms of *P. aeruginosa* that had been exposed to 125 µg/ml of DLAP-2. Micrographs were taken on the Olympus BX63 OFM. Observation of cells was achieved using a 60X oil immersion objective lens (Scale Bar: 20 µm). A- DIC Grey; B- FUN-1 fluorescent dye; C- Multitrack mode; D- Con A fluorescent dye. Green fluorescence- all intact cells (dead or alive) and biofilm matrix; red fluorescence- metabolically active cells.

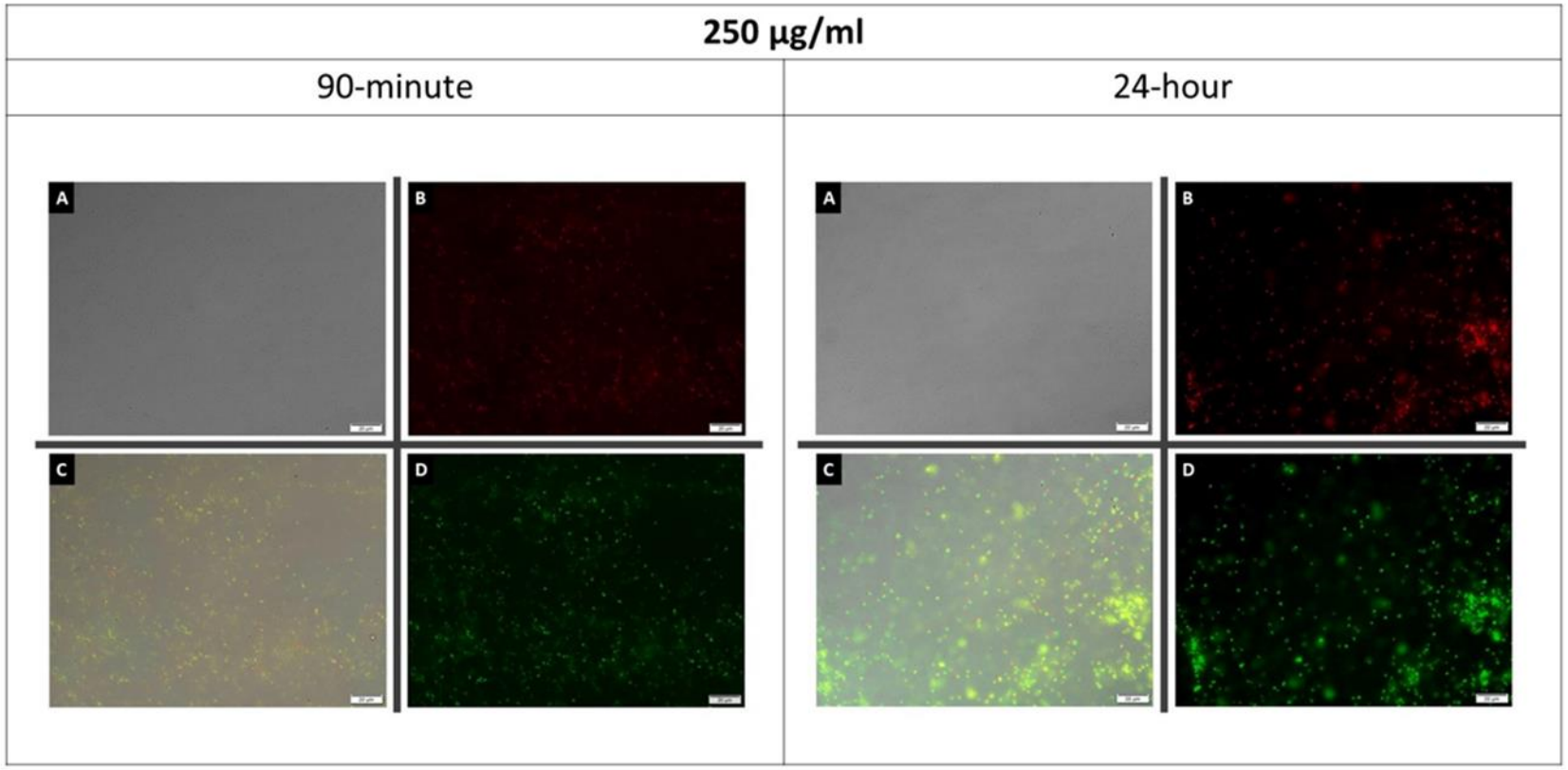

Figure 3.14. Micrographs for the 90-minute and 24-hour biofilms of *P. aeruginosa* that had been exposed to 250 µg/ml of DLAP-2. Micrographs were taken on the Olympus BX63 OFM. Observation of cells was achieved using a 60X oil immersion objective lens (Scale Bar: 20 µm). A- DIC Grey; B- FUN-1 fluorescent dye; C- Multitrack mode; D- Con A fluorescent dye. Green fluorescence- all intact cells (dead or alive) and biofilm matrix; red fluorescence- metabolically active cells.

3.4.2 Polymicrobial Biofilms

Combination or mixed cell cultures (*C. auris* MRL 6057 and *P. aeruginosa* ATCC 27853)

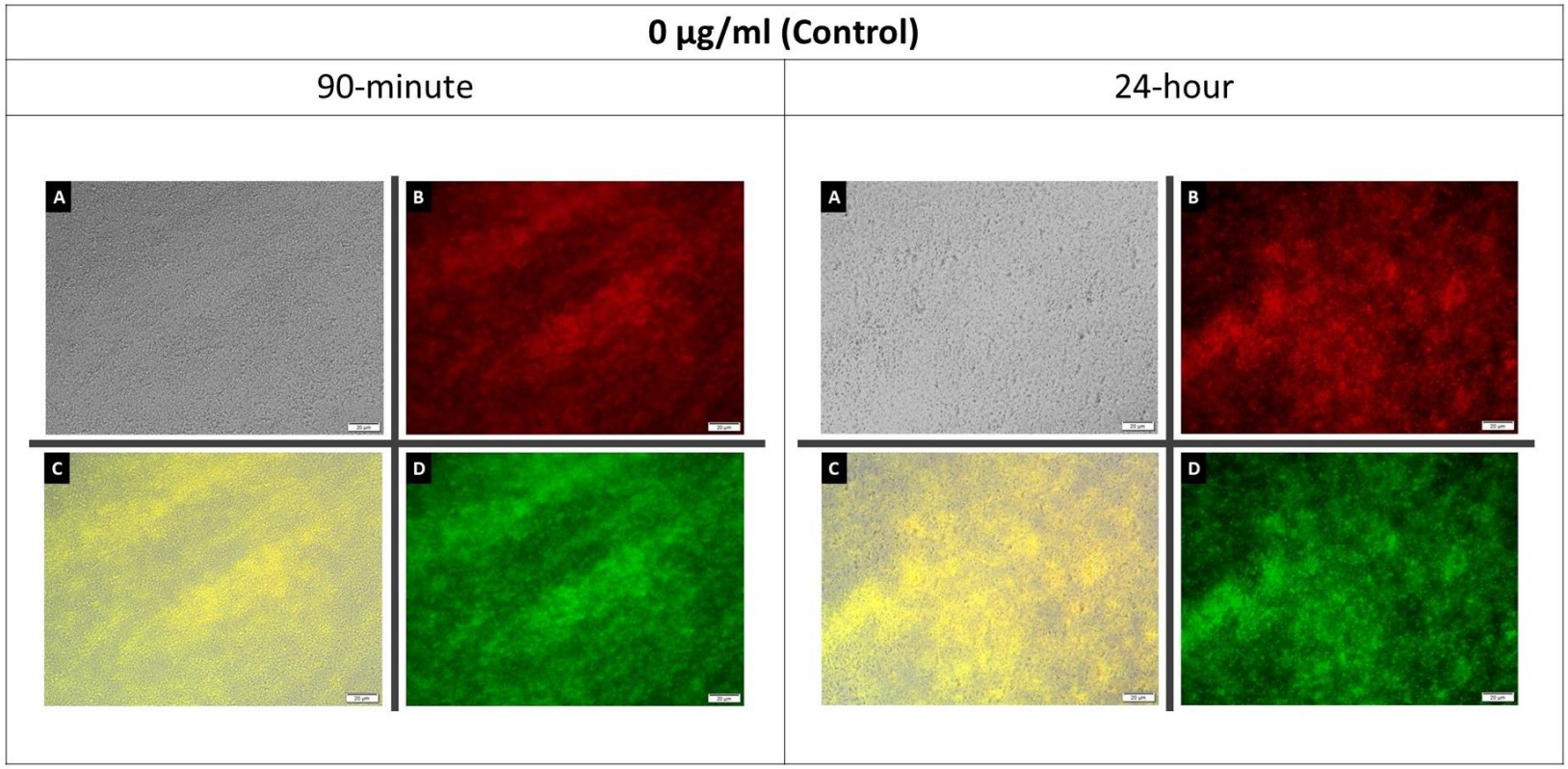

Figure 3.15. Micrographs for the 90-minute and 24-hour controls of polymicrobial biofilms (*C. auris* and *P. aeruginosa*). Micrographs were taken on the Olympus BX63 OFM. Observation of cells was achieved using a 60X oil immersion objective lens (Scale Bar: 20 µm). A- DIC Grey; B- FUN-1 fluorescent dye; C- Multitrack mode; D- Con A fluorescent dye. Green fluorescence- all intact cells (dead or alive) and biofilm matrix; red fluorescence- metabolically active cells.

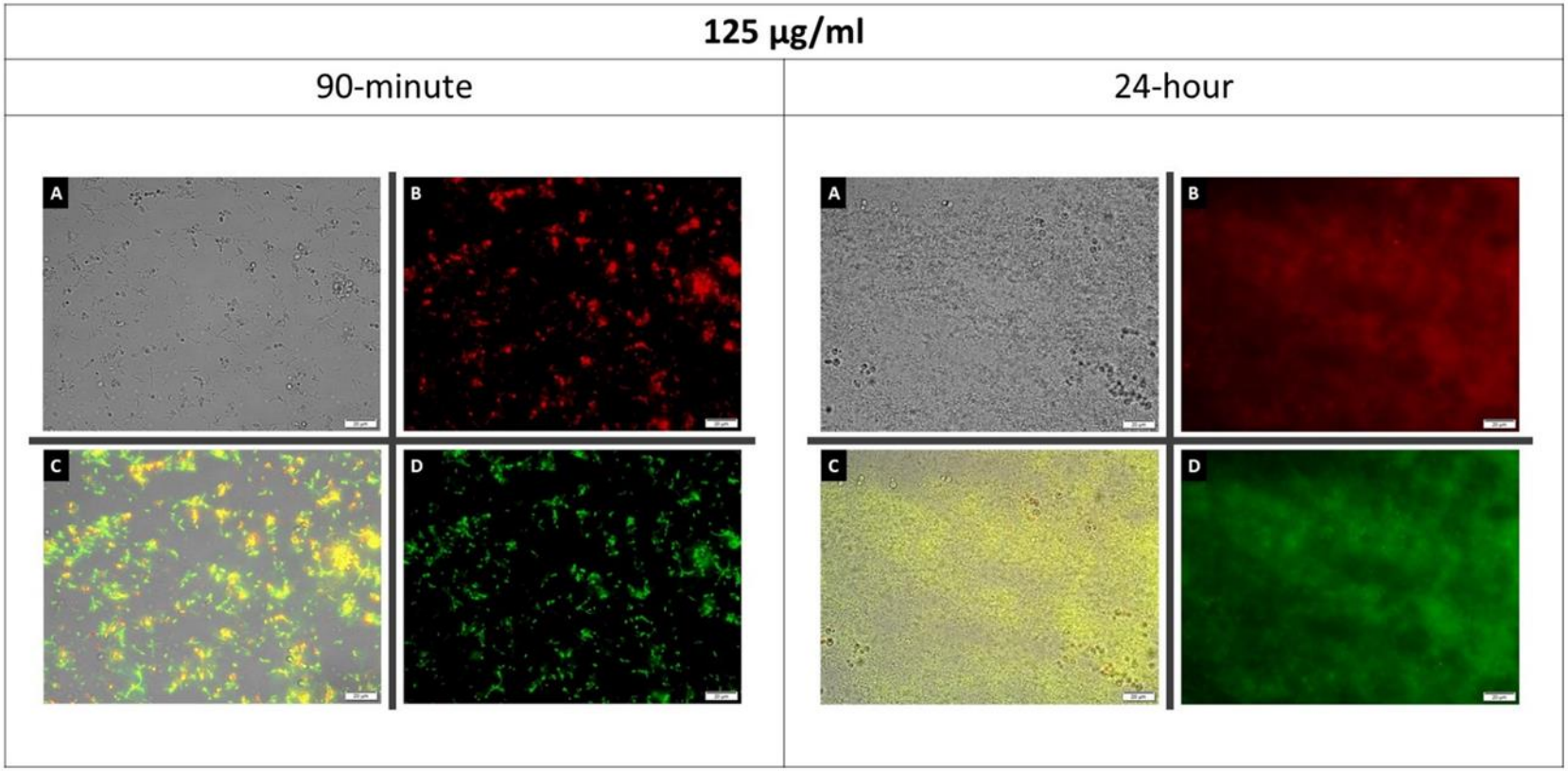

Figure 3.16. Micrographs for the 90-minute and 24-hour combination or polymicrobial biofilms (*C. auris* and *P. aeruginosa*) that were exposed to 125 µg/ml of DLAP-2. Micrographs were taken on the Olympus BX63 OFM. Observation of cells was achieved using a 60X oil immersion objective lens (Scale Bar: 20 µm). A- DIC Grey; B- FUN-1 fluorescent dye; C- Multitrack mode; D- Con A fluorescent dye. Green fluorescence- all intact cells (dead or alive) and biofilm matrix; red fluorescence- metabolically active cells.

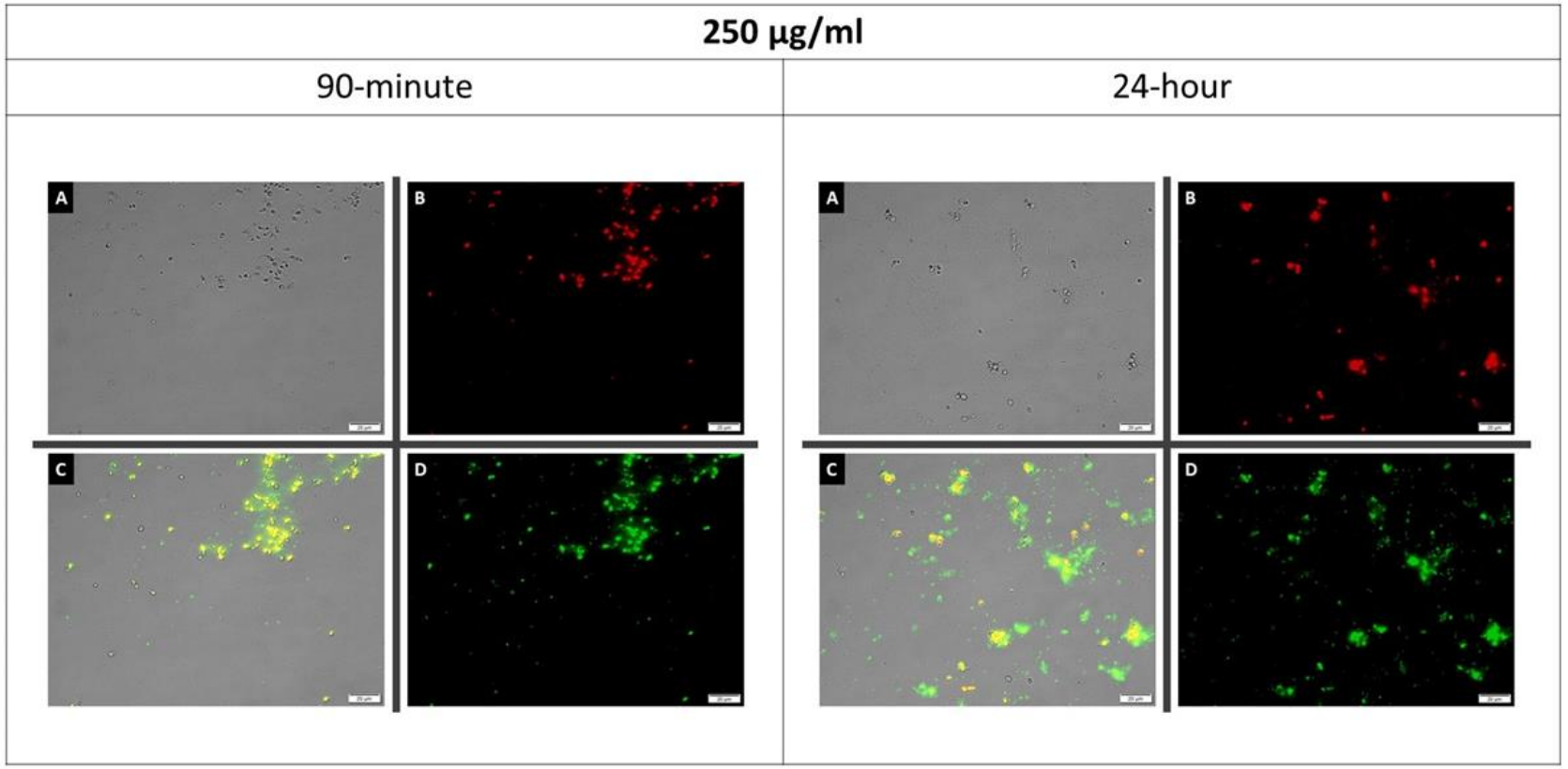

Figure 3.17. Micrographs for the 90-minute and 24-hour combination or polymicrobial biofilms (*C. auris* and *P. aeruginosa*) that were exposed to 250 µg/ml of DLAP-2. Micrographs were taken on the Olympus BX63 OFM. Observation of cells was achieved using a 60X oil immersion objective lens (Scale Bar: 20 µm). A- DIC Grey; B- FUN-1 fluorescent dye; C- Multitrack mode; D- Con A fluorescent dye. Green fluorescence- all intact cells (dead or alive) and biofilm matrix; red fluorescence- metabolically active cells.

3.5 Cell membrane integrity

The micrographs under investigation include Figure 3.18, Figure 3.19, and Figure 3.20. *C. auris* cells in single microbial cell suspensions were exposed to DLAP-2 at concentrations of 62,5 µg/ml (MIC) and 125 µg/ml (MFC) (please see Figure 3.18). Not only were there fewer cells in the exposed samples than when compared to the negative control, but also a significant number of these cells illustrated PI-positive staining (through orange fluorescence) and therefore indicated compromised cell membrane integrity. The same trend was seen in single cell-suspensions of *P. aeruginosa* (please see Figure 3.19), as well as in combination cell suspensions (please see Figure 3.20), which demonstrated higher MIC (125 µg/ml) and MBC/MFC (250 µg/ml) values as recorded in the AST section of this study. The level of fluorescence in each of these samples was on par with or greater than that of the established positive controls. This stands in stark contrast with the results of the negative control, as these healthy cells illustrated minimal to no fluorescence. In the negative control photomicrographs where some fluorescence can be seen, it can be attributed to the phenomenon known as programmed cell death. These cells are either no longer needed or have aged, and therefore undergo a process of apoptosis and die. This is a natural part of the cell cycle and the few cells which appear to have compromised cell membranes in the growth control photomicrographs are not because of exposure to environmental stress or toxic and antimicrobial compounds, as they are in the MIC and MBC/MFC samples.

These results, therefore, indicate that DLAP-2 has some antibacterial and antifungal effect on planktonic cells. It can further be concluded that compromising cell membrane integrity and consequently causing intracellular component leakage, is *one* of the mechanisms of action that this antimicrobial agent (DLAP-2) utilises to bring about cell death. However, further studies would need to be conducted to conclusively prove this to be the agent's exclusive mechanism of antimicrobial action.

3.5.1 Single planktonic cell-suspensions

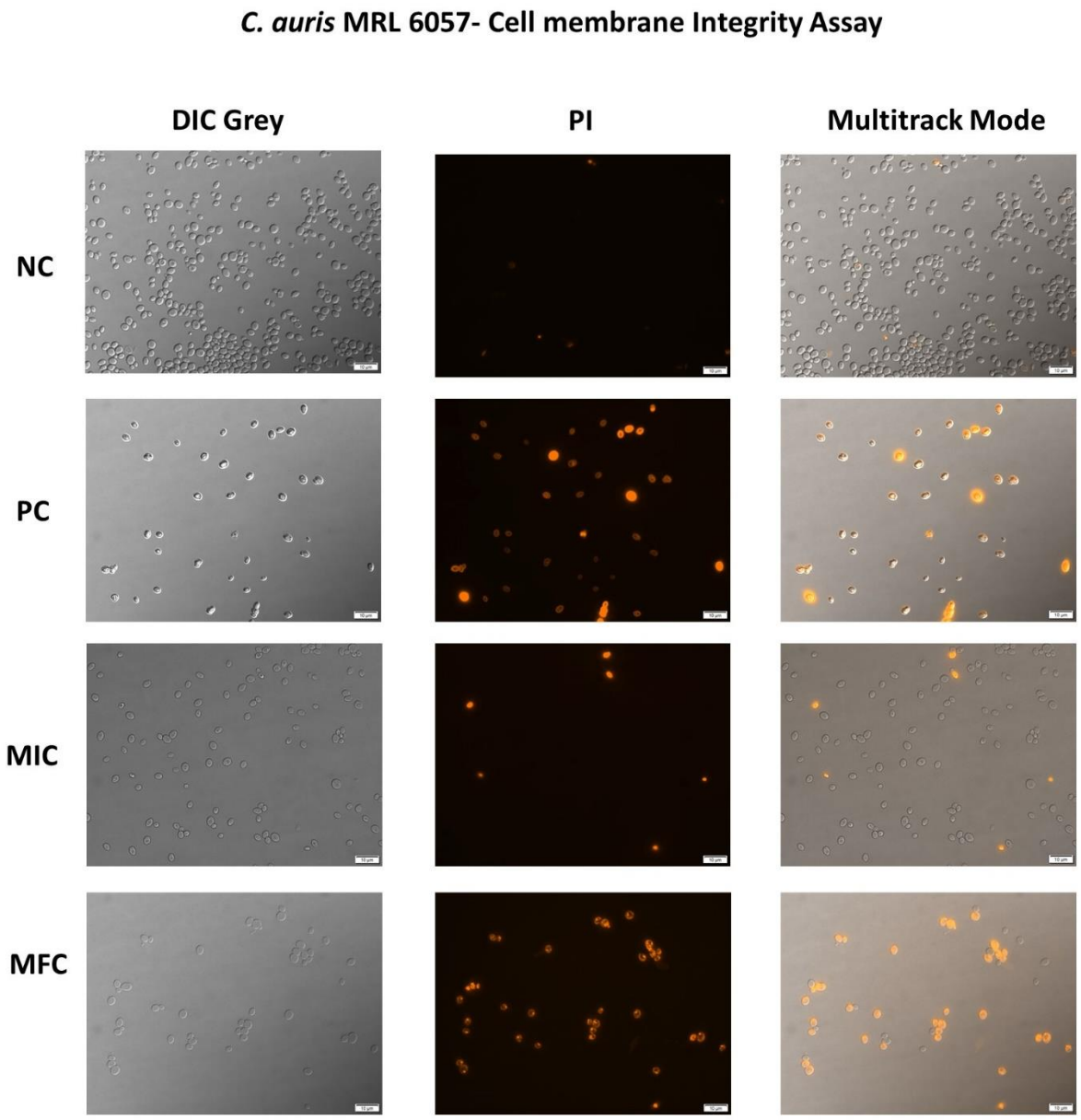

Figure 3.18. Micrographs of cell membrane integrity for *C. auris* planktonic cells, monitored by PI. NC- negative control sample, PC- positive control sample set up using hydrogen peroxide (H_2O_2). MIC- for *C. auris* is 62,5 µg/ml (DLAP-2) and MFC- 125 µg/ml (DLAP-2). Micrographs were captured using a 100X oil immersion objective (Scale Bar: 10 µm) on the Olympus BX63 OFM. Orange/red fluorescence indicates cells with compromised cell membranes.

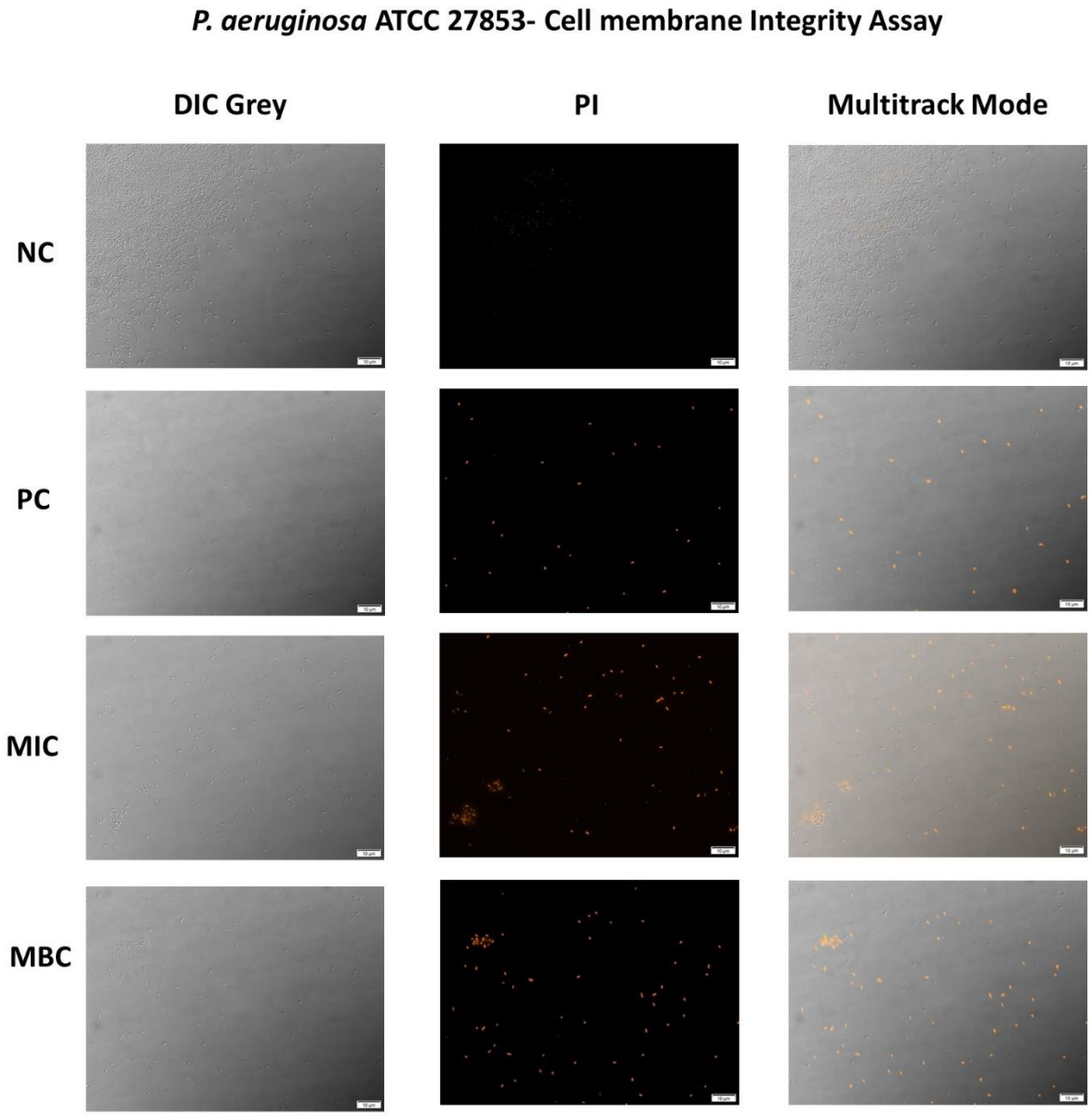

Figure 3.19. Micrographs of cell membrane integrity for *P. aeruginosa* planktonic cells, monitored by PI. NC- negative control sample, PC- positive control sample set up using hydrogen peroxide (H_2O_2). MIC- for *P. aeruginosa* 125 µg/ml (DLAP-2) and MBC- 250 µg/ml (DLAP-2). Micrographs were captured using a 100X oil immersion objective (Scale Bar: 10 µm) on the Olympus BX63 OFM. Orange/red fluorescence indicates cells with compromised cell membranes.

3.5.2 Mixed planktonic cell-suspensions

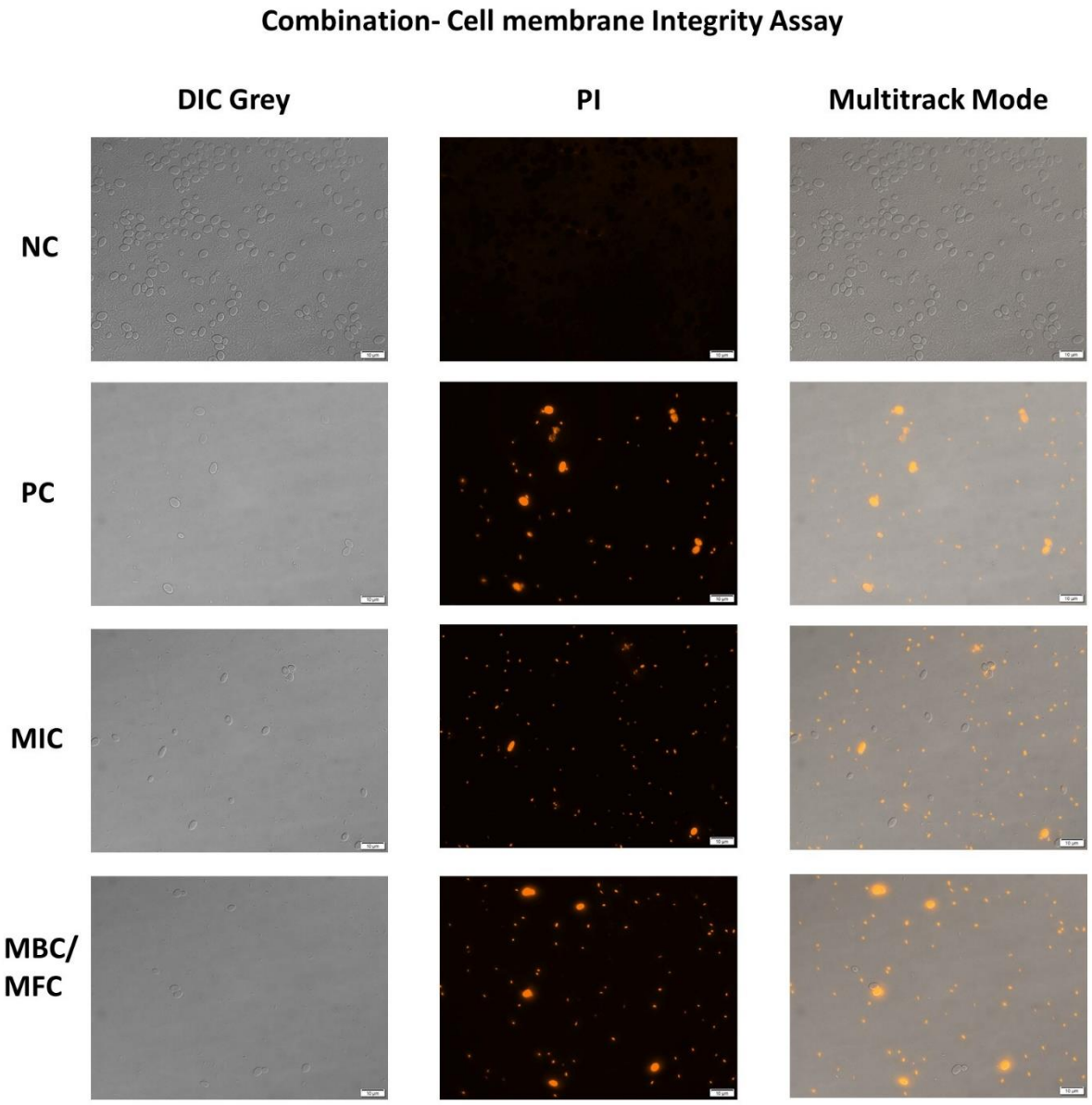

Figure 3.20. Micrographs of cell membrane integrity for combination (*C. auris* and *P. aeruginosa*) planktonic cell suspensions, monitored by PI. NC- negative control sample, PC- positive control sample set up using hydrogen peroxide (H_2O_2). MIC- for combination suspensions is 125 µg/ml (DLAP-2) and MBC/MFC- 250 µg/ml (DLAP-2). Micrographs were captured using a 100X oil immersion objective (Scale Bar: 10 µm) on the Olympus BX63 OFM. Orange/red fluorescence indicates cells with compromised cell membranes.

3.6 Cytotoxicity

For this experiment, equine blood was used. For comparison, a 1% Triton X-100 sample was set up as the positive control. At low concentrations, Triton X-100 is known for its ability to disintegrate mammalian RBCs. This chemical achieves this by removing cell membrane associated lipids and increasing membrane permeability. This leads to compromised cell membrane integrity and eventual cell lysis (Thermo Fisher Scientific, 2023). A negative control was also established, containing RBCs suspended in PBS. These samples brought about approximately 100% and 0% haemolysis, respectively. Figure 3.21 shows two of the most important steps that were involved in the experimental procedure for determining the haemolytic activity of DLAP-2. At varying concentrations (MIC, 2xMIC and 3xMIC), the compound, DLAP-2, showed haemolytic activity ranging from 0%- 82,9% (as seen in Table 3.4, and Figure 3.22).

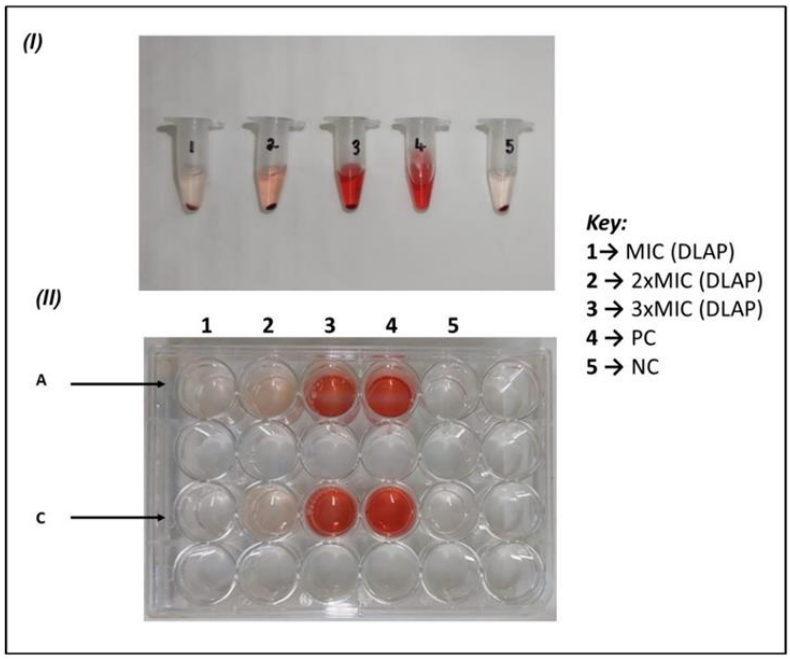

Figure 3.21. Haemolytic assay procedure. **(*I*)** shows the labelled samples which were incubated and centrifuged to separate the supernatant and pellet. **(*II*)** shows the 24-well plate into which the supernatants were aliquoted. From here, these plates underwent spectrophotometry. Samples 1, 2 and 3 contain DLAP-2 concentrations of 125 µg/ml (MIC), 250 µg/ml (2XMIC) and 375 µg/ml (3XMIC), respectively. Sample 4 is the positive control, which contains Triton X-100 which causes complete (or 100%) haemolysis. Lastly, sample 5 is the negative control which contains RBCs and PBS only, no (or 0%) haemolysis occurs in this control.

Table 3.4. Mean percentage haemolysis values for varying concentrations of DLAP-2 and their respective standard deviations.

Concentration	Percentage Haemolysis (%) Mean *(n=6)*	Standard Deviation
MIC (125 µg/ml)	0,83	2,04
2XMIC (250 µg/ml)	10	5,22
3XMIC (375 µg/ml)	82,83	9,02

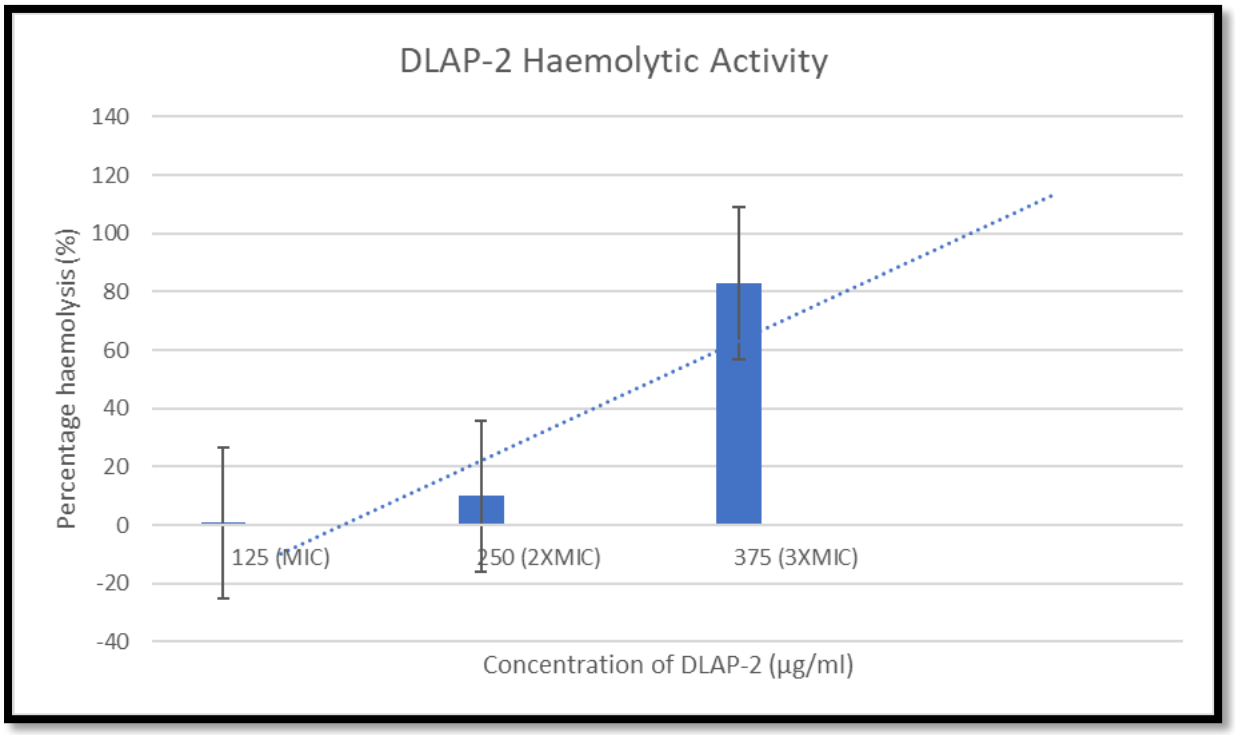

Figure 3.22. The haemolysis of RBCs at varying concentrations of DLAP-2 (p-value < 0,0001). 1% Triton X-100 was used as a positive control (100% haemolysis) and PBS was used as a negative control (0% haemolysis).

A comparison was made across three concentrations using a one-way ANOVA test, the results of which are summarised in Appendix III. Statistically significant results yielded from an ANOVA are an indication that the group means are not all equal. However, this test does not identify which differences between sets of means are statistically significant. For this reason, a *post hoc* analysis was conducted using the Bonferroni method. The ANOVA showed an overall p-value > 0,0001, indicating statistical significance. The Bonferroni test showed that, when comparing the 125 µg/ml and 250 µg/ml concentration groups, the difference between the two was not significant (p-value = 0,062), indicating similar levels of haemolysis. Additionally, the difference between groups 125 µg/ml and 375 µg/ml (p-value > 0,001), as well as

between 250 µg/ml and 375 µg/ml (p-value > 0,001), were highly significant, meaning that haemolysis levels at concentrations of 375 µg/ml were considerably higher. The standard deviations for each concentration level also shows that the variability in experimental repeats was higher for the 250 µg/ml and 375 µg/ml concentration groups.

CHAPTER 4: DISCUSSION

4.1 Contextualization of study findings

As discussed in the literature review, the continuous development of AMR is a serious challenge that is currently plaguing the world of medicine (Fletcher, 2015). Cases of pan-drug resistant infections are on the rise, and healthcare workers remain desperate for the discovery of new and effective antimicrobials (Bassetti *et al.,* 2018; (Du *et al.,* 2020). Additionally, fungi and bacteria have been described as two of the greatest etiological contributors to global infections and associated mortality rates (Horton and Nett, 2020; Zhang *et al.,* 2022). *C. auris* and *P. aeruginosa* were contextualized as being two pathogens of major concern when it comes to the advancement of AMR. This is true on a global scale as well as locally, i.e., in South Africa. These key pathogens also share a few other qualities which make them important within the field of medicine. These qualities include high levels of infectiousness, especially within an immunocompromised population, and the proficiency to form complex and protective biofilm structures. Consequently, this study aimed to provide more data on the antimicrobial and antibiofilm activity of a promising defensin compound known as, DLAP-2.

Defensins have been characterized as small, immunogenic molecules, secreted by various human bodily tissues (Liu *et al.,* 2008). Their function forms a component of innate immunity, a system aimed at destroying and eradicating potentially harmful organisms or substances that have invaded or been introduced into the body of a human host (Liu *et al.,* 2008). Antimicrobial peptides have become an area of interest which is attributable to their non-specific mechanism of action. This trait promises broad-spectrum activity against a myriad of infections, but also an unlikely tendency for the development of associated resistance. Furthermore, since their discovery, scientists have attempted to synthetically engineer linear analogues of these traditionally endogenous peptides to develop a novel class of antimicrobial agent (Liu *et al.,* 2008).

Many scientific articles can be found on the varying origins, targets, and effectiveness of these defensin peptides. Papers have been written and published on their presence in marine life (fish) (Barroso *et al.,* 2021), plants (Henrik *et al.,* 2009), insects (Otvos,

2000) and especially in mammals (Hughes, 1999), just to name a few. This study, however, has focused on human defensins (Dhople *et al.,* 2006).

Consequently, this study involved performing several experiments to help define the clinical potential of a synthetic defensin-like protein for use as an effective antimicrobial and antibiofilm remedy.

4.2 Antimicrobial activity

The antimicrobial activity assays for this study were very important in establishing the minimum concentrations of DLAP-2 which would still have inhibitory or even lethal effects on microbial cells. These MIC and MBC/MFC concentrations were needed as they were used to evaluate the antibiofilm activity of DLAP-2.

The results showed that DLAP-2 had good antibacterial and antifungal capabilities at relatively low concentrations with a stronger inhibitory effect against *C auris*. However, an interesting decrease in DLAP-2's inhibitory effect against *C. auris* was observed when these cells were in mixed cell suspensions with *P. aeruginosa*. This finding supported reports by the existing literature that polymicrobial cell cultures have the potential to exhibit increased resistance to antimicrobial agents (Orazi and O'Toole, 2019). This same increase in MIC and MBC/MFC readings was not seen for *P. aeruginosa*. Further studies would need to be completed to conclusively account for this one-sided change. Nevertheless, one might assume that *P. aeruginosa* was responsible for this increase in resistance and facilitated the continued survival of *C. auris* cells even at higher antimicrobial concentrations. The microorganisms of interest were also assessed for their resistance profiles against mainstream antimicrobial agents, commonly used to treat clinical infections. *C. auris* was run against amphotericin B to which it was found to be resistant. The observed MIC value (15,62 µg/ml) was significantly higher than that of the tentative MIC breakpoint value (≥ 2 µg/ml) as recommended by the CDC (Centers for Disease Control and Prevention, 2020). *P. aeruginosa* on the other hand, was run against gentamicin (MIC of 3,91 µg/ml), to which it was found to be susceptible when compared to the tentative MIC breakpoints (≥ 16 µg/ml), as stipulated by the CLSI (Clinical and Laboratory Standards Institute, 2022).

Tentative breakpoints could not be found for both pathogens from the same institute as there is no available data for amphotericin B against any *Candida* species in official CLSI documents (Uprety and Lockhart, 2022). This poses a challenge for healthcare professionals when treating serious cases of candidemia. However, most clinical, and diagnostic laboratory staff use the tentative breakpoints as stipulated by the results of a small study conducted for amphotericin B against most *Candida* species. This method of approach has not been without its problems, as recent reports have shown that in certain parts of the world, more than 33% of collected isolates of *C. auris* have an MIC value against amphotericin B that far exceed the stipulated acceptable limits (Uprety and Lockhart, 2022). Our chosen strain of *C. auris*, therefore, falls within this same category. Moreover, discrepancies in the recorded MIC value of *C. auris* against amphotericin B in our study and another study conducted before 2020 (Srivastava and Ahmad, 2020), shows a substantial increase in the resistance of this pathogen to the chosen antifungal. This difference is thought to be attributed to increased levels of resistance obtained by this pathogen over the ±3-year period or, differences in laboratory and researcher conditions.

While no scientific articles could be found that investigated a peptide with an identical amino acid sequence to that of DLAP-2, a few papers were found on HβD-3 and its linear analogues. As mentioned in the literature review above, HβD-3 has the most similar amino acid sequence (or primary structure) to DLAP-2 and can be described as the naturally occurring defensin from which DLAP-2 was modelled. For this reason, a comparison will be drawn from the results in this study to those completed using HβD-3 and its synthetically engineered linear analogues. One study found MIC_{90} values (minimum inhibitory concentrations needed to cause 90% mortality rates in the pathogen under investigation) (Dhople *et al.,* 2006) for HβD-3 against *P. aeruginosa* ATCC 27853 as well as for *C. albicans* 99788, a strain known to be resistant to amphotericin B. These MIC_{90} values were as follows; 13 µg/ml and 18 µg/ml, respectively (Dhople *et al.,* 2006). Compared to the MIC and MBC/MFC values established in this study for *P. aeruginosa* ATCC 27853 and for *Candida.* MRL 6057 against DLAP-2, our recordings showed much weaker inhibitory effects. The first important observation that can be made is the fact that this paper was published in 2006 (Dhople *et al.,* 2006). This means that the increase in AST values for the identical strain of *P. aeruginosa* could be due to the development of resistance in the ±17-years

since this paper was published. However, this difference in antimicrobial potentials could also be due to significant disagreements in the chemical structure and properties of naturally occurring HβD-3, and the synthetically constructed DLAP-2. Nevertheless, nothing can be stated for certain, as a myriad of contributing factors may be at play here and further research would be needed to enhance our understanding of this observed change. It has been established, however, that the antimicrobial activity of HβD-3 and its linear analogues can be attributed to unique structure-function relationships as well as an ability to interact with liposomes within the human body. It is these interactions that contribute to its antimicrobial action in Gram-positive and Gram-negative bacteria specifically, with an MIC value ranging from 25-150 µg/ml (Dhople *et al.,* 2006). Therefore, despite the discrepancies mentioned earlier, the results for this study (Gram-negative *P. aeruginosa* had an MIC of 125 µg/ml) are still in alignment with the findings in this existing literature (Dhople *et al.,* 2006).

A second study conducted in 2008 also investigated the antimicrobial activity of wild-type HβD-3 and a few of its synthetically engineered linear analogues. The two compounds most closely related (by amino acid sequence) to DLAP-2, were wild-type HβD-3 and a synthetic linear analogue coded as C(Acm)6 (Liu *et al.,* 2008). Both peptides were recorded as having the following amino acid sequence; **CIINTLQKYYCRVRCCRC-AVLSCLPKEEQICKCSTRCRKCCRRKK.** Similar to the first study, the wild-type HβD-3 and synthetic C(Acm)6 shared amino acid sequence similarities with DLAP-2 only in the second portion of the described sequence; (**AVLSCLPKEEQICKCSTRCRKCCRRKK)**. Comparisons and results, however, will still be discussed, but it is important to note that additional research is needed to understand the impact of the amino acid sequence discrepancies on the varying antimicrobial activities that were observed for each peptide. With this in mind, we can summarise the antimicrobial activity results as follows; against an undisclosed strain of *P. aeruginosa,* wild-type HβD-3 showed MIC values of 2,7 µg/ml and an MBC of 11,4 µg/ml (Liu *et al.,* 2008). Furthermore, the synthetic linear analogue, C(Acm)6, demonstrated an MIC value of 11,2 µg/ml and an MBC of 24,7 µg/ml. From this we can see that the human engineered linear analogue which had an identical amino acid sequence to that of the wild-type HβD-3, for an unknown reason, had lower antimicrobial activity against the same strain of *P. aeruginosa.* This same trend was observed for the 3 other species of bacteria that were investigated—*Escherichia coli*,

Staphylococcus aureus and *Bacillus cereus* (Liu *et al.,* 2008). This implies that the naturally occurring peptide (wild-type HβD-3) seems to possess additional attributes which increase its antimicrobial activity, attributes which were not replicated in the synthetically engineered linear analogues. Comparatively, when these MIC and MBC values are compared to those obtained for DLAP-2 against *P. aeruginosa,* DLAP-2 showed lower antimicrobial activity with higher MIC and MBC values. A direct comparison, however, would also not be appropriate considering the strain of *P. aeruginosa* under investigation in the study is unknown.

4.3 Biofilms and DLAP-2

Determining the antibiofilm activity of DLAP-2 included performing: (a) a colorimetric assay (MTT assay) for determining cell metabolic activity, (b) a microbial cell viability assessment, and (c) growing untreated and treated biofilms for visualisation on a fluorescence microscope. The major take-away trend which could be confirmed when looking at the results for all three assessments was that as the concentration of DLAP-2 increased, so the density and number of viable cells present in these biofilms decreased. This trend was confirmed quantitatively through experiments (a) and (b) and was also easily visualised (qualitatively) using method (c). However, significant differences in the levels of biofilm inhibition could not always be observed when comparing immature and mature biofilms.

The results of the MTT assay indicated that the highest levels of biofilm inhibition occurred in the polymicrobial biofilms which were made up of *C. auris* and *P. aeruginosa* cells together. Additionally, the lowest levels of inhibition were seen in monomicrobial biofilms that were made up of *P. aeruginosa*. This was true for immature and mature biofilms at the two highest concentrations of DLAP-2. This finding was surprising as it was expected that the inverse would be observed. Polymicrobial biofilms were expected to show the lowest levels of inhibition whilst monomicrobial biofilms were expected to exhibit the highest levels of biofilm inhibition. These anticipated findings would have been in alignment with previous literature which stipulates that biofilms that are made up of multiple species of microorganisms exhibit higher levels of resistance to antimicrobial agents (Orazi and O'Toole, 2019). This

unexpected outcome could be because of an unexplained interspecies relationship between *C. auris* and *P. aeruginosa* cells when grown in the same biofilm. An additional explanation would be that the treated wells in this study were each compared to their own untreated controls. Since these controls could not be identical when following the stipulated procedures for this experiment, some data bias could be at play. Repeating these experiments using an alternative method may help to clarify any limitations or additional variables that are contributing to these unexpected outcomes. The issue with this assay, is that determining cell viability by means of optical density is not always highly accurate. MTT is capable of staining more than just viable cells. The colour changes due to MTT staining that was observed could have been due to the presence of biofilm matrix or other substances within the reaction vessel. For this reason, a second more sensitive antibiofilm assay was conducted, to verify the findings, namely the microbial cell viability assessment.

The results from the microbial cell viability assessments, on the other hand, were a better representation of this expected trend in most of the datasets. When compared to polymicrobial Log10 CFU/ml values, a greater decrease in the number of viable cells after exposure to the highest concentrations of DLAP-2 was observed in immature and mature monomicrobial biofilms of *P. aeruginosa*. The same can be said for immature monomicrobial biofilms made up of *C. auris*. Nonetheless, in mature monomicrobial biofilms of *C. auris*, whilst the number of viable cells was greater when compared to polymicrobial biofilm values for *C. auris*, the overall decline in the number of viable cells was not as significant. Moreover, the statistical analysis for the microbial cell viability assessment revealed that there was a significant difference between the number of viable cells found in immature and mature biofilms. As duration—the period for which biofilms were allowed to develop—increased, so the number of viable cells increased, even in post-treated samples. This confirms the idea that more well-established biofilms have superior tendencies for resisting the effects of antimicrobials (Sharma, Misba and Khan, 2019). When comparing the calculated 98% reduction in viable cells in treated samples that were exposed to 125 µg/ml of DLAP-2 or more, for this assay, to the biofilm percentage reduction values in the previous assay, the microbial cell viability assessment boasted much higher levels of inhibition/reduction. Using optical density and an MTT stain to determine the number of viable cells within a biofilm is not as accurate as the microbial cell viability method. This is because MTT

is capable of staining cells, biofilm matrix along with other components within the reaction vessel. This leads to potential errors in the observed readings. Therefore, for this study it is believed that the microbial cell viability results are a better reflection of the true inhibitory action of DLAP-2 on biofilms.

For the qualitative or visual portion of this study, two fluorescent dyes were utilised. Fluorescence microscopy is a commonly used technique for studying microorganisms in microbiology. A wide variety of chemical substances exist which act as biological markers in the form of emitted light. When a sample that is stained with a fluorescent dye is exposed to light at the appropriate wavelength on a microscope slide, chemical compounds known as fluorochromes can absorb that light and reach a state known as excitation. These fluorochromes then re-emit this absorbed energy as light at an emission wavelength which can then be detected and interpreted (Molinari, 2015). Con A and FUN-1 staining on micrographs also showed that when DLAP-2 concentrations were increased, the number of cells and biofilm density was decreased significantly.

When taking all three sets of data into consideration, some discrepancies have obviously arisen. These would need to be further evaluated using a larger sample size as well as an experimental plan to decrease the contributions of unexplained or unidentified relationships or variables. One challenge was the lack of existing literature on *C. auris* and *P. aeruginosa* in mixed cell suspensions and polymicrobial biofilms. This makes it difficult to offer more insight into the dynamics of co-inhabited sites of infection. However, this means that this study is contributing significant new data and offers a starting point for addressing a clear gap in the existing body of literature.

The analysis of existing literature yielded three relevant scientific papers on the antimicrobial and antibiofilm activity of defensin molecules, more specifically, HβD-3 against multispecies biofilms and cell suspensions from isolated samples (Lee *et al.,* 2013; Song *et al.,* 2009; Zhu *et al.,* 2013). It is important to reiterate that HβD-3 is the naturally occurring peptide on which the synthetically engineered DLAP-2 was modelled.

The results of the studies conclusively agreed that HβD-3 exhibited impressive, broad-spectrum antimicrobial and antibiofilm effects against all the pathogenic strains under investigation (Lee *et al.,* 2013; Song *et al.,* 2009; Zhu *et al.,* 2013). The potency of

antimicrobial activity did, however, differ depending on the species and strain of the pathogens under investigation (Song *et al.,* 2009). Furthermore, HβD-3 treated biofilms exhibited high levels of sessile cell death (Lee *et al.,* 2013). It was also found that cells closer to the surface of the biofilms were more negatively affected by the antibiofilm agents (Lee *et al.,* 2013). This study also acknowledged that the superior antimicrobial activity of HβD-3 on bacterial biofilms may suggest that there are additional mechanisms of action by which this peptide is able to clear microbial infections, outside of the already discussed cell membrane permeabilization (Lee *et al.,* 2013). Additional research would be needed to confirm this hypothesis. HβD-3 was also found to inhibit continued biofilm development as well as reduce biofilm density in pre-existing or mature structures by interfering with the production of extracellular matrix components such as polysaccharides in bacteria (Zhu *et al.,* 2013).

Additionally, a study conducted on polymicrobial biofilms that were made up of *Candida albicans* and *Staphylococcus aureus* also had similar findings. When biofilms were treated with *Lactobacillus* metabolite extracts at MIC and MBC/MFC concentrations, inhibition of biofilms occurred at concentration-dependent levels. Higher concentrations of compound led to increased biofilm inhibition as well as more significant reductions in the number of viable cells found within these biofilm structures (Rather *et al*., 2023). The outlined conclusions are, therefore, in agreement with the findings of our study which utilised a synthetic linear analogue of HβD-3 (namely DLAP-2), against *C. auris* and *P. aeruginosa.*

4.4 Cell membrane integrity

The function of the cell membrane in both bacteria and fungi has been well documented (National Human Genome Research Institute, 2023). This essential cellular structure serves to contain and protect the internal cell components, as well as to regulate the transport of essential substances and waste products, both into and out of the cell (National Human Genome Research Institute, 2023). Due to its crucial role in the functioning and survival of microorganism cells, it is often a popular target for antimicrobial therapies. Additionally, as previously mentioned, PI is a fluorescent dye (orange-red fluorescence) used to detect cells that have damaged cell

membranes. For this reason, it is often used to identify drugs which target the cell membrane as a mechanism of antimicrobial action. Therefore, for this study, planktonic cells suspended in PBS under single and mixed conditions of *C. auris* and *P. aeruginosa* were exposed to MIC and MBC/MFC concentrations of DLAP-2. Positive controls (cells suspended in PBS and exposed to hydrogen peroxide), and negative controls (cells suspended in PBS), were also established for reference and comparison. Hydrogen peroxide (H_2O_2) was used to establish a positive control because of its oxidation properties. This chemical has highly reactive oxygen molecules which are able to remove electrons from the membranes of microorganisms and results in cellular destruction (Centers for Disease Control and Prevention, 2016).

In untreated negative controls, there was minimal to no indication of compromised cell membranes in single cell suspensions of *C. auris* or *P. aeruginosa*, as well as in combination cultures. However, in the established positive controls and treated samples, compromised membrane integrity was indicated by orange/red fluorescence. The main conclusion that can be drawn from these experiments is that, as the concentration of DLAP-2 increased, so the amount and intensity of orange/red fluorescence increased. This is directly linked to an increase in membrane permeabilization, which confirms the reported mechanism of action of defensin molecules (Pachón-Ibáñez *et al.,* 2017).

4.5 Cytotoxicity

When investigating potential antimicrobial drugs, an imperative characteristic that needs to be tested is the drug's safety for use in humans. Cytotoxicity can be described as the toxic effects caused by interactions between chemotherapeutic agents and living, mammalian, RBCs. A haemolytic assay focuses on quantifying the rupture or destruction of RBC's (haemolytic activity) brought about by a compound of interest (Amin and Dannenfelser, 2006). While the methodology for this assay remains largely conserved, the source of blood cells may differ. The blood needs to remain mammalian in origin for the results to be applicable, but the existing literature still reports the use of blood from a wide range of animal donors (e.g. leporine- rabbit or

hare, equine- horse, bovine- cow, ovine- sheep, murine- mice). A few studies also reported simply using human blood (Amin and Dannenfelser, 2006).

According to research published in 2006 by Amin and Dannenfelser, the acceptable limits or boundaries for percentage haemolysis in *in vitro*, mammalian RBC studies, lie between 10% and 25%. Values <10% are considered nonhemolytic, and those that are >25% are considered haemolytic. This means that anything that falls within the 10-25% buffer zone would be considered "indeterminate". According to these guidelines, the DLAP-2 compound can be considered nonhemolytic at lower—MIC (125 µg/ml) and 2xMIC (250 µg/ml)—concentrations. Any concentrations higher than 3xMIC (375 µg/ml), would have dangerously high levels of haemolysis (>83%). From a clinical point of view, this would mean that, unless the negative interactions between living RBCs and the DLAP-2 compound at higher concentrations could be mitigated through further manipulation of pharmacokinetic and pharmacodynamic characteristics, acceptable concentrations for patient use would have to be below 250 µg/ml.

Researchers have also reported that immunogenic responses are unlikely to be stimulated by HβD-3 analogues, because they mimic the identity of endogenous HβD-3 molecules within the body. For this reason, this article described these small peptides as potentially powerful antimicrobial and "non-immunogenic" therapies (Liu *et al.,* 2008). To test this hypothesis, a haemolytic assay was performed. Rabbit mammalian RBCs were exposed to varying concentrations of wild-type HβD-3 and its synthetic linear analogue (C(Acm)6). Concentrations of the antimicrobial peptides ranged from 3- 100 µg/ml and no haemolytic effect was detected (Liu *et al.,* 2008).
This experimental procedure was also performed on HβD-3 analogues in a second study; using RBCs from sheep. Similarly, the results indicated that at concentrations of 150-200 µg/ml, no cytotoxic effects could be detected (Dhople *et al.,* 2006). It is a positive sign that the results from this study's haemolytic assay agree with these previous findings. However, further studies would be needed to describe the significant haemolytic activity identified at higher concentrations in this study.

A collective review of the analysed data supports the view that defensin molecules are an underexploited and under-researched category of antimicrobial and antibiofilm

agents for use in the treatment of clinically significant infections. DLAP-2's promising affinity for compromising microbial cells, as well as for eradicating complex and polymicrobial biofilms shows that it has the potential to be an exciting drug which would be one of the first of its kind. Further investigation and development of these peptides should therefore be prioritised (Liu *et al.,* 2008).

CHAPTER 5: CONCLUSION

5.1 Closing statements

This study focused on two pathogens from distinctive biological kingdoms, but with similar and problematic tendencies for the development of resistance to available mainstream drugs. Under *in vitro* conditions, DLAP-2 demonstrated good antimicrobial activity against single and mixed cell suspensions of *C. auris* (MIC- 62,5 µg/ml; MFC- 125 µg/ml) and *P. aeruginosa*, (MIC- 125 µg/ml; MBC- 250 µg/ml) with stronger inhibitory effects against *C. auris* on its own. Additionally, DLAP-2s inhibitory effects were decreased for *C. auris* when in mixed populations (MIC- 125 µg/ml; MBC/MFC- 250 µg/ml).

When investigated for its antibiofilm capabilities on immature and mature biofilms, the most substantial percentages in biofilm inhibition were observed at the highest concentrations of DLAP-2. More specifically, polymicrobial biofilms showed above 60% inhibition at concentrations of 250 µg/ml. Moreover, the number of viable cells found within mono- and polymicrobial biofilms were also found to decrease with an increase in DLAP-2 concentrations. Overall, biofilm inhibition and reduction values ranged from 20%- 98% for mono- and polymicrobial biofilms made up of *C. auris* and *P. aeruginosa*. Concentrations of DLAP-2 that exceeded 125 µg/ml were found to be most effective at eradicating previously established biofilms.

A cell membrane integrity assay found that when planktonic cells were exposed to increasing concentrations of DLAP-2 (MIC and MBC/MFC), so the intensity and prevalence of orange/red fluorescence due to PI staining increased. This confirmed the existing literatures report that defensins bring about antimicrobial effects by disrupting cell membranes and inevitably causing cell lysis.

Based on the results of the haemolytic assay, at lower concentrations (125 µg/ml and 250 µg/ml), DLAP-2 exhibited minimal (≤ 10%) cytotoxic effects on mammalian RBCs. This, however, severely increased to above 82% when MIC concentrations were tripled (375 µg/ml). This means that unless additional pharmacological changes can

be made to DLAP-2 to decrease its haemolytic activity at higher concentrations, this compound would only be suitable for use in mammals at lower concentrations.

DLAP-2 can therefore be considered a promising antimicrobial and antibiofilm agent against single and mixed cell suspensions as well as mono- and polymicrobial biofilms that are made up of *C. auris* and *P. aeruginosa*.

5.2 Study limitations and future recommendations

- The data provided by this study is only applicable for *in vitro* scenarios, further testing will be required to determine the efficacy of the treatment for biofilm infections within living hosts (*in vivo* scenarios).
- Due to time and resource constraints this study only utilised one strain of each pathogen of interest which means extrapolation of results to other clinically significant strains will not be possible. To broaden the study profile, researchers may extend the pathogenic strains under investigation to include strains with fewer associated virulence factors, strains most isolated within clinical settings or even more virulent strains, and strains that are resistant to last-line antimicrobials (*C. auris* resistant to echinocandins and *P. aeruginosa* resistant to carbapenems or polymyxins).
- Further studies using confocal laser scanning microscopy (CLSM) and scanning electron microscope (SEM) microscopy could also be completed as these techniques offer more detailed photomicrographs of a cells structure and surface before and after exposure to anti-infectives. This study lacked access to such microscopes for analysis of larger sets of samples.
- The papers that can be found on scientific databases only describe in detail the relationship that exists between some Gram- positive (*Staphylococcus aureus*) and Gram-negative (*P. aeruginosa*) bacteria with more common species of *Candida* such as *C. albicans*. However, very little information is known about these same relationships with the newly emerging *C. auris*. Therefore, a study to verify the nature of the relationship (synergistic or antagonistic) that exists between *C. auris* and other clinically relevant bacteria within mixed microbial cell populations may be extremely useful.

- Studies have been done that verify the synergistic effects of using synthetic defensins in combination with mainstream antimicrobials when treating complex infections. It would be relevant to determine if the same relationship exists with DLAP-2.
- Quorum sensing and the production of toxins have been identified as other important diseases associated virulence factors within microorganism species such as *P. aeruginosa*. It may be useful to determine if DLAP-2 is capable of inhibiting or dismantling such virulence systems.
- From a molecular microbiology point of view, determining whether DLAP-2 can inhibit the expression of genes that are associated with virulence factors and worsened disease outcomes, may also be useful.
- Finally, it was speculated that defensin and defensin-like peptides may use multiple modes or mechanisms of antimicrobial activity to bring about cell death and biofilm inhibition. Additional studies which identify these multiple modes of action, outside of membrane permeabilization, would therefore be extremely useful.

REFERENCES

Amin, K., and Dannenfelser, R. (2006). *In vitro* hemolysis: guidance for pharmaceutical scientists. *J Pharm Sci* [online]. 95(6): pp. 1173-6. Available from: https://doi.org/10.1002/jps.20627 .

Barroso, C.; Carvalho, P.; Gonçalves, J.; Rodrigues, P., and Neves, J. (2021). Antimicrobial Peptides: Identification of two Beta-Defensins in a Teleost Fish, the European Sea Bass (Dicentrarchus labrax). *J. Pharm*.[online]. 14 (566). Available from: https://doi.org/10.3390/ph14060566.

Bassetti, M.; Vena, A.; Croxatto, A.; Righi, E., and Guery B. (2018). How to manage *Pseudomonas aeruginosa* infections. *Drugs Context* [online]. 29(7): pp. 212527. Available from: https://doi.org/10.7573%2Fdic.212527

Baylor College of Medicine. (2023). *Introduction to Infectious Diseases.* [online]. Available from: https://www.bcm.edu/departments/molecular-virology-and-microbiology/emerging-infections-and-biodefense/introduction-to-infectious-diseases . (Accessed 16 January 2024).

Centers for Disease Control and Prevention. (2016). *Infection Control-Chemical Disinfectants* [online]. Available from: https://www.cdc.gov/infectioncontrol/guidelines/disinfection/disinfection-methods/chemical.html#:~:text=Hydrogen%20peroxide%20works%20by%20producing,and%20other%20essential%20cell%20components. (Accessed 12 December 2023).

Centers for Disease Control and Prevention. (2020). *Antifungal Susceptibility Testing and Interpretation* [online]. Available from: https://www.cdc.gov/fungal/candida-auris/c-auris-antifungal.html#:~:text=Recent%20pharmacokinetic%2Fpharmacodynamic%20analysis%20of,should%20now%20be%20considered%20resistant. (Accessed 18 December 2023).

Centers for Disease Control and Prevention. (2021). *Immunization: The Basics* [online]. Available from: https://www.cdc.gov/vaccines/vac-gen/imz-basics.htm#:~:text=Vaccine%3A%20A%20preparation%20that%20is,or%20sprayed%20into%20the%20nose. (Accessed 19 January 2024).

Centers for Disease Control and Prevention. (2022). *Treatment and Management of C. auris Infections and Colonization*. [online]. Available from: https://www.cdc.gov/fungal/candida-auris/c-auris-treatment.html (Accessed 9 January 2024).

Cheong, H.; Kang, C.; Wi, Y.; Kim, E.; Lee, J.; Ko, K.; Chung, D.; Lee, N.; Song, J., and Peck, K. (2008). Clinical significance and predictors of community-onset *Pseudomonas aeruginosa* bacteremia. *Am J Med* [online]. 121(8): pp. 709-714. Available from: https://doi.org/10.1016/j.amjmed.2008.03.034.

Cleveland Clinic. (2023). *Candida Auris.* [online]. Available from: https://my.clevelandclinic.org/health/diseases/25152-candida-auris (Accessed 9 January 2024).

Cleveland Clinic. (2023). *Pseudomonas Aeruginosa* Infection. [online]. Available from: https://my.clevelandclinic.org/health/diseases/25164-pseudomonas-infection . (Accessed 10 January 2024).

Clinical and Laboratory Standards Institute. (2022). *Performance Standards for Antimicrobial Susceptibility Testing, 32nd edition. CLSI standards M100* [online]. Available from: file:///D:/2022%20CLSI%20M100.pdf .

Dhople, V.; Krukemeyer, A., and Ramamoorthy, A. (2006). The human beta-defensin-3, an antibacterial peptide with multiple biological functions. *Biochem Biophys Acta Gen Subj – Biomembranes* [online]. 1758 (9): pp. 1499-1512. Available from: https://doi.org/10.1016/j.bbamem.2006.07.007.

Diaz Caballero, J.; Wheatley, R.; Kapel, N.; López-Causapé, C.; Van der Schalk, T.; Quinn, A.; Shaw, L.; Ogunlana, L.; Recanatini, C.; Xavier, B.; Timbermont, L.; Kluytmans, J.; Ruzin, A.; Esser, M.; Malhotra-Kumar, S.; Oliver, A., and MacLean, C. (2023). Mixed strain pathogen populations accelerate the evolution of antibiotic resistance in patients. *at Commun* [online]. 14, 4083. Available from: https://doi.org/10.1038/s41467-023-39416-2.

Diggle, S., and Whiteley, M. (2020). Microbe Profile: *Pseudomonas aeruginosa*: opportunistic pathogen and lab rat. *J. Microbiol* [online]. 166 (1), pp. 30-33. Available from: https://doi.org/10.1099/mic.0.000860.

Du, H.; Bing, J.; Hu, T.; Ennis, C.; Nobile, C., and Huang G. (2020). *Candida auris:* Epidemiology, biology, antifungal resistance, and virulence. *PLoS Pathog* [online]. 16(10): pp. e1008921. Available from: https://doi.org/10.1371/journal.ppat.1008921

Fernandes, L.; Fortes, B.; Lincopan, N., and Ishida, K. (2020). Caspofungin and polymyxin B reduce the cell viability and total biomass of mixed biofilms of carbapenem-resistant *Pseudomonas aeruginosa* and *Candida* spp. *Front Microbiol* [online]. 11(1664-302X): pp. 573263. Available from: https://doi.org/10.3389/fmicb.2020.573263.

Fletcher, S. (2015). Understanding the contribution of environmental factors in the spread of antimicrobial resistance. *Environ Health Prev Med* [online]. 20: pp. 243–252. Available from: https://doi.org/10.1007/s12199-015-0468-0.

Fourie, R., and Pohl, C. (2019). Beyond Antagonism: The Interaction Between *Candida* Species and *Pseudomonas aeruginosa*. *J Fungi (Basel)* [online]. 5(2):34. Available from: https://doi.org/10.3390%2Fjof5020034.

Gaynes, R. (2017). The Discovery of Penicillin—New Insights After More Than 75 Years of Clinical Use. *Emerg. Infect. Dis* [online]. 23(5): pp. 849–853. Available from: https://doi.org/10.3201%2Feid2305.161556.

Ghannoum, M., and Rice L. (1999). Antifungal agents: mode of action, mechanisms of resistance, and correlation of these mechanisms with bacterial resistance. *Clin Microbiol Rev* [online]. 12(4): pp. 501-17. Available from: https://doi.org/10.1128%2Fcmr.12.4.501 .

Gleichmann, G. (2021). *Prokaryotes vs Eukaryotes: What Are the Key Differences?* Technology Networks [online]. Available from: https://www.technologynetworks.com/cell-science/articles/prokaryotes-vs-eukaryotes-what-are-the-key-differences-336095 (Accessed 5 February 2024).

Gray, A., and Sharara, F. (2022). Global and regional sepsis and infectious syndrome mortality in 2019: a systematic analysis. *Lancet Glob. Health* [online]. 10(S2): 2214-109X. Available from: https://doi.org/10.1016/S2214-109X(22)00131-0.

Gustavo, B., and Lorenz, A. (2021). What do we know about the biology of the emerging fungal pathogen of humans Candida auris? *Microbiol. Res*. [online]. 242(0944-5013): pp. 126621. Available from: https://doi.org/10.1016/j.micres.2020.126621 .

Gutiérrez, L.; Stepien, G.; Pérez-Hernández, M.; Pardo, J.; Grazú, V., and de la Fuente, J. (2017). Nanotechnology in Drug Discovery and Development. Chackalamannil, S.; Rotella, D., and Ward, S (eds.). Comprehensive Medicinal Chemistry III [online]. Oxford: Elsevier, pp. 264-295. Available from: https://doi.org/10.1016/B978-0-12-409547-2.12292-9 .

Hayes, A. Investopedia. (2023). *Multiple Linear Regression (MLR) Definition, Formula, and Example* [online]. Available from: https://www.investopedia.com/terms/m/mlr.asp (Accessed 11 December 2023).

Healthline Medical Network. (2023). *Side Effects of Antibiotics: What They Are and How to Manage Them* [online]. Available from: https://www.healthline.com/health/how-do-antibiotics-work (Accessed 9 January 2024).

Henrik, U.; Stotz, J., and Wang. (2009). Plant defensins- Defense, development, and application. *Plant Signal. Behav* [online]. 4: pp. 1010-1012. Available from: https://doi.org/10.4161/psb.4.11.9755.

Horton, M., and Nett, J. (2020). *Candida auris* infection and biofilm formation: going beyond the surface. *Curr Clin Microbiol Rep* [online]. 7(3): pp. 51-56. Available from: https://doi.org/10.1007/s40588-020-00143-7.

Horton, M.; Johnson, C.; Kernien, J.; Patel, T.; Lam, B.; Cleveland, A.; Meudt, J.; Shanmuganayagam, D.; Kalan, L., and Nett, J. (2020). *Candida auris* Forms High-Burden Biofilms in Skin Niche Conditions and on Porcine Skin. *ASM* [online]. 5(1): pp. e00910-19. Available from: https://doi.org/10.1128/mSphere.00910-19.

Houšť, J.; Spížek, J.; Havlíček, V. (2020). Antifungal Drugs. *Metabolites* [online]. 10(3):106. Available from: https://doi.org/10.3390/metabo10030106 .

Hughes, A. (1999). Evolutionary diversification of the mammalian defensins. CMLS. *Cell. Mol. Life Sci* [online]. 56: pp 94–103. Available from: https://doi.org/10.1007/s000180050010.

Jeffery-Smith, A., Taori, S., Schelenz, S., Jeffery, K., Johnson, E., Borman, A., Manuel, R., and Brown, C. (2018). *Candida auris*: a Review of the Literature. *Clin. Microbiol. Rev*.

[online]. 31(1): pp. 10.1128/cmr.00029-17. Available from: https://doi.org/10.1128/cmr.00029-17.

Klüver, E.; Adermann, K., and Schulz, A. (2006), Synthesis and structure–activity relationship of β-defensins, multi-functional peptides of the immune system. *J. Peptide Sci*. [online]. 12: 243-257. Available from: https://doi.org/10.1002/psc.749 .

LaBauve, A., and Wargo, (2012). M. Growth and laboratory maintenance of *Pseudomonas aeruginosa*. *Curr Protoc Microbiol* [online]. Chapter 6: Unit 6E.1. Available from: https://doi.org/10.1002%2F9780471729259.mc06e01s25 .

Lee, J.; Chang, S.; Perinpanayagam, H.; Lim, S.; Park, Y.; Han, S.; Baek, S.; Zhu, Q.; Bae, K., and Kum, K. (2013). Antibacterial Efficacy of a Human-β-Defensin-3 Peptide on Multispecies Biofilms. *J. Endod*. [online]. 39(12): pp. 1625-1629. Available from: https://doi.org/10.1016/j.joen.2013.07.035 .

Li, H; Zhang, C; Liu, P; Liu, W; Gao, Y., and Sun, S. (2015). *In vitro* interactions between fluconazole and minocycline against mixed cultures of *Candida albicans* and *Staphylococcus aureus*. *J Microbiol Immunol Infect* [online]. 48(6): pp. 655–661. Available from: https://doi.org/10.1016/j.jmii.2014.03.010.

Liu, S.; Zhou, L.; Li, J.; Suresh, A.; Verma, C.; Foo, Y.; Yap, E.; Tan, D., and Beuerman, R. (2008). Linear Analogues of Human β-Defensin 3: Concepts for Design of Antimicrobial Peptides with Reduced Cytotoxicity to Mammalian Cells. *ChemBioChem* [online]. 9: pp. 964-973. Available from: https://doi.org/10.1002/cbic.200700560.

Lone, S., and Ahmad, A. (2020). Inhibitory effect of novel Eugenol Tosylate Congeners on pathogenicity of *Candida albicans. BMC complement. med. ther*. [online]. 20(1): pp. 1-14. Available from: https://doi.org/10.1186%2Fs12906-020-02929-0

Marshall, J.; Warrington, R.; Watson, W., and Kim, H. (2018). An introduction to immunology and immunopathology. *Allergy Asthma Clin Immunol* [online]. 14(Supplement 2): Article number 49. Available from: https://doi.org/10.1186/s13223-018-0278-1 .

McDermott, A. (2022). Drug-resistant fungi on the rise. *Acad. Sci* [online]. 199 (48) pp. e2217948119. Available from: https://doi.org/10.1073/pnas.2217948119 .

Microbiology by numbers. (2011). *Nat Rev Microbiol*. [online]. 9, (1740-1534): 628. Available from: https://doi.org/10.1038/nrmicro2644 (Accessed 21 January 2024).

Molinari, G. (2015). Fluorescence Microscopy for Microbiology. McGenity, T.; Timmis, K., and Nogales, B (eds.). *Hydrocarbon and Lipid Microbiology Protocols*. Springer Protocols Handbooks. Berlin: Springer [online], pp. 49–69. https://doi.org/10.1007/8623_2015_108.

Narayanan, A.; Selvakumar, P.; Siddharthan, R., and Sanyal, K. (2022). ClaID: a Rapid Method of Clade-Level Identification of the Multidrug Resistant Human Fungal Pathogen *Candida auris. ASM* [online]. 10(2): pp. e00634-22. Available from: https://doi.org/10.1128/spectrum.00634-22.

National Human Genome Research Institute. (2023). *CELL MEMBRANE (PLASMA MEMBRANE)* [online]. Available from: https://www.genome.gov/genetics-glossary/Cell-Membrane (Accessed 12 December 2023).

Nett, J., and Andes, D. (2015). Antifungal Agents Spectrum of Activity. *Clin. Pharmacol. Ther.* [online]. 30(1): pp. 51-83. Available from: http://dx.doi.org/10.1016/j.idc.2015.10.012.

OneHealthTrust. (2024). *ResistanceMap. Antibiotic resistance* [online]. Available from: https://resistancemap.onehealthtrust.org/AntibioticResistance.php. (Accessed 13 January 2024).

Orazi, G., and O'Toole, G. (2019). "It Takes a Village": Mechanisms Underlying Antimicrobial Recalcitrance of Polymicrobial Biofilms. *J Bacteriol* [online]. 202(1): pp. e00530-19. Available from: https://doi.org/10.1128%2FJB.00530-19 .

O'Toole, G.; Kaplan, H., and Kolter, R. (2000). Biofilm Formation as Microbial Development. *Annu. Rev. Microbiol* [online]. 54: pp. 49-79. Available from: https://doi.org/10.1146/annurev.micro.54.1.49.

Otvos, L. (2000). Antibacterial peptides isolated from insects. *J Pept Sci*. [online]. 6(10): pp. 497-511. Available from: https://doi.org/10.1002/1099-1387(200010)6:10%3C497::aid-psc277%3E3.0.co;2-w.

Pachón-Ibáñez, M.; Smani, P.; Pachón, J., and Sánchez-Céspedes, J. (2017). Perspectives for clinical use of engineered human host defense antimicrobial peptides. *FEMS Microbiol. Rev* [online]. 41(3) pp. 323–342. Available from: https://doi.org/10.1093/femsre/fux012 .

Piketh, A.; Alam, H., and Ahmad, A. (2023). Quorum Sensing as an Alternative Approach to Combatting Multidrug Resistance. Mohmmad, Y., and Ahmad, A. (eds) *Non-traditional Approaches to Combat Antimicrobial Drug Resistance*. Singapore: Springer, pp 191–220. Available from: https://doi.org/10.1007/978-981-19-9167-7_8 .

Rasamiravaka, T.; Labtani, Q.; Duez, P., and El Jaziri, M. (2015). The Formation of Biofilms by *Pseudomonas aeruginosa*: A Review of the Natural and Synthetic Compounds Interfering with Control Mechanisms. *Biomed Res. Int*. [online]. 2015 (Article ID 759348). Available from: https://doi.org/10.1155/2015/759348

Rather, I.; Wani, M.; Kamli, M.; Sabir, J.; Hakeem, K.; Firoz, A.; Park, Y., and Hor, Y. (2023). *Limosilactobacillus fermentum* KAU0021 Abrogates Mono- and Polymicrobial Biofilms Formed by *Candida albicans* and *Staphylococcus aureus. Pharmaceutics* [online]. (15)-1079 Available from: http://dx.doi.org/10.3390/pharmaceutics15041079.

Reynolds, D., and Kollef, M. (2021). The Epidemiology and Pathogenesis and Treatment of *Pseudomonas aeruginosa* Infections: *An Update. Drugs* [online]. 81: 2117–2131.Available from: https://doi.org/10.1007/s40265-021-01635-6.

Rhodes, J., and Fisher, M. (2019). Global epidemiology of emerging *Candida auris*. *Curr. Opin. Microbiol*. [online]. 52, pp. 84-89. Available from: https://api.semanticscholar.org/CorpusID:195819933.

Salam, A.; Al-Amin, Y.; Pawar, J.; Akhter, N., and Lucy, I. (2023). Conventional methods and future trends in antimicrobial susceptibility testing. *Saudi J. Biol. Sci* [online]. 30(1319-562X), pp. 103582. Available from: https://doi.org/10.1016/j.sjbs.2023.103582 .

Scheunemann, G.; Fortes, B.; Lincopan, N., and Ishida, K. (2021). Caspofungin inhibits mixed biofilms of *Candida albicans* and methicillin resistant *Staphylococcus aureus* and displays effectiveness in coinfected *Galleria mellonella* larvae. *Microbiol Spectr* [online]. 9(2): pp. e0074421. Available from: https://doi.org/10.1128/Spectrum.00744-21.

Shaffer, C. (2023). *Biofilms in Human Disease* [online]. News-Medical.Net. Available from: https://www.news-medical.net/life-sciences/Biofilms-in-Human-Disease.aspx#:~:text=Infections%20related%20to%20biofilms%20can,can%20be%20difficult%20to%20treat. (Accessed 21 January 2024).

Sharma, D.; Misba, L., and Khan, A. (2019). Antibiotics versus biofilm: an emerging battleground in microbial communities. *Antimicrob Resist Infect Control* [online]. 8 (76). Available from: https://doi.org/10.1186/s13756-019-0533-3 .

Sikora, A., and Zahra, F. (2023). Nosocomial Infections. *NLM* [online]. Treasure Island (FL): StatPearls. Available from: https://www.ncbi.nlm.nih.gov/books/NBK559312/ .

Song, W.; Shi, Y.; Xiao, M.; Lu, H.; Qu, T.; Li, P.; Wu, G., and Tian, Y. (2009). *In vitro* bactericidal activity of recombinant human β-defensin-3 against pathogenic bacterial strains in human tooth root canal. *Int. J. Antimicrob. Agents* [online]. 33(0924-8579): pp. 237-243. Available from: https://doi.org/10.1016/j.ijantimicag.2008.05.022 .

Srivastava, V., and Ahmad, A. (2020). Abrogation of pathogenic attributes in drug resistant *Candida auris* strains by farnesol. *PLoS One* [online]. 15(5): pp. e0233102. Available from: https://doi.org/10.1371/journal.pone.0233102.

Srivastava, V., and Dubey, A. (2016). Anti-biofilm activity of the metabolites of *Streptomyces chrestomyceticus* strain ADP4 against *Candida albicans*. *J Biosci Bioeng* [online].; 122(4): pp. 434-40. Available from: https://doi.org/10.1016/j.jbiosc.2016.03.013.

StatisticsHowTo.com. (2023). *Wald Test: Definition, Examples, Running the Test* [online]. Available from: https://www.statisticshowto.com/wald-test/ (Accessed 11 December 2023).

Suchodolski, J.; Feder-Kubis, J., and Krasowska, A. (2017). Antifungal activity of ionic liquids based on (−) menthol: A mechanism study. *Microbiol* [online]. 197: pp. 56-64. Available from: https://doi.org/10.1016/j.micres.2016.12.008.

ThermoFisher Scientific Inc. (2023). *Invitrogen™- FUN™ 1 Cell Stain* [online]. Available from: https://www.thermofisher.com/order/catalog/product/F7030?gclid=CjwKCAiAjrarBhAWEiwA2qWdCFPo8SWGU41IfTrX8NvhkxqZDyz6CGcuD4L_KKgssB7J9uiipznlSBoChxMQA

vD_BwE&ef_id=CjwKCAiAjrarBhAWEiwA2qWdCFPo8SWGU41IfTrX8NvhkxqZDyz6CGcuD4L_KKgssB7J9uiipznlSBoChxMQAvD_BwE:G:s&s_kwcid=AL!3652!3!447292198766!!!g!!!10506731179!109642167771&cid=bid_pca_iva_r01_co_cp1359_pjt0000_bid00000_0se_gaw_dy_pur_con&gad_source=1 (Accessed 4 December 2023).

ThermoFisher Scientific Inc. (2023). *Preparing Fixed Cells for Labeling- The basics of fixation and permeabilization* [online]. Available from: https://www.thermofisher.com/za/en/home/life-science/cell-analysis/cell-analysis-learning-center/molecular-probes-school-of-fluorescence/imaging-basics/sample-considerations/preparing-fixed-cells-imaging.html#:~:text=membrane%2Dsurface%20antigens.-,Permeabilization,%2C%20in%20PBS)%20for%20permeabilization (Accessed 13 December 2023).

Theuretzbacher, U. (2017). Global antimicrobial resistance in Gram-negative pathogens and clinical need. *Curr. Opin. Microbiol* [online]. 39, pp. 106-112. Available from: https://api.semanticscholar.org/CorpusID:22901274 .

United States National Science Foundation. (2021). *Seven degrees from one trillion species of microbes* [online]. Available from: https://new.nsf.gov/news/seven-degrees-one-trillion-species-microbes#:~:text=The%20Earth%20contains%20about%20one,serves%20an%20ecosystem%20of%20microbes. (Accessed 4 January 2024).

Uprety, P., and Lockhart, S. (2022). AST News Update June 2022: Hot Topic- *Candida auris* Update: Method Variability with Amphotericin B Susceptibility Testing. *The Clinical and Laboratory Standards Institute*. [online]. Available from: https://clsi.org/about/blog/ast-news-update-june-2022-hot-topic/. (Accessed 17 January 2024).

Wang, M.; Liu, Z.; Liao, X.; Sun, R.; Li, R.; Liu, Y.; Fang, L.; Sun, J.; Liu, Y., and Zhang, R. (2021). Retrospective Data Insight into the Global Distribution of Carbapenemase-Producing *Pseudomonas aeruginosa*. *J. Antibiot* [online]. 10, 548. Available from: https://doi.org/10.3390/antibiotics10050548.

Watkins, R.; Gowen, R.; Lionakis, M., and Ghannoum, M. Update on the Pathogenesis, Virulence, and Treatment of *Candida auris*. (2022). *Pathog Immun* [online]. 7(2): pp. 46-65. Available from: https://doi.org/10.20411%2Fpai.v7i2.535

Wolcott, R.; Costerton, J.; Raoult, D., and Cutler, S. (2013). The polymicrobial nature of biofilm infection. *Clin Microbiol Infect*. [online]. 19(2): pp. 107-12. Available from: https://doi.org/10.1111/j.1469-0691.2012.04001.x.

World Health Organization. (2024). *A Brief History of Vaccination* [online]. Available from: https://www.who.int/news-room/spotlight/history-of-vaccination/a-brief-history-of-vaccination?topicsurvey=ht7j2q)&gclid=Cj0KCQiA2KitBhCIARIsAPPMEhLlIeUPSmuGlwM2mrLZBdMEO_lofhSCLiHCv7rR3teoPsg2GguVFgIaAvwlEALw_wcB (Accessed 19 January 2024).

Zhang, Y.; Li, Y.; Zeng, J.; Chang, Y.; Han, S.; Zhao, J.; Fan, Y.; Xiong, Z.; Zou, X.; Wang, C.; Li, B.; Li, H.; Han, J.; Liu, X.; Xia, Y.; Lu, B., and Cao, B. (2020). Risk Factors for Mortality of Inpatients with *Pseudomonas aeruginosa* Bacteremia in China: Impact of Resistance Profile in the Mortality. *Infect Drug Resist* [online]. 12(13): pp. 4115-4123. Available from: https://doi.org/10.2147%2FIDR.S268744 .

Zhu, C.; Tan, H.; Cheng, T.; Shen, H.; Shao, J.; Guo, Y.; Shi, S., and Zhang, X. (2013). Human β-defensin 3 inhibits antibiotic-resistant *Staphylococcus* biofilm formation. *J. Surg. Res.* [online]. 183(1): pp. 204-213. Available from: https://doi.org/10.1016/j.jss.2012.11.048 .

APPENDICES

Appendix I: Ethical clearance

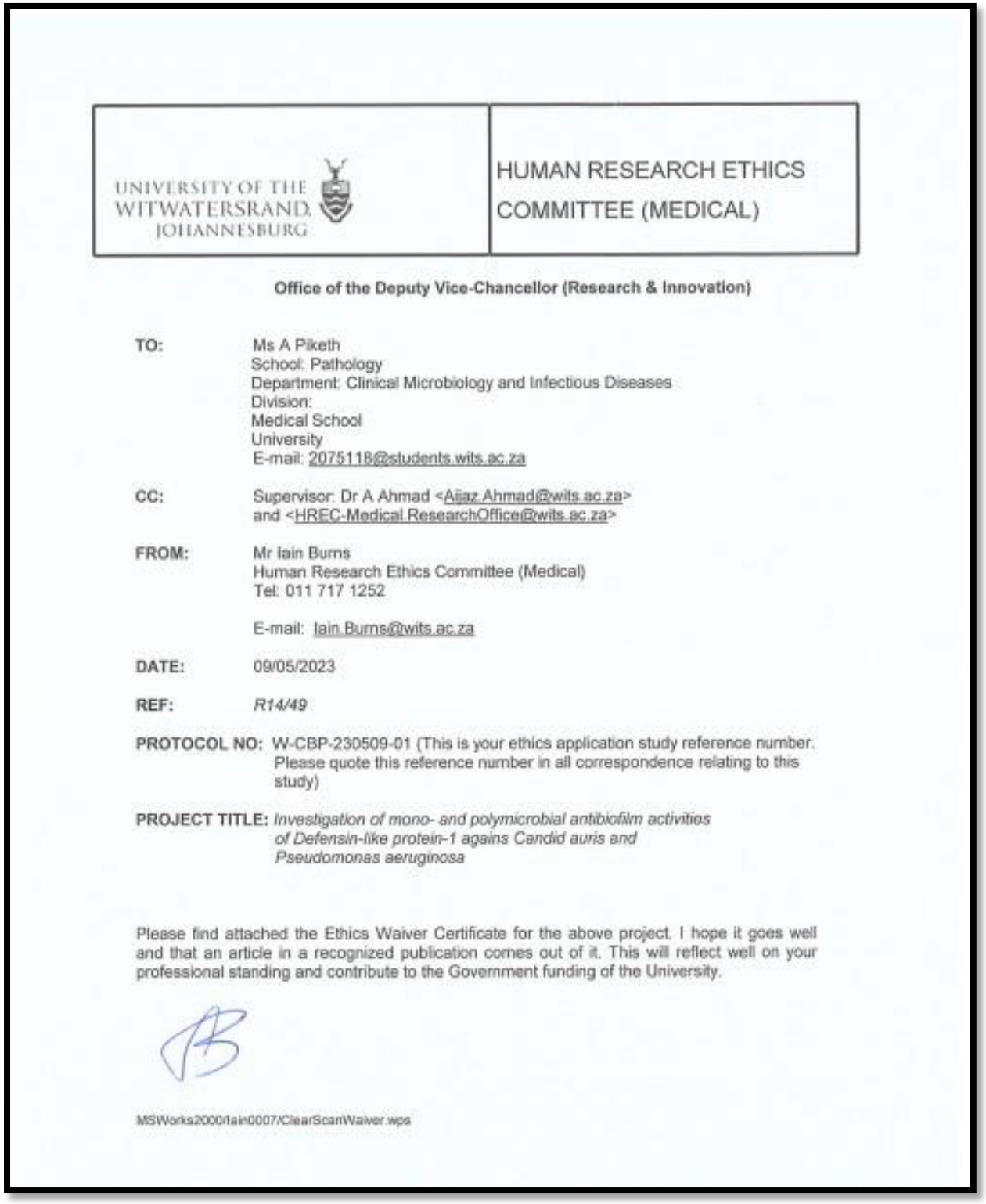

UNIVERSITY OF THE WITWATERSRAND, JOHANNESBURG

HUMAN RESEARCH ETHICS COMMITTEE (MEDICAL)

Office of the Deputy Vice-Chancellor (Research & Innovation)

TO: Ms A Piketh
School: Pathology
Department: Clinical Microbiology and Infectious Diseases
Division:
Medical School
University
E-mail: 2075118@students.wits.ac.za

CC: Supervisor: Dr A Ahmad <Aijaz.Ahmad@wits.ac.za>
and <HREC-Medical.ResearchOffice@wits.ac.za>

FROM: Mr Iain Burns
Human Research Ethics Committee (Medical)
Tel: 011 717 1252

E-mail: Iain.Burns@wits.ac.za

DATE: 09/05/2023

REF: *R14/49*

PROTOCOL NO: W-CBP-230509-01 (This is your ethics application study reference number. Please quote this reference number in all correspondence relating to this study)

PROJECT TITLE: *Investigation of mono- and polymicrobial antibiofilm activities of Defensin-like protein-1 agains Candid auris and Pseudomonas aeruginosa*

Please find attached the Ethics Waiver Certificate for the above project. I hope it goes well and that an article in a recognized publication comes out of it. This will reflect well on your professional standing and contribute to the Government funding of the University.

MSWorks2000/Iain0007/ClearScanWaiver.wps

UNIVERSITY OF THE WITWATERSRAND, JOHANNESBURG

HUMAN RESEARCH ETHICS COMMITTEE (MEDICAL)

Office of the Deputy Vice-Chancellor (Research & Innovation)

TO: Ms A Piketh
School: Pathology
Department: Clinical Microbiology and Infectious Diseases
Division:
Medical School
University
E-mail: 2075118@students.wits.ac.za

CC: Supervisor: Dr A Ahmad <Aijaz.Ahmad@wits.ac.za>
and <HREC-Medical.ResearchOffice@wits.ac.za>

FROM: Mr Iain Burns
Human Research Ethics Committee (Medical)
Tel: 011 717 1252

E-mail: Iain.Burns@wits.ac.za

DATE: 09/05/2023

REF: *R14/49*

PROTOCOL NO: W-CBP-230509-01 (This is your ethics application study reference number. Please quote this reference number in all correspondence relating to this study)

PROJECT TITLE: *Investigation of mono- and polymicrobial antibiofilm activities of Defensin-like protein-1 agains Candid auris and Pseudomonas aeruginosa*

Please find attached the Ethics Waiver Certificate for the above project. I hope it goes well and that an article in a recognized publication comes out of it. This will reflect well on your professional standing and contribute to the Government funding of the University.

MSWorks2000/Iain0007/ClearScan/Waiver.wps

Appendix II: Raw data

A.2.1 Antibiofilm activity (section 3.2)

Table A.1. Raw data for the antibiofilm activity of mono- and polymicrobial biofilms.

Organism	DLAP-2 Concentration (µg/ml)	Repeat	Percentage Biofilm Inhibition (%)
***C. auris* MRL 6057**			
Immature biofilms			
	62,5	1	46,59
		2	23,63
		3	19,28
		4	27,86
		5	44,95
		6	39,45
Mean:			**33,63**
Standard deviation:			**11,57**
	125	1	61,06
		2	44,59
		3	50
		4	46,43
		5	60,47
		6	56,46
Mean:			**53,17**
Standard deviation:			**7,15**
	250	1	57,57
		2	55,07
		3	52,86
		4	49,29
		5	59,47
		6	58,97
Mean:			**55,54**
Standard deviation:			**3,94**
Mature biofilms			
	62,5	1	49,55
		2	51,25
		3	41,33
		4	23,34
		5	47,57
		6	39,63
Mean:			**42,11**

Standard deviation:			**10,27**
	125	1	70,52
		2	60,89
		3	37,04
		4	35,33
		5	41,21
		6	40,69
Mean:			**47,61**
Standard deviation:			**14,51**
	250	1	68,54
		2	71,66
		3	56,31
		4	35,33
		5	60,28
		6	47,47
Mean:			**56,60**
Standard deviation:			**13,56**
***P. aeruginosa* ATCC 27853**			
Immature biofilms			
	62,5	1	25,72
		2	21,01
		3	21,01
		4	19,09
		5	46,4
		6	16,55
Mean:			**21,46**
Standard deviation:			**12,02**
	125	1	45,07
		2	51,35
		3	29,83
		4	29,83
		5	51,88
		6	51,27
Mean:			**38,23**
Standard deviation:			**9,40**
	250	1	52,92
		2	52,4
		3	34,13
		4	49,88
		5	57,36
		6	52,49
Mean:			**49,86**

Standard deviation:			**8,08**
Mature biofilms			
	62,5	1	20,77
		2	1,76
		3	1,76
		4	20,77
		5	53,03
		6	38,94
Mean:			**19,08**
Standard deviation:			**22,25**
	125	1	40,32
		2	41,9
		3	18,45
		4	13,79
		5	50,68
		6	44,81
Mean:			**34,99**
Standard deviation:			**15,11**
	250	1	40,32
		2	37,15
		3	20,78
		4	20,78
		5	60,08
		6	53,62
Mean:			**38,79**
Standard deviation:			**16,29**
Combination Immature biofilms			
	62,5	1	58,85
		2	61,65
		3	35,36
		4	37,27
		5	59,76
		6	36,59
Mean:			**48,25**
Standard deviation:			**13,02**
	125	1	41,54
		2	35,46
		3	56,9
		4	54,51
		5	67,48
		6	65,85
Mean:			**53,62**

Standard deviation:			**12,88**
	250	1	66,8
		2	57,44
		3	61,69
		4	61,21
		5	67,48
		6	66,67
Mean:			**63,55**
Standard deviation:			**4,05**
Mature biofilms			
	62,5	1	51,2
		2	62,17
		3	15,56
		4	11,47
		5	38,73
		6	16,18
Mean:			**32,55**
Standard deviation:			**21,28**
	125	1	65,57
		2	68,22
		3	62,43
		4	30,07
		5	53,76
		6	53,18
Mean:			**55,54**
Standard deviation:			**13,90**
	250	1	70,11
		2	68,22
		3	71,36
		4	66,89
		5	54,91
		6	56,07
Mean:			**64,59**
Standard deviation:			**7,23**

A.2.2 Biofilm microbial cell viability (section 3.3)

Table A.2. Raw data for the microbial cell viability assessment of mono- and polymicrobial biofilms.

Organism	DLAP-2 Concentration (µg/ml)	Repeat	CFUs/ml in original sample	Log10 CFUs/ml
***C. auris* MRL 6057**				
Immature biofilms				
	0 (NC)	1	4,2 x10^{10}	10,62
		2	4,73 x10^{10}	10,67
		3	7,033 x10^{10}	10,85
	Mean:		**5.321 x10^{10}**	**10,71**
	Standard deviation:		**1,51 x10^{10}**	**0,12**
	62,5	1	6000000	6,78
		2	5033333,33	6,7
		3	7400000	6,87
	Mean:		**6144444,44**	**6,78**
	Standard deviation:		**1189926,86**	**0,09**
	125	1	273333,33	5,44
		2	3333,33	3,52
		3	316666,67	5,5
	Mean:		**197777,78**	**4,82**
	Standard deviation:		**169782**	**1,13**
	250	1	333,33	2,52
		2	333,33	2,52
		3	26666,67	4,43
	Mean:		**27333,33**	**3,16**
	Standard deviation:		**15203,56**	**1,1**
Mature biofilms				
	0	1	9,867 x10^{10}	10,99
		2	9,53 x10^{10}	10,98
		3	8,033 x10^{10}	10,9
	Mean:		**9,143 x10^{10}**	**10,96**
	Standard deviation:		**9762286276**	**0,05**
	62,5	1	6,53 x10^{10}	10,81
		2	7,8 x10^{10}	10,89
		3	8,9 x10^{10}	10,95
	Mean:		**7,743 x10^{10}**	**10,88**
	Standard deviation:		**1,186 x10^{10}**	**0,07**
	125	1	1023333000	9,01
		2	1066666667	9,03
		3	870000000	8,94

	Mean:		**986666555,7**	**8,99**
	Standard deviation:		**103333274,3**	**0,05**
	250	1	44666700	7,65
		2	30000000	7,48
		3	30000000	7,48
	Mean:		**34888900**	**7,54**
	Standard deviation:		**8467823,19**	**0,1**
***P. aeruginosa* ATCC 27853**				
Immature biofilms				
	0 (NC)	1	7,03 x10^{10}	10,85
		2	4,73 x10^{10}	10,68
		3	8,83 x10^{10}	10,95
	Mean:		**6,866 x10^{10}**	**10,83**
	Standard deviation:		**2,06 x10^{10}**	**0,14**
	62,5	1	49666666,67	7,7
		2	41333333,33	7,62
		3	65333333,33	7,82
	Mean:		**52111111,11**	**7,71**
	Standard deviation:		**12185297,76**	**0,1**
	125	1	113333,33	5,05
		2	76666,67	4,88
		3	13333,33	4,12
	Mean:		**67777,78**	**4,68**
	Standard deviation:		**50589,12**	**0,5**
	250	1	10000	4
		2	9666,67	3,99
		3	333,33	2,52
	Mean:		**6666,67**	**3,5**
	Standard deviation:		**5487,36**	**0,85**
Mature biofilms				
	0 (NC)	1	9,967 x10^{12}	12,99
		2	9,033 x10^{12}	12,96
		3	9,967 x10^{12}	12,99
	Mean:		**9,66 x10^{12}**	**12,98**
	Standard deviation:		**5,7 x10^{12}**	**0,02**
	62,5	1	1,67 x10^{10}	10,22
		2	2,43 x10^{10}	10,39
		3	2,467 x10^{10}	10,39
	Mean:		**2,189 x10^{10}**	**10,33**
	Standard deviation:		**4498477520**	**0,1**
	125	1	15666666,67	7,19
		2	33000000	7,52
		3	20666666,67	7,32
	Mean:		**23111111,11**	**7,34**
	Standard deviation:		**8921468,07**	**0,17**

	250	1	10000	4
		2	10000	4
		3	10000	4
	Mean:		**10000**	**4**
	Standard deviation:		**0**	**0**
Combination				
Immature biofilms				
C. auris				
	0 (NC)	1	13666666,67	7,14
		2	15666666,67	7,19
		3	19000000	7,28
	Mean:		**16111111,11**	**7,20**
	Standard deviation:		**2694301,25**	**0,07**
	62,5	1	50000	4,7
		2	323333,33	5,51
		3	36666,67	4,56
	Mean:		**136666,67**	**4,92**
	Standard deviation:		**161795,48**	**0,5**
	125	1	2000	3,3
		2	4000	3,6
		3	5333,33	3,73
	Mean:		**3777,77**	**3,54**
	Standard deviation:		**1677,74**	**0,22**
	250	1	66,67	1,82
		2	66,67	1,82
		3	66,67	1,82
	Mean:		**66,67**	**1,82**
	Standard deviation:		**0**	**0**
P. aeruginosa				
	0 (NC)	1	2166666667	9,34
		2	4266666667	9,63
		3	2066666667	9,32
	Mean:		**2833333334**	**9,43**
	Standard deviation:		**1242309677**	**0,17**
	62,5	1	47000000	7,67
		2	22333300	7,35
		3	10333300	7,01
	Mean:		**26555533,33**	**7,34**
	Standard deviation:		**18694442,03**	**0,33**
	125	1	20000	4,3
		2	13333,33	4,12
		3	26666,67	4,43
	Mean:		**20000**	**4,28**
	Standard deviation:		**6666,67**	**0,16**
	250	1	2766,67	3,44

		2	33,33	1,52
		3	33,33	1,52
	Mean:		**944,44**	**2,16**
	Standard deviation:		**1578,09**	**1,11**
Mature biofilms				
C. auris				
	0 (NC)	1	986667000	8,99
		2	600000000	8,78
		3	826667000	8,92
	Mean:		**804444666,7**	**8,9**
	Standard deviation:		**194289002**	**0,11**
	62,5	1	1733333,33	6,24
		2	2633333,33	6,42
		3	4633333,33	6,67
	Mean:		**2999999,997**	**6,44**
	Standard deviation:		**1484362,94**	**0,22**
	125	1	533333,33	5,73
		2	433333,33	5,64
		3	766666,67	5,88
	Mean:		**577777,78**	**5,75**
	Standard deviation:		**171053,39**	**0,12**
	250	1	133333,33	5,12
		2	366666,67	5,56
		3	233333,33	5,37
	Mean:		**244444,44**	**5,35**
	Standard deviation:		**117062,82**	**0,22**
P. aeruginosa				
	0 (NC)	1	$1,4x10^{11}$	11,15
		2	$1,5\ x10^{11}$	11,18
		3	$3,9\ x10^{11}$	11,59
	Mean:		**$2,267\ x10^{11}$**	**11,31**
	Standard deviation:		**$1,42\ x10^{11}$**	**0,25**
	62,5	1	5000000000	9,7
		2	2233333333	9,35
		3	5000000000	9,7
	Mean:		**4077777778**	**9,58**
	Standard deviation:		**1597335745**	**0,2**
	125	1	70000000	7,85
		2	103333333,3	8,01
		3	36666666,67	7,56
	Mean:		**69999999,99**	**7,81**
	Standard deviation:		**33333333,32**	**0,23**
	250	1	866666,67	5,94
		2	866666,67	5,94
		3	1433333,33	6,16
	Mean:		**1055555,56**	**6,01**
	Standard deviation:		**4348988,82**	**0,13**

A.2.3 Cytotoxicity (section 3.6)

Table A.3. Raw data for the haemolytic assay of DLAP-2 on RBCs

	DLAP-2 Concentration		
Repeat	**MIC (125 µg/ml)**	**2XMIC (250 µg/ml)**	**3XMIC (375 µg/ml)**
	Percentage haemolysis (%)		
1	5,44	12,3	72,58
2	0	6,77	74,33
3	0	7,39	81,44
4	0	2,9	81,77
5	0	17,12	93,81
6	0	14,01	93,28
Average:	**0,91**	**10,08**	**82,87**
Standard deviation:	**2,22**	**5,29**	**9,06**

Appendix III: Statistical analysis

A.3.1 Antibiofilm activity (section 3.2)

```
2 . regress Inhibition i.Concentration i.Duration Concentration# Duration

      Source |       SS       df       MS              Number of obs =      36
-------------+------------------------------           F(5, 30)      =    3.94
       Model |      2358.25     5     471.65            Prob > F      =  0.0073
    Residual |      3592.5     30     119.75           R-squared     =  0.3963
-------------+------------------------------           Adj R-squared =  0.2957
       Total |      5950.75    35  170.021429           Root MSE      =  10.943

------------------------------------------------------------------------------
  Inhibition | Coefficient  Std. err.      t    P>|t|     [95% conf. interval]
-------------+----------------------------------------------------------------
Concentration |
         125 |    19.33333   6.317964     3.06   0.005     6.43033    32.23634
         250 |    21.83333   6.317964     3.46   0.002     8.93033    34.73634
             |
    Duration |
        1440 |         8.5   6.317964     1.35   0.189    -4.403003    21.403
             |
Concentration#Duration |
    125 1440 |   -13.83333   8.93495     -1.55   0.132    -32.08094    4.414269
    250 1440 |        -7.5   8.93495     -0.84   0.408     -25.7476    10.7476
             |
       _cons |    33.66667   4.467475     7.54   0.000     24.54287    42.79047
------------------------------------------------------------------------------

3 . testparm Concentration# Duration

 ( 1)  125.Concentration#1440.Duration = 0
 ( 2)  250.Concentration#1440.Duration = 0

       F(  2,    30) =    1.20
            Prob > F =    0.3148
```

Figure A.1. The MLR model analysis for the monomicrobial *C. auris* percentage biofilm inhibition study.

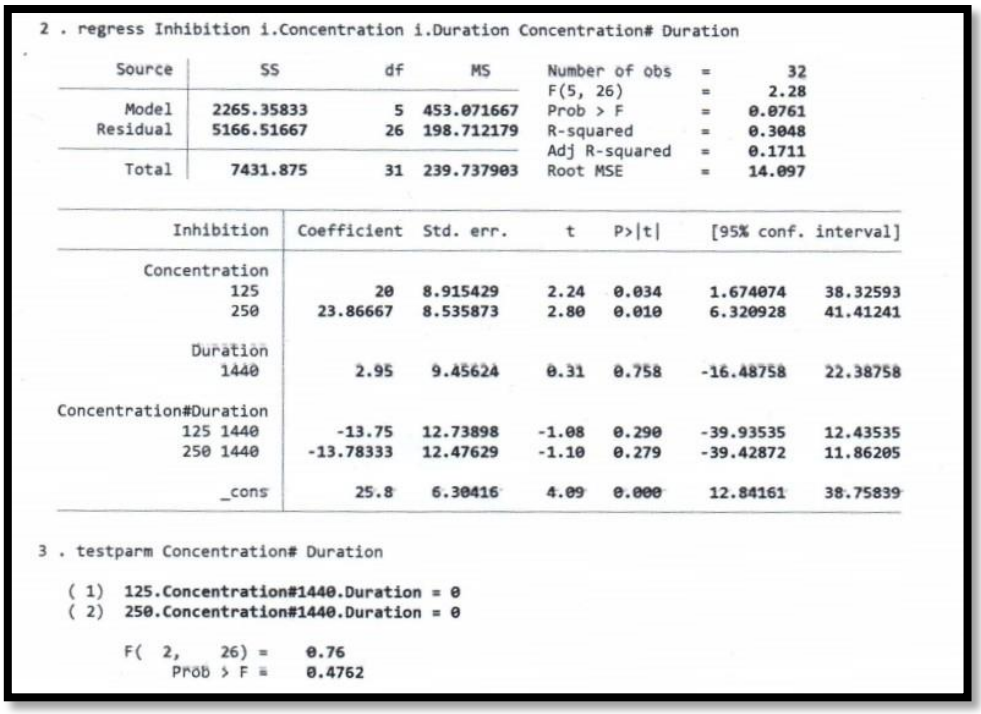

```
2 . regress Inhibition i.Concentration i.Duration Concentration# Duration

      Source |       SS       df       MS              Number of obs =      32
-------------+------------------------------           F(5, 26)      =    2.28
       Model |  2265.35833     5  453.071667            Prob > F      =  0.0761
    Residual |  5166.51667    26  198.712179            R-squared     =  0.3048
-------------+------------------------------           Adj R-squared =  0.1711
       Total |    7431.875    31  239.737903            Root MSE      =  14.097

------------------------------------------------------------------------------
  Inhibition | Coefficient  Std. err.      t    P>|t|     [95% conf. interval]
-------------+----------------------------------------------------------------
Concentration |
         125 |          20   8.915429     2.24   0.034     1.674074    38.32593
         250 |    23.86667   8.535873     2.80   0.010     6.320928    41.41241
             |
    Duration |
        1440 |        2.95   9.45624     0.31   0.758    -16.48758    22.38758
             |
Concentration#Duration |
    125 1440 |       -13.75  12.73898    -1.08   0.290    -39.93535    12.43535
    250 1440 |   -13.78333   12.47629    -1.10   0.279    -39.42872    11.86205
             |
       _cons |        25.8   6.30416     4.09   0.000     12.84161    38.75839
------------------------------------------------------------------------------

3 . testparm Concentration# Duration

 ( 1)  125.Concentration#1440.Duration = 0
 ( 2)  250.Concentration#1440.Duration = 0

       F(  2,    26) =    0.76
            Prob > F =    0.4762
```

Figure A.2. The MLR model analysis for the monomicrobial *P. aeruginosa* percentage biofilm inhibition study.

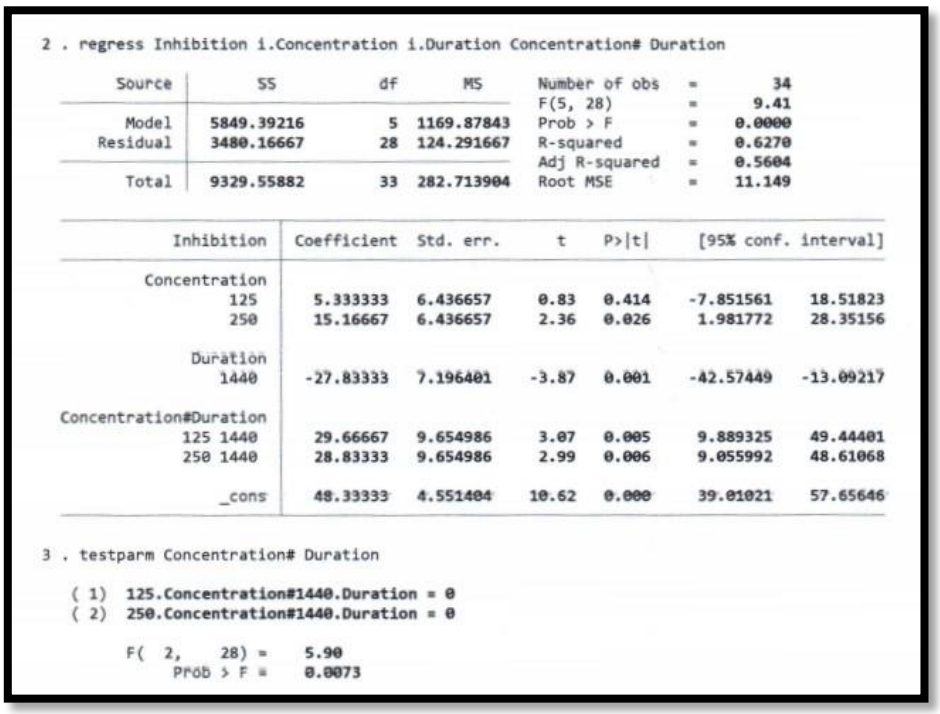

```
2 . regress Inhibition i.Concentration i.Duration Concentration# Duration

      Source |       SS       df       MS              Number of obs =      34
-------------+------------------------------           F(5, 28)      =    9.41
       Model |  5849.39216     5  1169.87843            Prob > F      =  0.0000
    Residual |  3480.16667    28  124.291667            R-squared     =  0.6270
-------------+------------------------------           Adj R-squared =  0.5604
       Total |  9329.55882    33  282.713904            Root MSE      =  11.149

------------------------------------------------------------------------------
  Inhibition | Coefficient  Std. err.      t    P>|t|     [95% conf. interval]
-------------+----------------------------------------------------------------
Concentration |
         125 |    5.333333   6.436657     0.83   0.414    -7.851561    18.51823
         250 |    15.16667   6.436657     2.36   0.026     1.981772    28.35156
             |
    Duration |
        1440 |   -27.83333   7.196401    -3.87   0.001    -42.57449   -13.09217
             |
Concentration#Duration |
    125 1440 |    29.66667   9.654986     3.07   0.005     9.889325    49.44401
    250 1440 |    28.83333   9.654986     2.99   0.006     9.055992    48.61068
             |
       _cons |    48.33333   4.551404    10.62   0.000     39.01021    57.65646
------------------------------------------------------------------------------

3 . testparm Concentration# Duration

 ( 1)  125.Concentration#1440.Duration = 0
 ( 2)  250.Concentration#1440.Duration = 0

       F(  2,    28) =    5.90
            Prob > F =    0.0073
```

Figure A.3. The MLR model analysis for the combination percentage biofilm inhibition study.

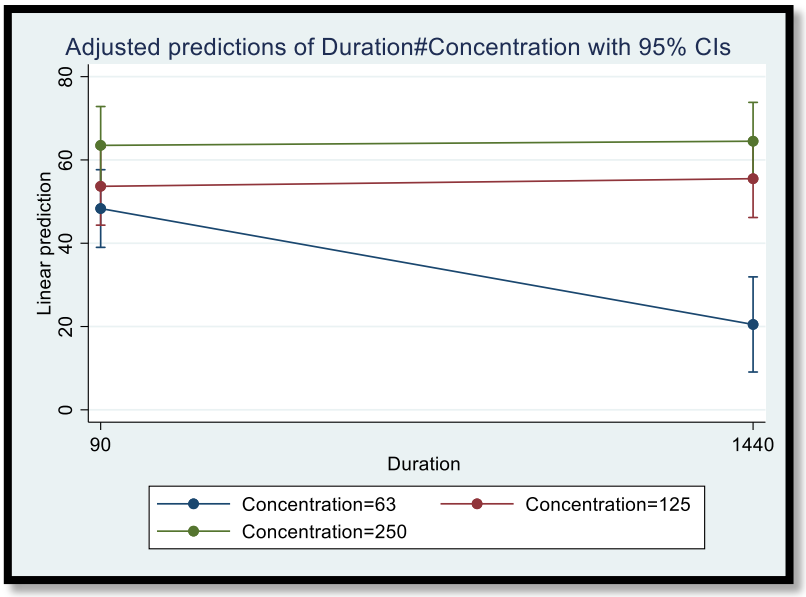

Figure A.4. Linear prediction graph showing the nature of the interaction between duration and concentration in the percentage biofilm inhibition dataset for the combination biofilm plates. The 62,5 µg/ml-concentration category has been set as 63 (rounded off value) in all the statistical analyses graphs to improve the datasets compatibility with the chosen statistical analysis package. Duration, plotted on the x-axis is in units of minutes.

A.3.2 Biofilm microbial cell viability (section 3.3)

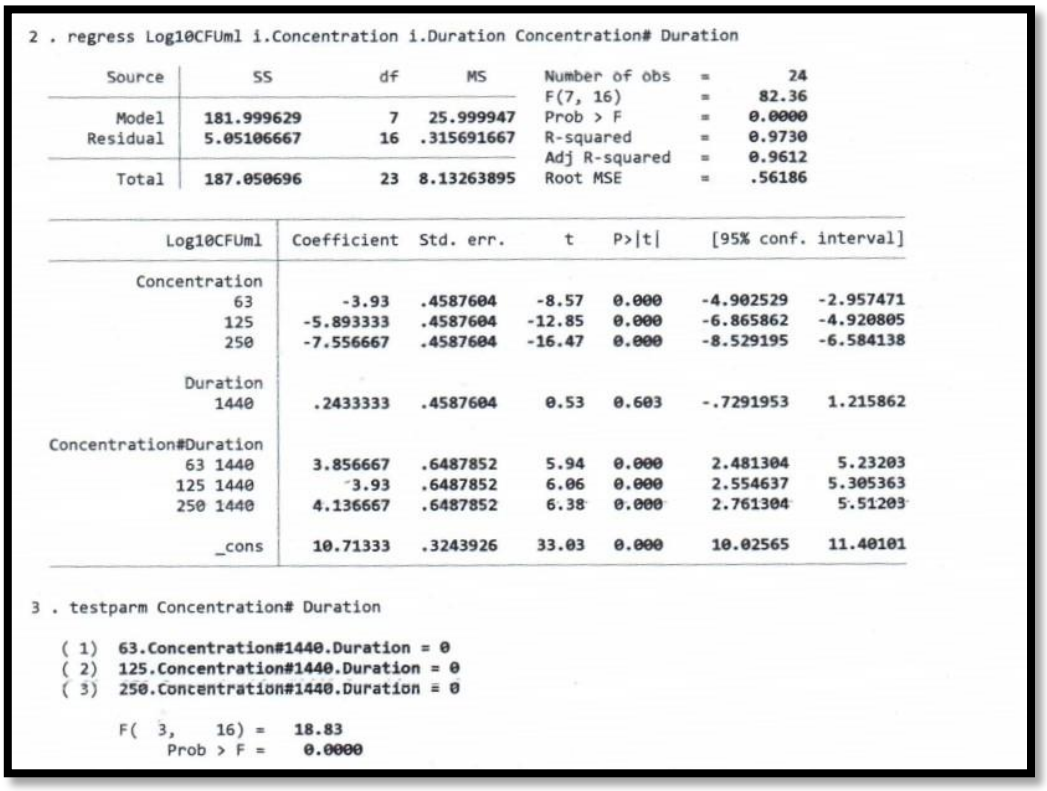

```
2 . regress Log10CFUml i.Concentration i.Duration Concentration# Duration

      Source |       SS       df       MS              Number of obs =      24
-------------+------------------------------           F(7, 16)      =   82.36
       Model |  181.999629     7  25.999947             Prob > F      =  0.0000
    Residual |  5.05106667    16  .315691667            R-squared     =  0.9730
-------------+------------------------------           Adj R-squared =  0.9612
       Total |  187.050696    23  8.13263895            Root MSE      =  .56186

------------------------------------------------------------------------------
     Log10CFUml | Coefficient  Std. err.      t    P>|t|     [95% conf. interval]
----------------+-------------------------------------------------------------
  Concentration |
             63 |       -3.93   .4587604    -8.57   0.000    -4.902529   -2.957471
            125 |  -5.893333   .4587604   -12.85   0.000    -6.865862   -4.920805
            250 |  -7.556667   .4587604   -16.47   0.000    -8.529195   -6.584138
                |
       Duration |
           1440 |   .2433333   .4587604     0.53   0.603    -.7291953    1.215862
                |
Concentration#Duration |
         63 1440 |   3.856667   .6487852     5.94   0.000     2.481304    5.23203
        125 1440 |       3.93   .6487852     6.06   0.000     2.554637    5.305363
        250 1440 |   4.136667   .6487852     6.38   0.000     2.761304    5.51203
                |
           _cons |   10.71333   .3243926    33.03   0.000     10.02565    11.40101
------------------------------------------------------------------------------

3 . testparm Concentration# Duration

 ( 1)  63.Concentration#1440.Duration = 0
 ( 2)  125.Concentration#1440.Duration = 0
 ( 3)  250.Concentration#1440.Duration = 0

       F(  3,    16) =   18.83
            Prob > F =    0.0000
```

Figure A.5. STATA MLR analysis of the *C. auris* in monomicrobial biofilms for cell viability assessment data.

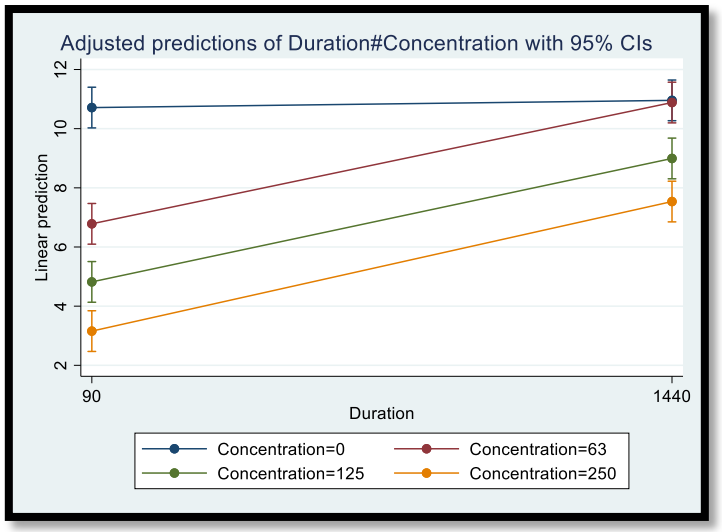

Figure A.6. Linear prediction graph showing the nature of the interaction between duration and concentration in the cell viability results for the monomicrobial *C. auris* dataset. The 62,5 µg/ml-concentration category has been set as 63 (rounded off value) in all the statistical analyses graphs to improve the datasets compatibility with the chosen statistical analysis package. Duration, plotted on the x-axis is in units of minutes.

```
2 . regress Log10CFUml i.Concentration i.Duration Concentration# Duration

      Source |       SS       df       MS              Number of obs =      24
-------------+------------------------------           F(7, 16)      =  281.46
       Model |  255.338096     7  36.4768708            Prob > F      =  0.0000
    Residual |      2.0736    16      .1296            R-squared     =  0.9919
-------------+------------------------------           Adj R-squared =  0.9884
       Total |  257.411696    23  11.1918129            Root MSE      =     .36

------------------------------------------------------------------------------
    Log10CFUml |      Coef.   Std. Err.      t    P>|t|     [95% Conf. Interval]
---------------+--------------------------------------------------------------
Concentration  |
            63 |  -3.113333   .2939388   -10.59   0.000    -3.736456   -2.490211
           125 |  -6.143333   .2939388   -20.90   0.000    -6.766456   -5.520211
           250 |  -7.323333   .2939388   -24.91   0.000    -7.946456   -6.700211
               |
      Duration |
          1440 |   2.153333   .2939388     7.33   0.000     1.530211    2.776456
               |
Concentration#Duration |
       63 1440 |   .4666667   .4156922     1.12   0.278    -.4145614    1.347895
      125 1440 |   .5066667   .4156922     1.22   0.241    -.3745614    1.387895
      250 1440 |  -1.656667   .4156922    -3.99   0.001    -2.537895   -.7754386
               |
         _cons |   10.82667   .2078461    52.09   0.000     10.38605    11.26728
------------------------------------------------------------------------------

3 . testparm Concentration# Duration

 ( 1)  63.Concentration#1440.Duration = 0
 ( 2)  125.Concentration#1440.Duration = 0
 ( 3)  250.Concentration#1440.Duration = 0

       F(  3,    16) =   11.97
            Prob > F =    0.0002
```

Figure A.7. STATA MLR analysis of the *P. aeruginosa* in monomicrobial biofilms for cell viability assessment data.

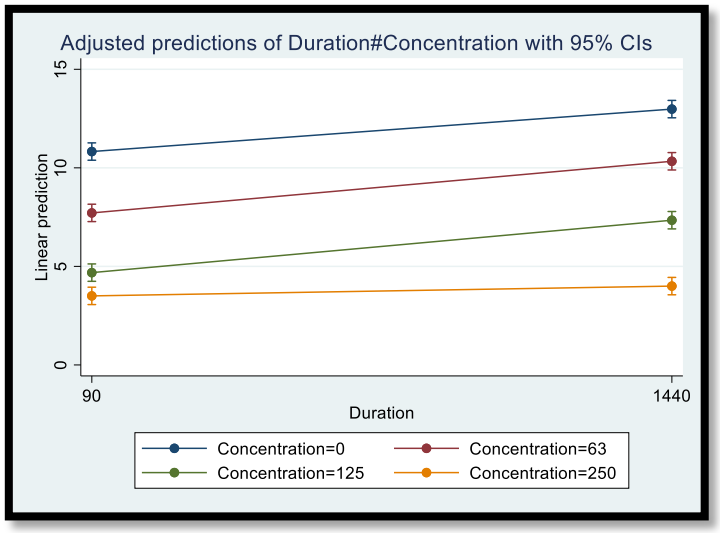

Figure A.8. Linear prediction graph showing the nature of the interaction between duration and concentration in the cell viability data for the *P. aeruginosa* dataset. The 62,5 µg/ml-concentration category has been set as 63 (rounded off value) in all the statistical analyses graphs to improve the datasets compatibility with the chosen statistical analysis package. Duration, plotted on the x-axis is in units of minutes.

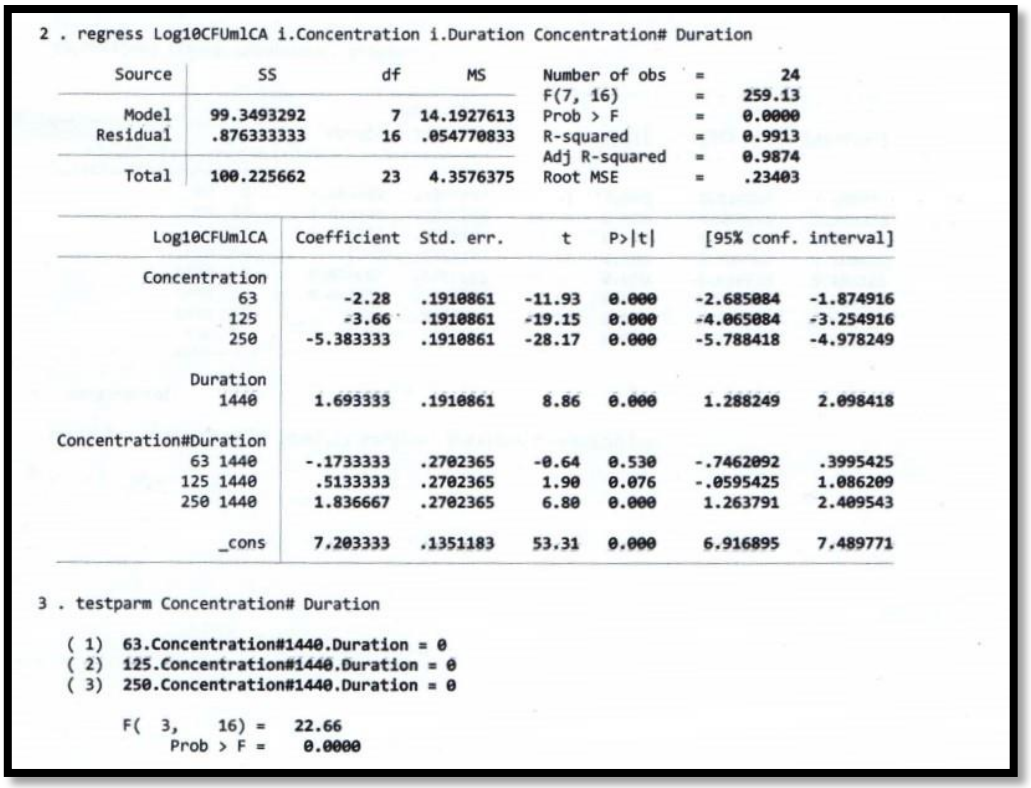

```
2 . regress Log10CFUmlCA i.Concentration i.Duration Concentration# Duration

      Source |       SS       df       MS              Number of obs =      24
-------------+------------------------------           F(7, 16)      =  259.13
       Model |  99.3493292     7  14.1927613            Prob > F      =  0.0000
    Residual |  .876333333    16  .054770833           R-squared     =  0.9913
-------------+------------------------------           Adj R-squared =  0.9874
       Total |  100.225662    23  4.3576375            Root MSE      =  .23403

------------------------------------------------------------------------------
   Log10CFUmlCA | Coefficient  Std. err.      t    P>|t|     [95% conf. interval]
----------------+-------------------------------------------------------------
  Concentration |
             63 |       -2.28   .1910861   -11.93   0.000    -2.685084   -1.874916
            125 |       -3.66   .1910861   -19.15   0.000    -4.065084   -3.254916
            250 |  -5.383333   .1910861   -28.17   0.000    -5.788418   -4.978249
                |
       Duration |
           1440 |   1.693333   .1910861     8.86   0.000     1.288249    2.098418
                |
Concentration#Duration |
        63 1440 |  -.1733333   .2702365    -0.64   0.530    -.7462092    .3995425
       125 1440 |   .5133333   .2702365     1.90   0.076    -.0595425    1.086209
       250 1440 |   1.836667   .2702365     6.80   0.000     1.263791    2.409543
                |
          _cons |   7.203333   .1351183    53.31   0.000     6.916895    7.489771
------------------------------------------------------------------------------

3 . testparm Concentration# Duration

 ( 1)  63.Concentration#1440.Duration = 0
 ( 2)  125.Concentration#1440.Duration = 0
 ( 3)  250.Concentration#1440.Duration = 0

       F(  3,    16) =   22.66
            Prob > F =    0.0000
```

Figure A.9. STATA MLR analysis of the *C. auris* in polymicrobial biofilms for cell viability assessment data.

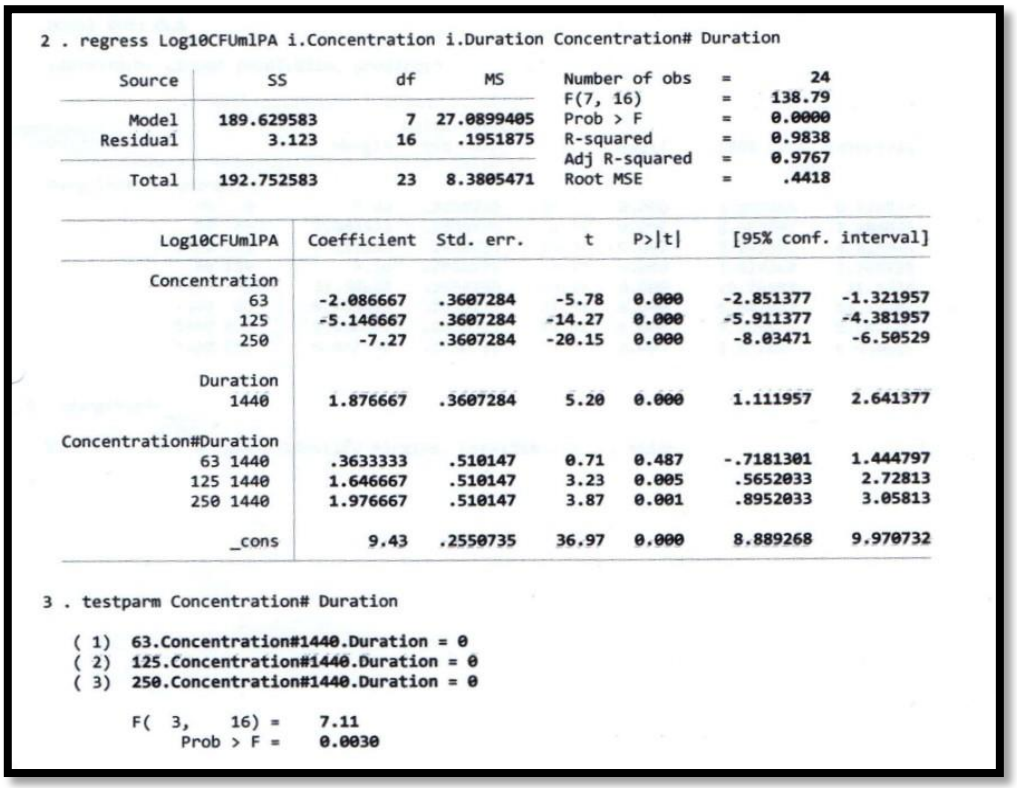

```
2 . regress Log10CFUmlPA i.Concentration i.Duration Concentration# Duration

      Source |       SS       df       MS              Number of obs =      24
-------------+------------------------------           F(7, 16)      =  138.79
       Model |  189.629583     7  27.0899405            Prob > F      =  0.0000
    Residual |      3.123    16  .1951875              R-squared     =  0.9838
-------------+------------------------------           Adj R-squared =  0.9767
       Total |  192.752583    23  8.3805471            Root MSE      =  .4418

------------------------------------------------------------------------------
   Log10CFUmlPA | Coefficient  Std. err.      t    P>|t|     [95% conf. interval]
----------------+-------------------------------------------------------------
  Concentration |
             63 |  -2.086667   .3607284    -5.78   0.000    -2.851377   -1.321957
            125 |  -5.146667   .3607284   -14.27   0.000    -5.911377   -4.381957
            250 |       -7.27   .3607284   -20.15   0.000     -8.03471    -6.50529
                |
       Duration |
           1440 |   1.876667   .3607284     5.20   0.000     1.111957    2.641377
                |
Concentration#Duration |
        63 1440 |   .3633333    .510147     0.71   0.487    -.7181301    1.444797
       125 1440 |   1.646667    .510147     3.23   0.005     .5652033     2.72813
       250 1440 |   1.976667    .510147     3.87   0.001     .8952033     3.05813
                |
          _cons |       9.43   .2550735    36.97   0.000     8.889268    9.970732
------------------------------------------------------------------------------

3 . testparm Concentration# Duration

 ( 1)  63.Concentration#1440.Duration = 0
 ( 2)  125.Concentration#1440.Duration = 0
 ( 3)  250.Concentration#1440.Duration = 0

       F(  3,    16) =    7.11
            Prob > F =    0.0030
```

Figure A.10. STATA MLR analysis of the *P. aeruginosa* in polymicrobial biofilms for cell viability assessment data.

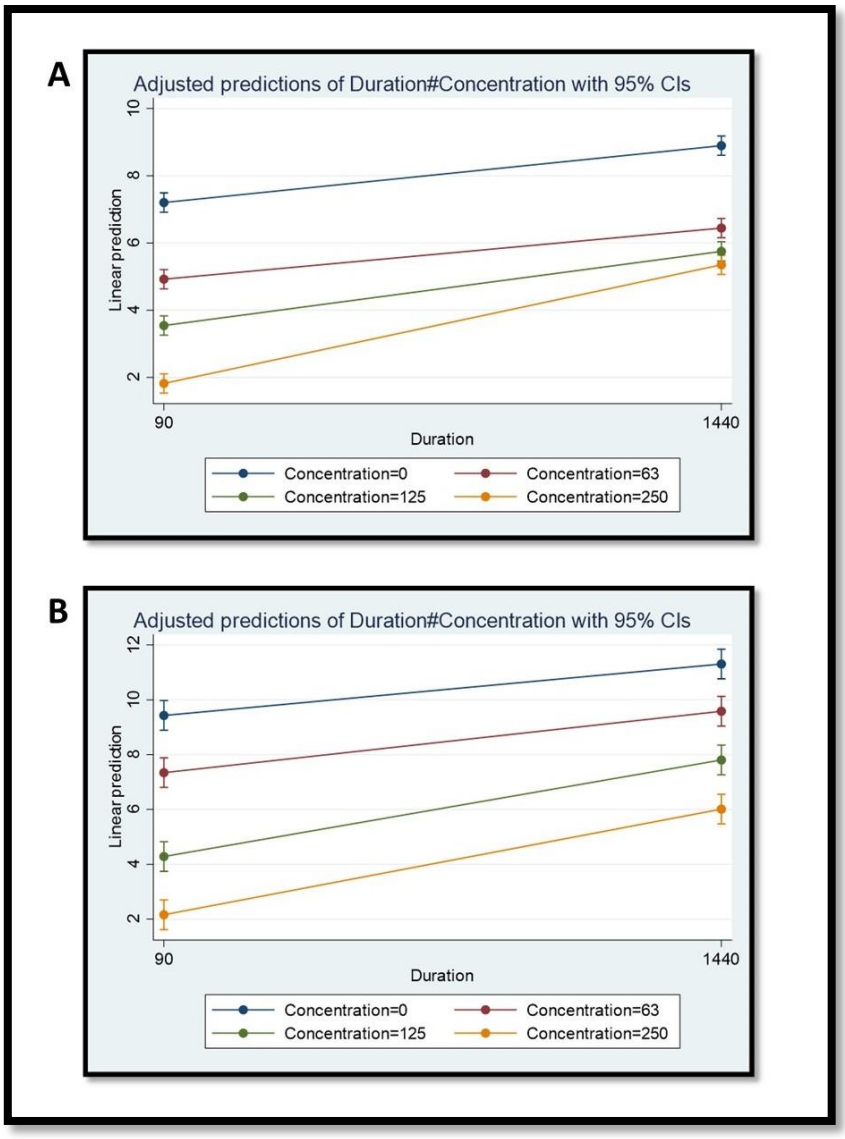

Figure A.11. Linear prediction graph showing the nature of the interaction between duration and concentration in the cell viability results for the polymicrobial, combination dataset (including both (**A**- *C. auris* and **B**- *P. aeruginosa* cells). The 62,5 µg/ml-concentration category has been set as 63 (rounded off value) in all the statistical analyses graphs to improve the datasets compatibility with the chosen statistical analysis package. Duration, plotted on the x-axis is in units of minutes.

A.3.3 Cytotoxicity (section 3.6)

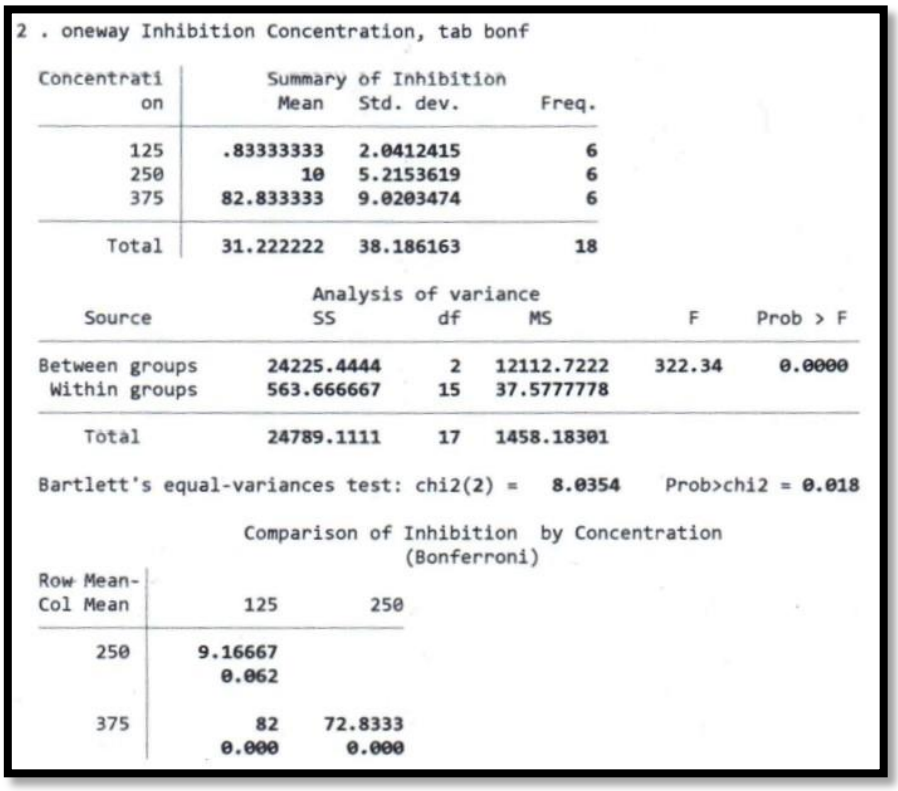

```
2 . oneway Inhibition Concentration, tab bonf

Concentrati |      Summary of Inhibition
         on |      Mean   Std. dev.       Freq.
------------+------------------------------------
        125 | .83333333   2.0412415           6
        250 |        10   5.2153619           6
        375 | 82.833333   9.0203474           6
------------+------------------------------------
      Total | 31.222222   38.186163          18

                        Analysis of variance
    Source              SS         df      MS            F     Prob > F
------------------------------------------------------------------------
Between groups      24225.4444      2   12112.7222     322.34     0.0000
 Within groups      563.666667     15   37.5777778
------------------------------------------------------------------------
     Total          24789.1111     17   1458.18301

Bartlett's equal-variances test: chi2(2) =   8.0354     Prob>chi2 = 0.018

                  Comparison of Inhibition by Concentration
                                (Bonferroni)
Row Mean-
Col Mean |        125         250
---------+--------------------------
     250 |    9.16667
         |      0.062
         |
     375 |         82     72.8333
         |      0.000       0.000
```

Figure A.12. The ANOVA (analysis of variance) results for the haemolytic activity assay.

Appendix IV: Preparation and recipes for broth, agar and buffers

Broth and agar

Sabouraud Dextrose Broth
SDB was used to grow suspended cells of fungal *C. auris*.

SDB powder (Merck, Germany)	30 g
Distilled water	1 L

Mueller Hinton Broth
MHB was used to grow suspended cells of the bacterial *P. aeruginosa*.

MHB powder (Merck, Germany)	22 g
Distilled water	1 L

Tryptone Soy Broth
TSB was used to grow suspended cells of both bacterial (*P. aeruginosa*) and fungal (*C. auris*) origin, in combination.

TSB powder (Merck, Germany)	30 g
Distilled water	1 L

Sabouraud 4% Glucose Agar
SDA was used to grow fungal cells of *C. auris* on a solid growth medium.

SDA powder (Merck, Germany)	30 g
Distilled water	1 L

Nutrient Agar (NA)
NA was used to grow bacterial cells of *P. aeruginosa.*

NA powder (Merck, Germany)	28 g
Distilled water	1 L

Buffers

Phosphate-buffered saline (PBS)
PBS was used throughout this experiment to suspend and wash cells.

PBS (Merck, Germany)	5 pellets
Distilled water	1 L

8.5% Saline

Saline solution was used throughout this experiment to suspend and wash cells.

NaCl salt crystals	8,5 g
Distilled water	1 L

Powder and crystals were mixed and dissolved in sterilised, 1 L, glass bottles. These bottles were then autoclaved on a liquid cycle at 121ºC for 15 minutes.

All bottles were left to reach room temperature once out of the autoclave. The bottle lids were tightly sealed and were stored on shelves in the laboratory, at room temperature, until they were needed. To prevent contamination, broth and buffers were aliquoted out into 50 ml falcon tubes to be used as needed. Additionally, agar was heated to 100ºC in a water bath to return the media to liquid before 25 ml was aliquoted into 90 mm Petri dish plates that were then allowed to solidify. These agar plates were stored in sealed boxes at 4 ºC. Sterility controls were established for all experiments to ensure zero contamination.

Appendix V: Similarity index report

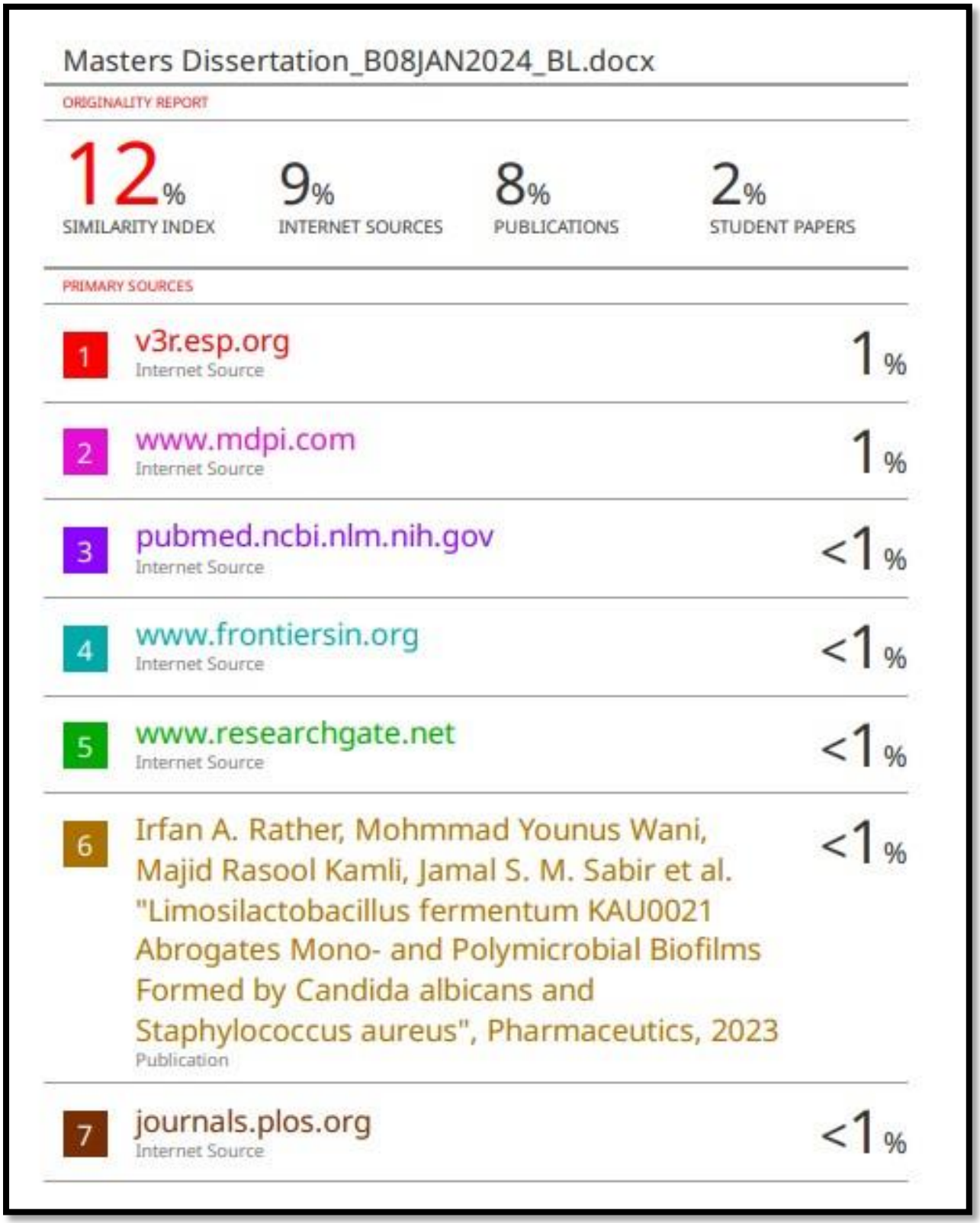

Masters Dissertation_B08JAN2024_BL.docx

ORIGINALITY REPORT

12%	9%	8%	2%
SIMILARITY INDEX	INTERNET SOURCES	PUBLICATIONS	STUDENT PAPERS

PRIMARY SOURCES

1	v3r.esp.org Internet Source	1%
2	www.mdpi.com Internet Source	1%
3	pubmed.ncbi.nlm.nih.gov Internet Source	<1%
4	www.frontiersin.org Internet Source	<1%
5	www.researchgate.net Internet Source	<1%
6	Irfan A. Rather, Mohmmad Younus Wani, Majid Rasool Kamli, Jamal S. M. Sabir et al. "Limosilactobacillus fermentum KAU0021 Abrogates Mono- and Polymicrobial Biofilms Formed by Candida albicans and Staphylococcus aureus", Pharmaceutics, 2023 Publication	<1%
7	journals.plos.org Internet Source	<1%